The Journal of Gemmology

Volume 28 No. 7 July 2003

The Gemmological Association and Gem Testing Laboratory of Great Britain

Gemmological Association and Gem Testing Laboratory of Great Britain

27 Greville Street, London EC1N 8TN
Tel: +44 (0)20 7404 3334 Fax: +44 (0)20 7404 8843
e-mail: gagtl@btinternet.com Website: www.gem-a.info

An anorthite-ruby-pargasite-picotite assemblage

Dr Karl Schmetzer[1], Dr Heinz-Jürgen Bernhardt[2] and Professor Edward J. Gübelin[3]

1. Taubenweg 16, D-85238 Petershausen, Germany
2. Central Microprobe Facility, Ruhr-University, D-44780 Bochum, Germany
3. Haldenstrasse 4, CH-6002 Lucerne, Switzerland

ABSTRACT: The mineral assemblage of cabochon-cut samples, probably from Myanmar, was determined by a combination of X-ray powder diffraction and electron microprobe analysis. The matrix consists of colourless plagioclase, which contains between 93 and 96 mol.% anorthite. The inclusions were determined as rubies, green chromium-bearing pargasites and black picotites. The possible origin of the samples is discussed.

Keywords: anorthite, Cr-pargasite, electron microprobe analyses, ruby

Introduction

In the mid-1990s, cabochons composed of ruby crystals in a transparent matrix of feldspar were briefly described by Koivula *et al.* (1994). These cabochons (*Figure 1*) were purchased by a German gem merchant in northern Thailand and were said to originate from Myanmar by local dealers. During further trips to Thailand, our supplier was able to obtain some similar cabochons with a colourless matrix and green inclusions (*Figure 2*); also some of the cabochons contained red and green minerals together as inclusions in a transparent matrix. In the mid-1990s cabochons of similar appearance (*Figure 3*) were also found elsewhere in the Asian market (Tay Thye Sun, pers. comm., 1995). Cathodoluminescence of this particular material was described recently by Ponahlo (2002).

The following study was undertaken to characterize the various components of this mineral assemblage.

Figure 1: *Ruby crystals in a matrix of colourless anorthite. Size of the sample on the left: 10.5 × 8.3 mm; photo by M. Glas.*

 ISSN: 1355–4565

Figure 2: *Pargasite crystals in a matrix of colourless anorthite. Size of the sample on the left: 21.3 × 16.3 mm; photo by M. Glas.*

Figure 3: *Ruby and pargasite crystals in a matrix of colourless anorthite. Size of the sample about 17 × 13 mm, photo by Tay Thye Sun.*

Materials and methods

For the present study about 40 cabochons in the range of about 3 to 20 ct were examined. For mineralogical phase determination, all four components of the cabochons were examined by microscope and by X-ray powder diffraction. Four samples were selected for electron microprobe analyses. After repolishing the originally slightly curved (almost plane) backs of these cabochons, analyses were made at 98 points in the different components of the mineral assemblage, namely 68 of the colourless to whitish matrix, 18 of the red component, eight of the green mineral and four of the black crystals.

Results

X-ray phase determination

Examination of the four components of the mineral assemblage by X-ray powder diffraction showed the following phases to be present (see *Figure 4*):

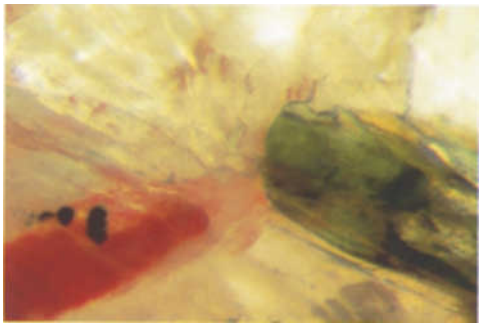

Figure 4: *Mineral assemblage with ruby, green pargasite and black picotite in a matrix of colourless anorthite. Photo by E.J. Gübelin, magnified 60 ×.*

- colourless to whitish matrix: plagioclase feldspar
- red inclusions: corundum (ruby)
- green inclusions: amphibole
- black inclusions: spinel

Microscopic observations

The crystals forming the colourless plagioclase matrix occasionally reveal parallel striations due to polysynthetic twinning. Healing feathers are also common. The ruby crystals show tabular habit with dominant basal pinacoids (0001) and appear as lath-like cross sections on the curved surfaces of the cabochons (*Figures 5 and 6*). Occasionally, the ruby crystals appear as if several platelets of different diameters are piled up to form an irregular stack. The green amphiboles are developed as long prismatic crystals (*Figure 7*). Cross sections typically consist of four {110} faces, some with two smaller {010} prisms (*Figure 8*). The spinels are small opaque grains or clusters with metallic lustre and sporadic development of small octahedral crystal faces (*Figures 4 and 9*).

Chemical compositions

The matrix consists of a transparent, colourless to light grey plagioclase feldspar. Microprobe analyses (*Table I*) showed that plagioclase is almost pure anorthite within the compositional range of 93 and 96 mol.% anorthite and 7 to 4 mol.% albite, thus showing only small variation.

The red corundum crystals (rubies) show a relatively large variation of chromium contents from 0.14 to 1.80 wt.% Cr_2O_3 (*Table II*). However, iron contents are small, titanium contents are extremely low and vanadium is below the detection limit of the electron microprobe.

The analyses of the green amphiboles (*Table I*) show a limited variability and reveal an aluminium-rich calcic amphibole with a composition close to pargasite:

$$NaCa_2(Mg, Fe^{2+})_4AlSi_6Al_2O_{22}(OH)_2$$

Figure 5: *Ruby crystals in a matrix of colourless anorthite. Size of the sample 19.0 × 13.4 mm; photo by M. Glas.*

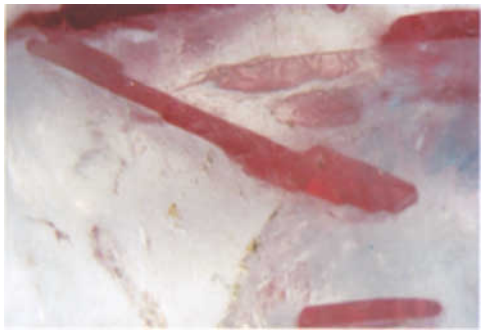

Figure 6: *Mineral assemblage with tabular ruby crystals in a matrix of colourless anorthite. Photo by K. Schmetzer, magnified 50 ×.*

Table I: *Compositional ranges of feldspars (F1-3), amphiboles (A1-3) and spinels (S1-3) shown by microprobe analyses of selected samples.*

Wt.%	*F1*	*F2*	*F3*	*Wt.%*	*A1*	*A2*	*A3*	*Wt.%*	*S1*	*S2*	*S3*
SiO_2	43.77	43.35	43.09	SiO_2	41.78	41.59	42.75	SiO_2	0.06	0.07	0.05
Al_2O_3	35.20	35.64	35.95	Al_2O_3	19.22	19.30	18.43	Al_2O_3	30.47	32.74	38.27
TiO_2	0.02	0.05	0.04	TiO_2	0.14	0.13	0.10	TiO_2	0.05	-	0.05
Cr_2O_3	0.02	0.05	0.06	Cr_2O_3	0.88	0.67	0.15	Cr_2O_3	31.44	29.44	25.11
MgO	-	-	-	MgO	14.85	15.01	15.43	MgO	4.21	4.51	6.36
FeO*	0.03	0.04	0.10	FeO*	5.09	4.90	5.11	FeO*	30.86	29.95	27.61
MnO	-	0.04	-	MnO	0.07	0.09	0.06	MnO	0.77	0.65	0.63
CaO	19.20	19.18	19.44	CaO	13.26	13.21	13.57	ZnO	0.63	0.74	0.70
Na_2O	0.78	0.53	0.42	Na_2O	2.50	2.47	2.54	CaO	0.13	0.10	0.07
K_2O	-	-	-	K_2O	0.50	0.55	0.49	Na_2O	0.03	0.01	-
								K_2O	-	-	-
Sum	**99.02**	**98.88**	**99.10**	**Sum**	**98.29**	**97.92**	**98.63**	**Sum**	**98.65**	**98.21**	**98.85**
Number of ions on the basis of 8 O				*Number of ions on the basis of 23 O*				*Number of ions on the basis of 4 O*			
Si	2.046	2.028	2.013	Si	5.918	5.916	6.032	Si	0.002	0.002	0.001
Al	1.939	1.964	1.980	Al	2.082	2.084	1.968	Al	1.152	1.226	1.374
Ti	0.001	0.002	0.001	**Sum T**	**8.000**	**8.000**	**8.000**	Ti	0.001	-	0.001
Cr	0.001	0.002	0.002	Al	1.133	1.151	1.097	Cr	0.798	0.740	0.605
Mg	-	-	-	Ti	0.015	0.014	0.011	Mg	0.201	0.214	0.289
Fe	0.001	0.002	0.004	Cr	0.098	0.075	0.017	Fe	0.828	0.796	0.704
Mn	-	-	-	Mg	3.144	3.181	3.241	Mn	0.021	0.018	0.016
Ca	0.961	0.961	0.974	Fe	0.605	0.583	0.603	Zn	0.015	0.017	0.016
Na	0.071	0.048	0.038	Mn	0.008	0.011	0.008	Ca	0.004	0.004	0.002
K	-	-	-	**Sum C**	**5.003**	**5.015**	**4.977**	Na	0.002	0.001	-
				Ca	2.018	2.013	2.050	K	-	-	-
				Na	0.689	0.682	0.695	**Sum**	**3.024**	**3.018**	**3.008**
				K	0.091	0.099	0.089				
				Sum A+ B	**2.798**	**2.794**	**2.834**				

* Total iron as FeO; - means below detection

Table II: *Compositional range and mean of ruby obtained from microprobe analyses.*

Wt.%	*Range (18 analyses)*	*Mean*
Al_2O_3	98.08–99.85	99.07
Cr_2O_3	0.14–1.80	0.77
Fe_2O_3	0.21–0.32	0.25
TiO_2	0.00–0.04	0.01
MnO	0.00–0.03	0.01

*Total iron as Fe_2O_3

The site occupancies of the T, C and A+B positions in the amphibole structure also show the presence of a limited percentage of the tschermakite molecule:

$$Ca_2(Mg, Fe^{2+})_3A_2lSi_6Al_2O_{22}(OH)_2$$

and a limited percentage of the sadanagaite molecule:

$$NaCa_2(Mg, Fe^{2+})_3Al_2Si_5Al_3O_{22}(OH)_2$$

(see Leake, 1997; Deer *et al.*, 1997). Small but distinct amounts of chromium are present in all the amphibole analyses. Consequently, the amphiboles are designated as chromium-bearing pargasites with about 10% each of the tschermakite and sadanagaite molecules.

The black spinels show a larger variation in chemical composition (*Table I*). These crystals are magnesium-iron-aluminium-chromium spinels with atomic ratios of Fe>Mg and Al>Cr. The compositions of these spinels lie in the range represented by the simplified formulae

$$(Mg_{0.2}Fe_{0.8})(Al_{1.2}Cr_{0.8})O_4 \text{ and}$$

$$(Mg_{0.3}Fe_{0.7})(Al_{1.4}Cr_{0.6})O_4$$

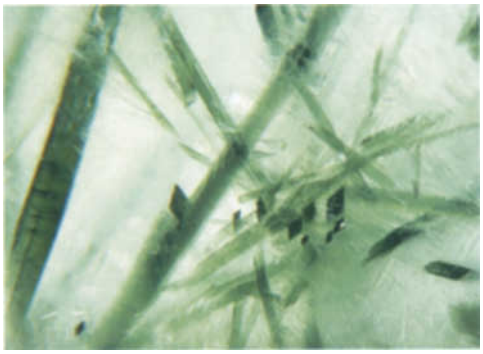

Figure 7: *Mineral assemblage with pargasite crystals in a matrix of colourless anorthite. Photo by K. Schmetzer, magnified 30 ×.*

Figure 8: *Cross section of a prismatic pargasite crystal consisting of four {110} and two smaller {010} prism faces. Photo by K. Schmetzer, magnified 60 ×.*

Figure 9: *Mineral assemblage with ruby and a black picotite grain in a matrix of colourless anorthite. Photo by K. Schmetzer, magnified 80 ×.*

Consequently, the spinels are chromian hercynite, which are also called picotite in the mineralogical nomenclature (see, for example, Deer *et al.*, 1975)

Discussion

The mineral assemblage described in this paper consists of a matrix of anorthite with major contents of Al-rich, chromium-bearing pargasites and rubies, and minor contents of chromium-bearing Fe-Al-spinels (picotite). Worldwide, ruby occurs mainly in three types of primary metamorphic rocks, i.e. in marbles, amphibolites (including anorthosites) and gneisses (Hunstiger, 1989, 1990 a, b). To date, two mineral assemblages in metamorphic rocks with ruby in an anorthitic matrix are known to the authors:

- in the ruby deposit of Rubinovoje, Polar Urals, Russia, ruby is found in metasomatic anorthosites and in mica-bearing anorthosites (Grygoriev *et al.*, 2000). Inclusions in ruby are black chromium-bearing spinel, plagioclase and chromium-bearing mica (fuchsite);

- in the ruby occurrence of Fiskenässet, Greenland, red corundum is found in an anorthosite matrix associated with green amphibole which is described as pargasite (Gübelin, 1979) or tschermakite (Petersen and Secher, 1985).

There are, in addition, several occurrences of rubies in amphiboles currently known, for example, Valle d'Arbedo, Switzerland; Chantel, France; Harts Range, Australia. A general overview is presented by Hunstiger (1989). The amphiboles found in these rocks are described as pargasites or tschermakites, and occasionally distinct percentages of chromium up to 1.15 wt.% Cr_2O_3 are reported from microprobe analyses. Frequently the feldspars in these mineral assemblages are anorthites or plagioclases with high percentages of the anorthite molecule. In rock specimens of the ruby-bearing zoisite-amphibolite from Longido, Tanzania, pargasitic amphiboles are found in association with anorthite and magnesium-iron-aluminium-chromium spinel (picotite). Amphibole analyses quoted by Leake (1971) and Hunstiger (1989) also show the presence of distinct amounts of chromium in the Longido pargasites.

Aluminium-rich pargasitic amphiboles similar to those analysed in our samples have also been described by Bunch and Okrusch (1973). These amphiboles were found in a corundum- and spinel-bearing marble from Pakistan (exact locality not given in the paper cited but confirmed subsequently as the Hunza area; M. Okrusch, pers. comm. 2002). The two hand specimens examined also contained anorthitic feldspars. Similar mineral assemblages were also mentioned later from the ruby marble deposit of Hunza, Pakistan (Okrusch *et al.*, 1976). The minerals described from Pakistan in these papers indicate the stability of this particular mineral assemblage – Al-rich pargasite, corundum, spinel and anorthite – not only in the anorthosites and amphibolites but also in metamorphic marbles. The ruby-bearing marble occurrence of Stirigma, Greece, in which pargasite and anorthite are also found, was briefly mentioned by Hunstiger (1990b).

Searching for the exact origin of the samples in this study which were quoted to come from Myanmar by local dealers in Thailand, marbles, amphibolites and anorthosites can therefore be considered. The most famous marble of Myanmar is known to all gemmologists as the host of the rubies in Mogok. Consequently, an origin for the samples from the large metamorphic mining area in Mogok, in which different types of metamorphic rocks other than marbles also occur, seems possible.

This assumption is supported by information obtained recently from T. Themelis (pers. comm. 2002),who reported that material similar to that described in this study was seen on several occasions during frequent visits to the Mogok area from 1994 to 2001.

It has to be mentioned, however, that there has also been a rumour in the trade about a possible origin for such samples from Africa, for example from Longido, indicating that the material was brought from its country of origin into Thailand and offered for sale in a local market in Northern Thailand. The similarity of chemical compositions of the anorthites, pargasites and picotites in our samples with data from the same minerals in Longido material could support this origin.

Acknowledgement

The authors are grateful to M. Steinbach of Köln, Germany, who submitted the samples used for the present study.

References

Bunch, T.E., and Okrusch, M., 1973. Al-rich pargasite. *American Mineralogist*, **58**, 721-6

Deer, W.A., Howie, R.A., and Zussman, J., 1975. *Rock-Forming Minerals. Volume 5, Non-Silicates, 7th impression.* Longman Group Ltd, London

Deer, W.A., Howie, R.A., and Zussman, J., 1997. *Rock-Forming Minerals. Volume 2B, Double-chain silicates*, 2nd edn. The Geological Society, London

Grygoriev, V.V., Burlakov, J.V., Polenov, J.A., and Kuznecov, V.I., 2000. Rubinovoje: Die roten Korunde von Rai-Iz im Polar-Ural. *Lapis*, **25**(9), 37-40

Gübelin, E.J., 1979. Fiskenässet. Rubinvorkommen auf Grönland. *Lapis*, **4**(3), 19-26

Hunstiger, C., 1989. Darstellung und Verleich primärer Rubinvorkommen in metamorphen Muttergesteinen - Petrographie und Phasenpetrologie. Teil I. *Z. Dt. Gemmol. Ges.*, **38**(4), 113-38

Hunstiger, C., 1990a. Darstellung und Vergleich primärer Rubinvorkommen in metamorphen Muttergesteinen – Petrographie und Phasenpetrologie. Teil II. *Z. Dt. Gemmol. Ges.*, **39**(1), 49-63

Hunstiger, C., 1990b. Darstellung und Vergleich primärer Rubinvorkommen in metamorphen Muttergesteinen – Petrographie und Phasenpetrologie. Teil III. *Z. Dt. Gemmol. Ges.*, **39**(2/3), 121-45

Koivula, J.I., Kammerling, R.C., and Fritsch, E. (Ed.), 1994. Gem News. Feldspar with ruby inclusions. *Gems & Gemology*, **30**(4), 274

Leake, B.E., 1971. On aluminous and edenitic hornblendes. *Mineralogical Magazine*, **38**(296), 389-407

Leake, B.E., *et al.*, 1997. Nomenclature of amphiboles: report of the subcommittee on amphiboles of the International Mineralogical Association, Commission on New Minerals and Mineral Names. *American Mineralogist*, **82**, 1019-37

Okrusch, M., Bunch, T.E., and Bank, H., 1976. Paragenesis and petrogenesis of corundum-bearing marble at Hunza (Kashmir). *Mineralium Deposita*, **11**, 278-97

Peterson, O.V., and Secher, K., 1985. *Grönland. Mineralien, Geologie, Geshichte.* Bochum, Verlag Bode & Partner KG

Ponahlo, J., 2002. Inclusions in gemstones: their cathodoluminescence (CL) and CL spectra. *Journal of Gemmology*, **28**(2), 85-100

An anorthite-ruby-pargasite-picotite assemblage

Identification of an impregnated quartz imitation of jade

T.L. Tan[1], T.S. Tay[2], B.L. Tan[1] and W.H. Tan[1]

1. Natural Sciences Academic Group, Nanyang Technological University, National Institute of Education, 1 Nanyang Walk, Singapore 637616, Singapore

2. Far East Gemological Laboratory, 400 Orchard Road #03-10, Orchard Towers, Singapore 238875, Singapore

ABSTRACT: The imitation of high-quality green jadeite has become more prevalent mainly because the jadeite commonly known as 'imperial jade' is now less commonly available. Fourier transform infrared (FTIR) and energy-dispersive X-ray fluorescence (EDXRF) spectroscopic techniques have been found to be accurate non-destructive techniques in identifying common imitations of jade. Therefore imitations of jade, natural jadeite (grade A jade) and treated jadeite (grade B jade) can be reliably distinguished. A selection of six stones was investigated to verify this assertion. The surface technique of EDXRF has a particular advantage in testing for jadeite close-set in jewellery on which measurements of refractive index and specific gravity can be impossible. In this study, transmission FTIR spectra of impregnated quartz imitations of jade show strong absorption peaks which correspond to those of quartz and of green polymers which are commonly used for impregnation of jadeite. Identification of the elemental content (C, O and Si) and calculations of X-ray peak intensity ratios of C/Si and O/Si in the investigated jadeite imitations and in quartz using EDXRF spectroscopy support the finding that the imitation is polymer-impregnated quartz. The EDXRF results from the imitations are compared to those of grade A and grade B jades, and specific gravity and ultraviolet fluorescence tests were conducted on all eight jade imitation and jadeite samples.

Keywords: energy-dispersive XRF, FTIR, jadeite, polymer

Introduction

Massive jadeitic rock, one of the two jade varieties, has always been highly valued in Asia and has often been associated with power, longevity and academic achievement (Chung, 2000). The proliferation of treated jadeite has been known in the jade market for at least ten years as the international jade business has expanded (Anon, 1991a, 1991b; Hurwit, 1989). As the skill of doctoring of jadeite by impregnation with polymers improves, more sensitive detection methods have become critical (Fritsch and McClure, 1993). In 1992, Fritsch *et al.* reported the successful application of transmission Fourier transform infrared (FTIR) spectroscopy in differentiating

 ISSN: 1355–4565

bleached and polymer-impregnated jadeite (grade B jade) from natural jadeite (grade A jade). Quek and Tan (1997) extended this infrared technique using diffuse reflectance on the surfaces of jadeite. Further studies of grades A and B jade on their elemental content by X-ray photoelectron spectroscopy (XPS) were reported by Tan *et al.* (1995). A polymer known as *polystyrene* was detected in some jadeite samples by Quek and Tan (1998) using the FTIR and XPS techniques. Tay *et al.* (1993) used a scanning electron microscope (SEM) to study damaged crystal structure in impregnated jadeites. Recently, dyed polymer-impregnated jadeite, considered as grade C, has become prevalent in the jade market (Tay, 2001).

Although scientific studies on treated jadeite have become more sophisticated and numerous (Gao and Zhang, 1998), studies on impregnated quartz imitations of jadeite remain very limited (Wu, 1991). An imitation or simulant usually displays a good colour such as translucent green to resemble a good jadeite, but it does not have the same physical properties. However, if an imitation gem is recognized with similar physical properties such as refractive index (RI), specific gravity (SG) and hardness, as the natural gem, then identification becomes difficult and a more sensitive scientific tool is required. Furthermore, accurate measurements of these physical properties are not possible for jewellery with close metal mountings.

In our present investigation, FTIR and EDXRF spectroscopic techniques were used together for the first time to accurately identify some material used for the imitation of jade.

Materials

Two samples of jade imitation (samples 1 and 2), two samples of natural quartz SiO_2 (samples 3 and 4), two samples of grade A jade, natural green jadeite (samples 5 and 6),

Figure 1: *The test stones, samples 1-8: impregnated quartz imitation of jade (1 and 2); natural quartz (3 and 4); grade A jade (5 and 6) and grade B jade (7 and 8).*

Table I: *Gemmological and spectroscopic data on jadeite imitation, natural quartz, grade A jade and grade B jade samples.*

Sample	*Sample No.*	*Description, microscopic observations*	*Behaviour in di-iodomethane (SG 3.32)*	*Fluorescence in LW UV radiation*	*Infrared absorption peaks (cm^{-1})*	*EDXRF elemental peaks*	*O/Si, C/Si intensity ratios*
Cabochons of imitation jade	1	Green veins, uneven patches of pale and dark green. Few fine fissures. No white or colourless areas.	float	weak chalky blue	2136, 2241, 2493, 2597, 2673 2873, 2932, 2965	C, O, Si	O/Si 1.21 C/Si 0.03
	2	Common green veins, uneven patches of pale and dark green. Fine fissures. No white areas.	float	weak chalky blue	2136, 2241, 2493, 2597, 2673 2873, 2932, 2965	C, O, Si	O/Si 0.22 C/Si 0.03
Quartz	3	Clear natural rock crystal with few fissures.	float	none	2136, 2241, 2493, 2597, 2673	O, Si	O/Si 0.11
	4	Clear natural quartz or 'rock crystal' some fissures, tinted with very light brown.	float	none	2136, 2241, 2493, 2597, 2673	O, Si	O/Si 0.12
Cabochons of grade A jadeite	5	Dark green with patches of white, fine fissures.	sink	none	2850, 2919	C, O, Na, Mg, Al, Si, Ca, Fe	O/Si 0.19 C/Si 0.01
	6	Light green with white and clear colourless patches, fine fissures.	sink	none	2850, 2919	C, O, Na, Mg, Al, Si, Ca, Fe	O/Si 0.18 C/Si 0.01
Cabochons of grade B jade	7	Green with white patches, large pit marks and fine fissures.	float	chalky-blue	2875, 2930, 2967, 3037, 3060	C, O, Na, Mg, Al, Si, Ca, Fe	O/Si 0.35 C/Si 0.05
	8	Green with large white patches, pit marks and fine fissures.	float	chalky-blue	2875, 2930, 2967, 3037, 3060	C, O, Na, Mg, Al, Si, Ca, Fe	O/Si 0.36 C/Si 0.06

Experimental methods

A Bio-Rad Excalibur Fourier transform infrared spectrometer was used to record the FTIR spectra of all samples with a resolution of 5 cm^{-1} in the wavenumber range of 400 to 4000 cm^{-1}. Immediately before the FTIR experiments the samples were thoroughly rinsed in propanol to remove any organic contaminant on their surfaces due to handling. Spectra were obtained from infrared transmission through whole samples and the investigations were non-destructive. Taking into account the spectrometric resolution of 5 cm^{-1} and other possible systematic errors, the positional accuracy of the absorption peak is ± 1 cm^{-1}.

All the samples were further tested using energy-dispersive X-ray fluorescence (EDXRF) to determine their chemical composition. The EDXRF spectra were collected using a scanning electron microscope JEOL JSM-5600LV SEM/ EDX with working accelerating voltage of 20 kV. Surface analysis by EDXRF is accomplished by bombarding a sample with high energy electrons and detecting and analysing the energy of the emitted X-rays. These electrons have penetrating power in a solid extending from 1 to 5 μm depending on their energy and the nature of the substance. EDXRF is a surface-sensitive technique of chemical characterization of the surface of a solid. The surfaces of all samples were thoroughly cleaned with a light dose of the volatile propanol in order to remove any contaminant present due to handling. The method has been shown to be useful in studies of gemstones (Muhlmeister and Devouard, 1992).

and two samples of grade B jade treated jadeite (samples 7 to 8) were used in this investigation and are shown in *Figure 1*. All the samples originated from Myanmar (Burma). The results of microscopic surface observations, immersion in di-iodomethane for SG estimates and exposure to ultraviolet radiation fluorescence are summarized in *Table I*.

The approximate test of immersion in di-iodomethane of SG 3.32 is commonly used to differentiate jade of grades A and B (Fritsch *et al.*, 1992; Tan *et al.*, 1995) The two jade imitation samples (1 and 2) and the quartz samples (3 and 4) were found to float. As expected, both grade A jade samples (5 and 6), which have an SG slightly above 3.32, sink in di-iodomethane. Both grade B jade samples (7 and 8), were found to float in the liquid because of their polymer impregnation which lowers the SG of the stones as a whole. Therefore the SG test is not effective in differentiating jadeite imitations from grade B jades.

The two jadeite imitation samples (1 and 2) and two grade B jade samples (7 and 8) give a strong chalky blue fluorescence under long wave ultraviolet radiation (*Table I*). The natural quartz and grade A jade samples are all inert in ultraviolet radiation. These results suggest that the jade imitations and the grade B jades were impregnated with a similar polymer material. Microscopic observation of the two jadeite imitations at 20× magnification showed that their colour is patchy pale and darker green with few fine fissures, and an absence of any white or colourless minerals. By comparison, the natural quartz is slightly smoky with transparent patches and some fine fissures. Of the four jadeite samples, three are patchy white and green, and only the grade B jade sample 7 was uniformly green and with an absence of white patches.

Results and discussion

In the FTIR transmission studies, the samples are nearly opaque to infrared radiation in the 400-2000 cm^{-1} region, and therefore the useful region of study is from 2000-4000 cm^{-1}. The positions (in cm^{-1}) of the infrared absorption peaks of all samples are listed in *Table I*. Typical sharp peaks in the infrared spectra of the jadeite imitation

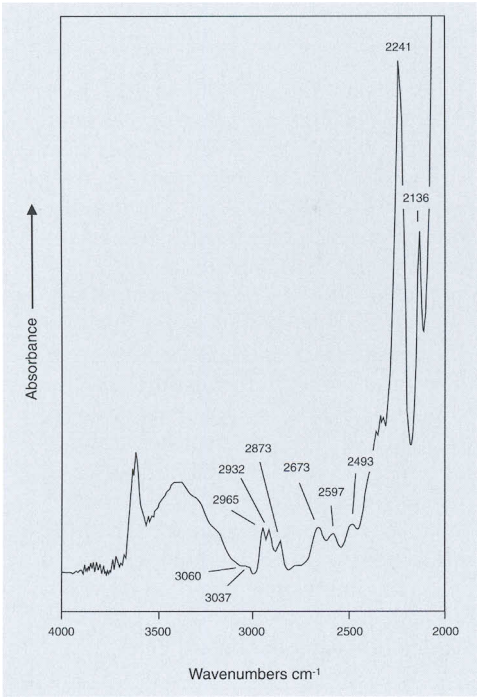

Figure 2: *Infrared absorption spectrum of impregnated quartz imitation of jade (samples 1 and 2).*

samples (1 and 2) are found at 2136, 2241, 2493, 2597, 2673, 2873, 2932 and 2965 cm^{-1}, while a broad absorption ranges from 3200 to 3700 cm^{-1}, as shown in *Figure* 2. A comparison in *Figure 3* of the spectra of the jade imitation (samples 1 and 2) with that of natural quartz (samples 3 and 4) reveals that both have common peaks at 2136, 2241, 2493, 2597 and 2673 cm^{-1}, and a broad absorption from 3200 to 3700 cm^{-1}. The agreement of these five absorption peaks strongly implies that the jadeite imitation is composed of quartz.

The transmission infrared spectra of the grade B and grade A jade samples are shown in *Figure 3c and d* respectively. Strong absorption peaks at 2875, 2930, and 2967 cm^{-1}, and weaker peaks at 3037 and 3060 cm^{-1} are typical of polymers in grade B jades (Fritsch *et al.*, 1992; Quek and Tan, 1998) The wax on the surface of grade A jade (*Figure 3d*) is manifested by two weak peaks at 2850 and 2919 cm^{-1}, in agreement with several previous works (e.g. Fritsch *et al.*, 1992, Quek and Tan, 1998). Three strong peaks at 2873, 2932, and 2965 cm^{-1} in jade imitations (samples 1 and 2) as shown in *Figure 2*, agree with those in grade B jade (*Figure 3c*) within experimental error of ± 1 cm^{-1}. This indicates the presence of polymers in the jade imitations. The spectra of the jade imitations (samples 1 and 2) and grade B jade (samples 7 and 8) are shown in *Figure 3b and c* and the presence in both of absorption peaks in the 2800-3000 cm^{-1} region clearly demonstrates the polymer contents.

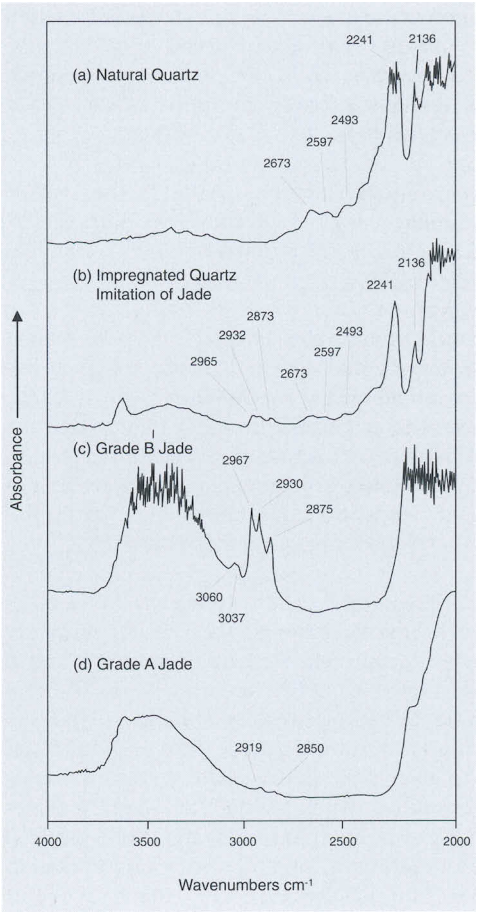

Figure 3: *Infrared absorption spectra of:*

a) Natural quartz (samples 3 and 4)
b) Jade imitation (samples 1 and 2)
c) Treated jade, grade B (samples 7 and 8)
d) Natural jade, grade A (samples 5 and 6)

Therefore all eight strong absorption peaks in the infrared spectra of the jade imitation samples (as given in *Table I*) could be assigned to natural quartz and the impregnation polymers typical of grade B jades. The absorption peaks in grade B jades, jade imitations and in natural quartz may be compared in *Figure 3 (c), (b) and (a)* respectively, and indicate that the jade imitations consist of green polymer-impregnated quartz material.

In the EDXRF experimental studies, a typical spectrum from the surface of a jade imitation (samples 1 and 2) is shown in *Figure 4b*. The spectrum recorded in the X-ray energy range of 0 to 9 keV indicates all the major elements present on the surface of the jadeite together with the gold coating added in sample preparation. The strong peaks from the sample are silicon Si $K_{\alpha 1}$ at 1.74 keV, oxygen O $K_{\alpha 1}$ at 0.525 keV and carbon C $K_{\alpha 1}$ at 0.277 keV (Blake, 1990). The presence of Si, O and C is consistent with the conclusions from FTIR work that the jadeite imitation is polymer-impregnated quartz, carbon (C) being attributed to the polymer. For sample 1, the X-ray peak intensity ratio of O/ Si is 0.21 and that of C/Si is 0.03 (*Figure 4b* and *Table I*). Corresponding values of 0.22 and 0.03 were obtained from sample 2.

The typical EDXRF spectrum of natural quartz (samples 3 and 4) is shown in *Figure 4a*. Si and O peaks are prominent, the O/Si ratio is 0.11 and carbon (C) was not detected (C/Si ratio is 0) in either sample. The presence of C and of higher O/Si ratio values in the jade imitation samples 1 and 2, compared to that in natural quartz indicate the presence of polymer in the imitations. These EDXRF results are in good agreement with the results of the FTIR work.

The EDXRF spectrum typical of grade B jade (samples 7 and 8) is shown in *Figure 4c*. The strong X-ray energy peaks of O, Na ($K_{\alpha 1}$ at 1.04 keV), Al ($K_{\alpha 1}$ at 1.49 keV), and Si are consistent with the ideal composition of jadeite, $NaAl(SiO_3)_2$. Traces of C, Mg ($K_{\alpha 1}$ at 1.25 keV), Ca ($K_{\alpha 1}$ at 3.69 keV) and Fe ($K_{\alpha 1}$ at

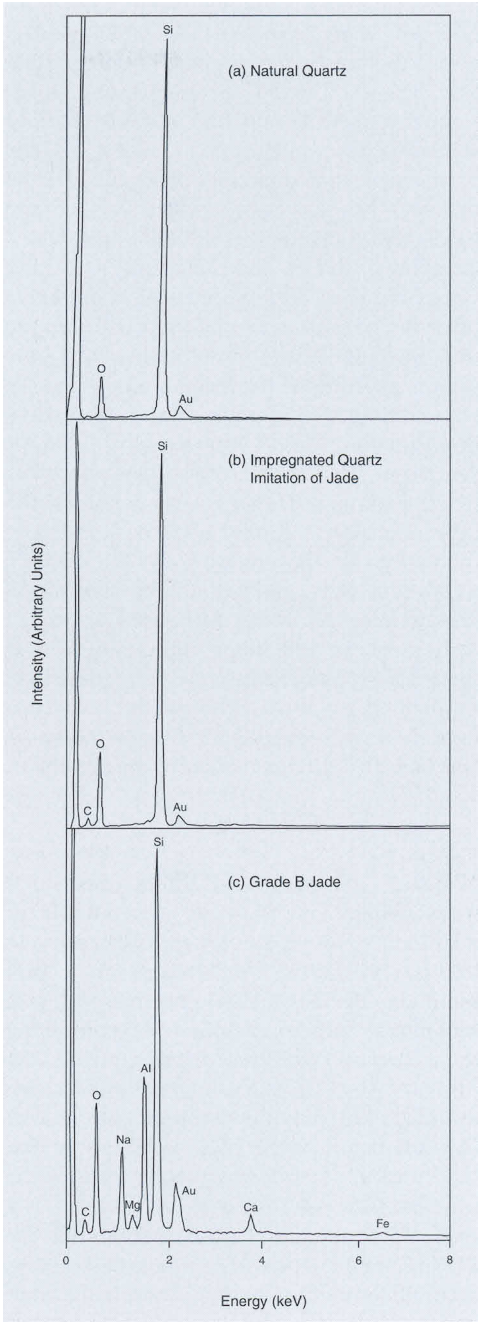

Figure 4: *EDXRF spectra of:*

(a) natural quartz (samples 3 and 4)
(b) jade imitation (samples 1 and 2)
(c) treated jade, grade B (samples 7 and 8)

6.40 keV) were also found. The carbon peak is due to the presence of polymer in the grade B jade. The O/Si and C/Si intensity ratios for sample 7 are 0.35 and 0.05 respectively, and similar values were obtained for sample 8. The presence of small quantities of Mg, Ca, and Fe in jadeite jade has been reported by Ou Yang (1993) and is not unexpected. For grade A jade (samples 5 and 6), the O/Si and C/Si ratio values are close to 0.19 and 0.01 respectively (*Table I*). The low values of C/Si of 0.01 indicate that the grade A jade samples have very little carbon, probably in the form of a thin layer of wax rather than the more extensive impregnation. This is supported by the FTIR spectrum in *Figure 3d*. The accurate determination of the various elements and the calculations of O/Si and C/Si peak intensity ratios for all the samples by the EXDRF techniques has proved to be useful in identifying the jade imitations, and in distinguishing imitations from natural and treated jades. Since Fritsch *et al.* (1992) described the method, advances in techniques now enable light elements such as C and O to be measured and make the detection of polymers possible.

Conclusion

Basic gemmological tests such as measurement of SG and observation of ultraviolet fluorescence can only provide limited indications for identifying a jade imitation. By using FTIR spectroscopy, jade imitations can be identified by comparing their spectra with standards and in the present investigation a jade imitation has been found to be polymer-impregnated quartz. One limitation of the FTIR technique is that the samples must be sufficiently thin for the transmission of infrared radiation. The present investigation has also shown that the EDXRF method provides a non-destructive, accurate technique for identification of a wide variety of elements including C and O present at the sample surface. Calculations of the X-ray peak peak intensity ratios O/Si and C/Si give useful quantitative chemical data for polymer-impregnated materials like quartz, which is used as a jade imitation, and of polymer-impregnated (grade B) jadeites.

References

Anon, 1991A. Green jadeite bleached then dyed emerald green. *Jewellery News Asia*, **79**, 122, 124

Anon, 1991b. New filler threatens jadeite sales in Japan. *Jewellery News Asia*, **82**, 1, 72

Blake, D., 1990. Scanning electron microscopy. In: Dale L. Perry (ed.), *Instrumental Surface Analysis of Geologic Materials*. VCH publisher, New York, U.S.A., 11-43

Chung, Y., 2000. Romancing the stone. *Asia week*, November 24 issue, p. 118

Fritsch, E., and McClure, S.F., 1993. Polymer impregnated jadeite. *ICA Laboratory Alert*, **75**

Fritsch, E., Wu S.-T. T., Moses, T., McClure, S.F., and Moon, M., 1992. Identification of bleached and polymer-impregnated jadeite. *Gems and Gemology*, **28**, 176-87

Gao, Y., and Zhang, B.L., 1998. Identification of B jade by FTIR spectrometer with near-IR fibre-optic probe accessory. *Journal of Gemmology*, **26**, 302-7

Hurwit, K,. 1989. Gem trade lab notes: Impregnated jadeite jade. *Gems and Gemology*, **25**, 239-40

Muhlmeister S., and Devouard B., 1992. Determining the natural or synthetic origin of rubies using energy-dispersive X-ray fluorescence (EDXRF). In: Alice S. Keller (ed.), *Proceedings of the International Gemological Symposium 1991*. Gemological Institute of America, Santa Monica, California, U.S.A., 139-40

Ou Yang, C.M., 1993. Microscopic studies of Burmese jadeite jade - 1. *Journal of Gemmology*, **23**, 278-84

Quek, P.L., and Tan, T.L., 1997. Identification of B jade by diffuse reflectance infrared Fourier transform (DRIFT) spectroscopy. *Journal of Gemmology*, **25**, 417-27

Quek, P.L., and Tan, T.L., 1998. Identification of polystyrene in impregnated jadeite. *Journal of Gemmology*, **26**, 168-173

Tan, T.L., Tay, T.S., Loh, F.C., Tan, K.L., and Tang, S.M., 1995. Identification of wax- and polymer-impregnated jadeite by X-ray photoelectron spectroscopy. *Journal of Gemmology*, **24**, 475-83

Tay, T.S., 2001. Far East Gemological Lab, private communications

Tay, T.S., Paul, S., and Puah, C.M., 1993. SEM studies of bleached and polymer-impregnated jadeite. *Australian Gemmologist*, **18**, 257-61

Wu S.-T.T., 1991. How to identify the new jadeite imitations [in Chinese]. *Jewelry Journal*, **2**, 6-8

Trace elements in Thai gem corundums

S. Saminpanya[1], D.A.C. Manning[2], G.T.R. Droop[3] and C.M.B. Henderson[3]

1. Department of General Science, Faculty of Science, Srinakharinwirot University, Sukhumvit 23, Watthana, Bangkok 10110, Thailand. Email: seriwat@hotmail.com

2. Department of Agricultural and Environmental Science, Faculty of Agriculture and Biological Sciences, University of Newcastle, Newcastle upon Tyne NE1 7RU, UK

3. Department of Earth Science, University of Manchester, Manchester M13 9PL

ABSTRACT: Thai gem corundums fall into two discrete populations on the basis of their trace element fingerprinting. Sapphires are rich in Ga (up to 0.101 wt % Ga_2O_3) and poor in Cr (<0.053 wt% Cr_2O_3) whereas rubies are rich in Cr (up to 0.564 wt% Cr_2O_3) and poor in Ga (<0.009 wt% Ga_2O_3). The trace element study of corundums from well-characterized geological environments suggests that Thai sapphires crystallized from syenitic gneiss metasomatised by a highly evolved magma such as carbonatite. Rubies could have crystallized in a metamorphic environment probably in a pre-existing metamorphic rock with mafic composition.

Keywords: EPMA, LA-ICP-MS, ruby, sapphire, Thailand, trace element

Introduction

Trace element geochemistry has been used to distinguish natural from synthetic corundums (e.g. Stern and Hänni, 1982; Tang *et al.*, 1989; Muhlmeister *et al.*, 1998; Joseph *et al.*, 2000) and to differentiate rubies from different localities (e.g. Tang *et al.*, 1988; Osipowicz *et al.*, 1995; Sanchez *et al.*, 1997; Calligaro *et al.*, 1999). However Sutherland *et al.* (1998b) were able to classify corundums derived from basaltic terrains into a metamorphic suite and a basaltic suite by use of their trace element contents and their metamorphic and magmatic mineral inclusions (previously studied by Sutherland and Coenraads, 1996; Sutherland and Schwarz, 1997). This differs from the model of corundum genesis proposed by Guo *et al.* (1996) who focused only on sapphire genesis. The mineral inclusions in rubies also may yield information on their provenance and clarify the options possible for corundum origin (e.g. Sutthirat *et al.*, 2001). However more research on the metamorphic-related genesis of rubies and sapphires needs to be done. In the present study, the trace element 'fingerprints' of corundums from Thailand are compared with those of other corundums from well-characterized geological environments as one of the approaches that can be used to deduce their origin.

Transition group elements (V, Ni, Fe, Mn, Cr, and Ti) are expected to substitute in the structure of corundum and some of them are known to cause body colour. For example Cr

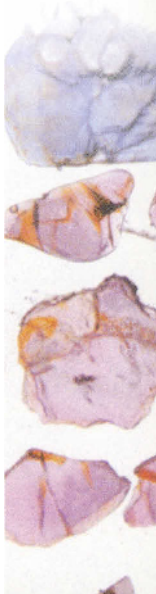

 ISSN: 1355–4565

is responsible for the red colour of ruby, Ti and Fe for the blue colour of sapphire (Nassau, 1983) and V, Cr, Ti and Fe for colour change sapphire (purple-red colour under incandescent light, blue-green colour under fluorescent light) (Schmetzer and Bank, 1980). Gallium is akin to Al and it uses the Al as a camouflage due to the closeness of their atomic radii (0.620 Å for Ga^{VI} and 0.535 Å for Al^{VI}) and charge, 3+ (Frye, 1974, 39-40; Krauskopf and Bird, 1995, 542-545). To determine the presence and quantity of other trace elements, laser ablation inductively coupled plasma mass spectrometry (LA-ICP-MS) was used (Pearce *et al.*, 1992). This gives an identification of all elements between Li and Pb in the periodic table, with only a few exceptions. On the basis of exploratory results obtained using LA-ICP-MS, the following elements were sought using the

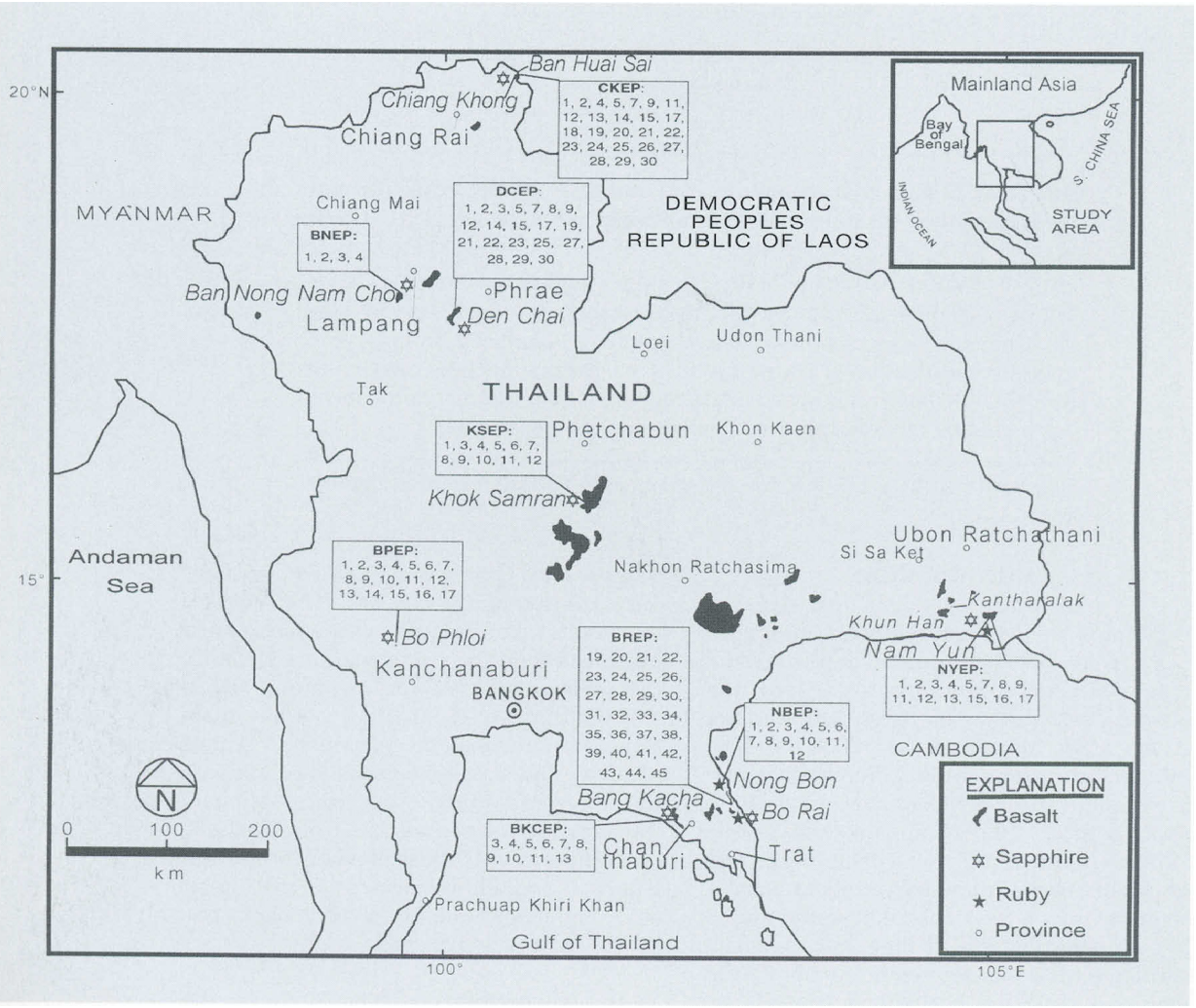

Figure 1: *Map of Thailand showing the localities of corundum samples (rubies and sapphires) and the distribution of basalts (modified from Vichit, 1992). The sample numbers are given in boxes.*

electron microprobe. Lanthanum (radius of La^{3+} = 1.032 Å for La^{VI}) and yttrium (radius of Y^{3+} = 0.900 Å for Y^{VI}) were investigated as possible substitutes for Al. Sn, Ta, Nb, W and Cu were examined in order to confirm unexpected high values indicated for some samples by LA-ICP-MS. Although Si prefers to substitute for Al in minerals with IV co-ordinated sites, VI co-ordinated Si is possible, and thus it was analysed for experimentally in corundum in this work. Moreover Si may be controlled by the presence of divalent cations, e.g. Fe^{2+} and Mg (Schmetzer and Bank, 1980).

Samples

The corundum samples from Thailand and Ban Huai Sai, in the Democratic People's Republic of Laos, were purchased from, or donated by, mine operators at the localities shown in *Figure 1*. They consist of rubies

Table 1: *Corundum samples from outside Thailand.*

Corundum variety	*Host rock composition*	*Rock type/main mineralogy*	*Locality*	*Reference*	*Field Nos (Fig. 4)*
sapphire (grey)	Al-rich 'diorite'	pegmatitic plumasite	? Natal, S. Africa	DuToit, 1918	1
sapphire (blue)	Al-rich pelite (restite)	corundum mullite buchite	Mull, Scotland	Thomas, 1922; Brearley, 1986; Schairer and Yagi, 1952	2
ruby (purple)	Al-rich pelite (restite)	corundum plagioclase hornfels	Bushveld, S. Africa	Willemse and Viljoen, 1970	
ruby (purple)	ultramafic	actinolite – gneiss	S. India (Kodaikanal)	–	3
sapphire (grey)	syenitic	syenite gneiss	Bancroft, Ontario, Canada	Moyd, 1949	4
sapphire (blue)	'normal pelitic'	corundum – biotite – hornfels	Loch Awe, Etive, Scotland	Droop and Treloar, 1981, Moazzen, 1999	5
sapphire (colourless in thin section)	'normal pelitic'	corundum – sillimanite – cordierite – hornfels	Belhelvie, Scotland	Droop and Charnley, 1985	
ruby (pink)	'normal pelitic'	corundum – staurolite – muscovite – schist	Stoer, NW. Scotland	Cartwright and Barnicoat, 1986	
sapphire (colourless in thin section)	Al, Mg rich pelitic (? restitic)	corundum cordierite gneiss	Baffin Island, Canada	–	6
ruby (purple)	Al, Mg – rich pelitic (? restitic)	corundum – biotite schist	Limpopo Belt, Zimbabwe	Droop, 1989	

Corundum variety	*Host rock composition*	*Rock type/main mineralogy*	*Locality*	*Reference*	*Field Nos (Fig. 4)*
sapphire (colourless in thin section)	Al, Mg – rich pelitic (? restitic)	garnet – sapphirine – granulite	Limpopo Belt, Zimbabwe	Droop, 1989; Horrocks, 1983	6
sapphire (colourless in thin section)	bauxitic	chloritoid – corundum – rock	Cape Emerion, Naxos, Greece	Feenstra, 1985	7
sapphire (colourless in thin section)	bauxitic	spinel – biotite – plagioclase granulite	Limpopo Belt, Zimbabwe	Droop, 1989	
sapphire (colourless in thin section)	Al – rich pelite (restite)	corundum – spinel – hornfels (emery)	Sithean Sluain, Scotland	Smith, 1969	
ruby (purple)	calcareous	corundum – marble	Mong Hsu, Myanmar	Peretti *et al.*, 1995; 1996	8
ruby (purple)	marly (Al, Ca, Si – rich)	corundum – zoisite rock	Tanzania	Game, 1954; Dirlam, *et al.*, 1992	
sapphire (blue)	unknown origin		Vietnam		
sapphire (blue)	unknown origin		Nigeria, Africa		
ruby (purple)	unknown origin		North Vietnam		
ruby (purple)	unknown origin		Africa		

Notes: A Igneous corundums fall in Field 1.

B Corundums in pelite xenoliths less than 10 cm across in mafic magma fall in Field 2.

C Corundums in metamorphosed igneous rocks fall in Fields 3 and 4.

D Corundums in metamorphosed sedimentary rocks fall in Fields 5, 6, 7 and 8.

E Corundums from unknown origin.

The data for mineral assemblages, sample numbers and geological setting for each rock are available from the author.

(red, pink and purple) and sapphires (blue, green, yellow, brown and black varieties and varieties with chatoyancy and asterism). The average diameter of the samples is *ca.* 5 mm.

Corundum samples from well-characterized geological environments elsewhere in the world were chosen to compare with Thai corundum samples. Eight types of host-rock composition ranging from igneous rock (pegmatitic plumasite), pelite xenoliths in dolerite and gabbro, and metamorphosed igneous rocks to metasedimentary rocks were studied. The descriptions of these rocks are presented in *Table I*.

Methods and techniques

Several techniques have been used to obtain trace-element concentrations in corundum: energy dispersive X-ray fluorescence (ED-XRF), proton-induced X-ray emission (PIXE) and neutron activation analysis (NAA) (e.g. Stern and Hänni, 1982; Tang *et al.*, 1989; Muhlmeister *et al.*, 1998). However laser ablation – inductively coupled plasma – mass spectroscopy (LA-ICP-MS) and electron probe microanalysis – wavelength dispersive spectrometry (EPMA-WDS) have been employed in this work as they have relatively low detection limits, easy sample preparation and are suitable for a large number of samples.

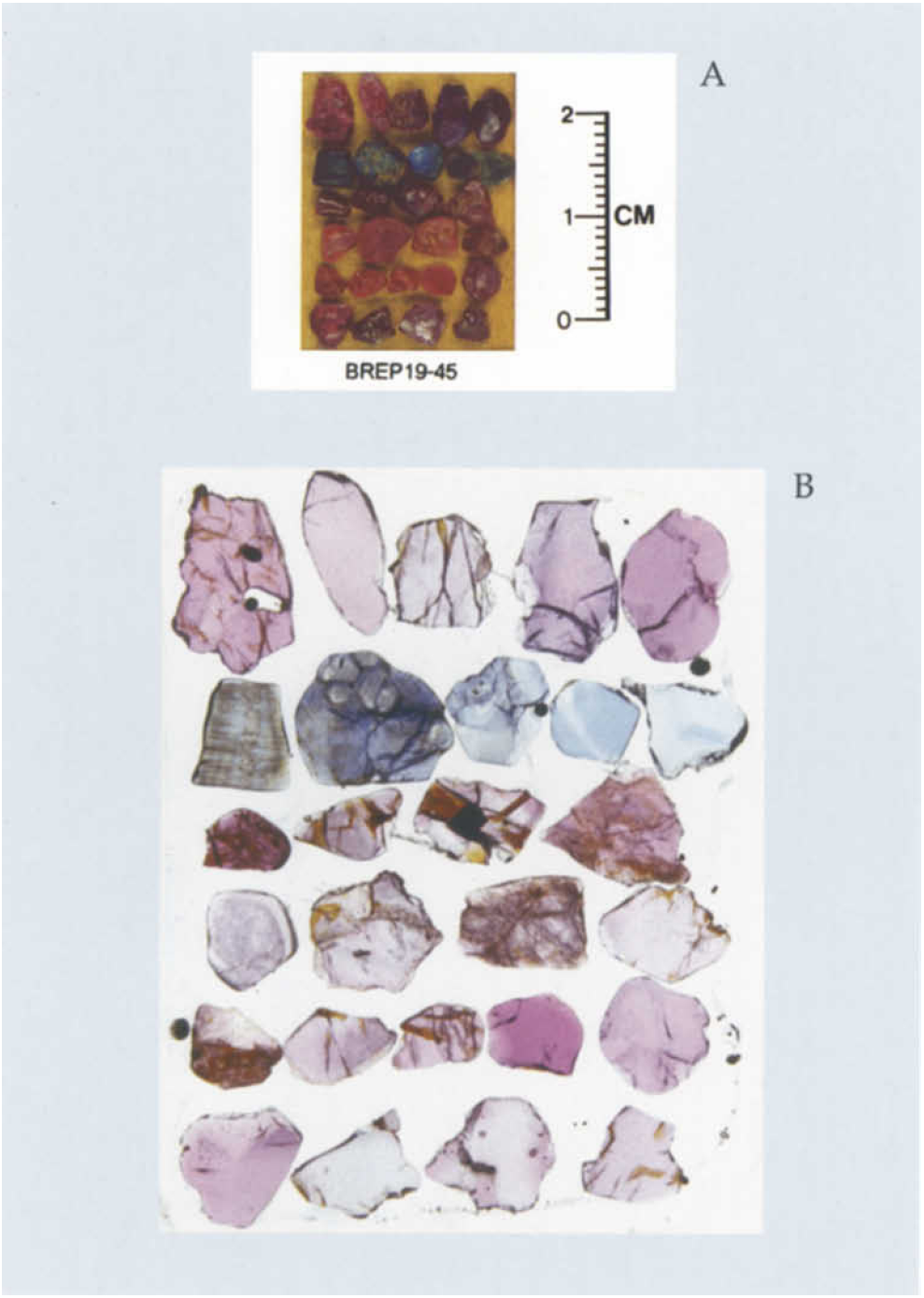

Figure 2: *(A) Corundum samples from Bo Rai, Thailand (sample numbers BREP 19-45, from left to right and top to bottom), being prepared to cut and polish and turn into the polished section as in (B).*

Table II: *Range of trace element concentrations (wt%) in corundum samples from Thailand and the Democratic People's Republic of Laos.*

Locality (prefix)	*Ban Huai Sai (CKEP)*	*Ban Nong Nam Cho (BNEP)*	*Den Chai (DCEP)*	*Bo Phloi (BPEP*	*Khok Samran (KSEP)*	*Bang Kacha (BKCEP)*	*Nam Yun (NYEP*	*Bo Rai (BREP*	*Bo Rai (BREP)*	*Nong Bon (NBEP)*	*Mean detection limit*
variety	sapphire								ruby		
V_2O_5	bdl-0.014	0.001-0.008	bdl-0.013	bdl-0.032	bdl-0.004	bdl-0.007	bdl-0.006	bdl-0.004	bdl-0.011	0.002-0.007	0.0026
Ga_2O_3	0.013-0.101	0.007-0.017	0.015-0.040	0.011-0.030	0.011-0.019	0.014-0.034	0.020-0.047	0.018-0.034	bdl-0.009	0.002-0.007	0.0019
Fe_2O_3	0.296-1.458	0.478-1.114	0.300-1.966	0.302-0.931	1.367-1.833	0.705-3.334	0.795-1.684	0.559-1.195	0.349-0.882	0.360-0.692	0.0047
MnO	bdl-0.001	bdl	bdl	bdl-0.001	bdl-0.003	bdl-0.007	bdl	bdl	bdl-0.004	bdl-0.003	0.0043
Cr_2O_3	bdl-0.042	bdl-0.011	bdl-0.018	bdl-0.053	bdl-0.007	bdl-0.007	bdl-0.010	bdl-0.003	0.086-0.564	0.028-0.355	0.0047
La_2O_3	bdl-0.003	bdl-0.003	bdl-0.002	bdl-0.003	bdl-0.002	bdl-0.005	bdl-0.003	bdl-0.002	bdl-0.002	bdl-0.004	0.0016
TiO_2	0.002-0.554	0.022-0.067	0.007-0.242	0.003-0.264	0.008-0.182	0.003-0.375	0.004-0.037	0.009-0.089	0.007-0.073	0.017-0.062	0.0003
SnO_2	bdl-0.075	bdl-0.001	bdl-0.004	bdl-0.004	bdl-0.004	bdl-0.005	bdl-0.003	bdl-0.001	bdl-0.005	bdl-0.003	0.0033
SiO_2	bdl-0.009	bdl-0.003	bdl-0.013	bdl-0.007	bdl-0.002	bdl	bdl-0.007	bdl-0.024	0.002-0.049	bdl-0.024	0.0059
Y_2O_3	bdl-0.005	bdl-0.004	bdl-0.004	bdl-0.004	bdl-0.001	bdl-0.004	bdl-0.004	bdl-0.001	bdl-0.007	bdl-0.006	0.0112
Ta_2O_5	bdl -0.271	na	na	bdl-0.006	na	na	na	na	na	na	0.0018
Nb_2O_5	bdl-0.382	na	na	bdl-0.003	na	na	na	na	na	na	0.0012
WO_3	bdl-0.023	na	na	bdl-0.093	na	na	na	na	na	na	0.0103
CuO	bdl-0.004	na	na	bdl-0.006	na	na	na	na	na	na	0.0037

Notes: The shaded cells contain the maximum values; na = not analysed; bdl = below detection limit; NiO was sought but not detected.

Table III: *Range of trace element concentrations (wt%) in corundum samples outside Thailand.*

Field Nos. (Fig. 4)	*1*	*2*	*3*	*4*	*5*	*6*	*7*	*8*	*9*	*10*
Locality (Sample No.)	Natal (Δ1556)	Mull (SVI/1) Bushveld (18058)	S. India (Δ793)	Bancroft (BC21)	Etive (MM125A) Behelvie (Δ1192) Stoer (Δ16136)	Baffin (Δ440) Limpopo (BB14A) Limpopo (BB29F)	Naxos (Δ577) Limpopo (BB19) Sithean Sluain (Δ1378)	Mong Hsu (TYEP, MSEP) Tanzania (CRM/ZOI-1)	Vietnam (VNEP) Nigeria (NAEP)	N. Vietnam (NVEP) Africa (AFEP)
variety*	sapphire	sapphire/ ruby	ruby	sapphire	sapphire/ CL/ruby	CL/ruby/CL	CL/CL/CL	ruby/ruby	sapphire/ sapphire	ruby/ruby
V_2O_5	bdl-0.005	0.046-0.196	0.002-0.004	bdl-0.002	0.001-0.046	0.002-0.009	bdl-0.045	bdl-0.102	0.001-0.012	bdl-0.047
Ga_2O_3	0.017-0.024	0.006-0.015	bdl-0.004	0.006-0.014	0.004-0.033	0.002-0.013	bdl-0.016	bdl-0.015	0.023-0.054	0.001-0.006
Fe_2O_3	1.191-1.467	0.150-0.451	0.497-0.521	0.209-0.354	0.098-0.257	0.129-0.653	0.383-4.895	bdl-0.216	0.247-1.431	0.001-0.281
MnO	bdl	bdl-0.001	bdl-0.001	bdl	bdl-0.004	bdl-0.001	bdl	bdl-0.001	bdl	bdl
Cr_2O_3	0.001-0.003	0.089-0.674	1.252-1.466	bdl-0.004	0.007-0.196	bdl-0.037	0.002-0.279	0.332-1.700	bdl-0.004	0.311-1.218
La_2O_3	bdl-0.002	bdl-0.002	bdl-0.000	bdl-0.004	bdl-0.003	bdl-0.002	bdl-0.004	bdl-0.003	bdl-0.002	bdl-0.001
TiO_2	0.007-0.043	0.095-0.600	0.005-0.007	0.002-0.060	0.005-0.915	0.007-0.030	0.004-0.469	0.003-0.502	0.008-0.047	0.009-0.188
SnO_2	bdl-0.004	0.000-0.004	bdl-0.001	bdl-0.003	bdl-0.003	bdl-0.005	bdl-0.004	bdl-0.003	bdl-0.002	bdl-0.001
SiO_2	bdl-0.097	bdl-0.040	bdl	bdl	bdl-0.098	bdl-0.053	bdl-0.256	bdl-0.044	bdl-0.016	bdl
Y_2O_3	bdl-0.325	bdl-0.006	bdl-0.397	bdl-0.001	bdl-0.006	bdl-0.003	bdl-0.009	bdl-0.003	bdl-0.004	bdl-0.004

* Purple and pink colours are called ruby for the purposes of this study and the other colours are called sapphires. CL = Colourless in thin section.
The shaded cells contain the maximum values. bdl = below detection limit; NiO was sought but not detected.

Analyses of minerals using LA-ICP-MS were made from a range of mineral groups using samples prepared in a variety of ways (see Jackson *et al.*, 1992; Pearce *et al.*, 1992; Jeffries *et al.*, 1995; Christensen *et al.*, 1995; Sylvester and Ghaderi, 1997). At this stage results were qualitative.

For EPMA investigation, single grains of corundum were hand-picked on the basis of colour, low abundance of cracks, and minimum degree of weathering and staining. The grains were placed, in an array, on a piece of adhesive tape in order to be able to recognize them (*Figure 2a*). They were then embedded in epoxy resin, cut, polished and made into sections without a cover glass as shown for example in *Figure 2b*. The sections are approximately 100 µm thick due to the high hardness of corundum. The samples of corundum-bearing rocks from outside Thailand were cut and polished in the standard way to a thickness of about 30 µm. All sections before analysis were coated with carbon by the carbon-arc technique to provide a conducting path for the probe current and thus prevent build-up of charge (Reed, 1996; Reed, 1997).

The polished sections were analysed with the CAMECA SX-100 electron microprobe at the Department of Earth Sciences, University of Manchester. Clean areas in the samples, without visible inclusions, were chosen for analysis. The computer software, SXRAY, was set to automatically run the machine under the 'trace analysis programme' (without collecting the count rates of Al and O) for collecting the count rates of 15 trace elements (V, Ni, Ga, Fe, Mn, Cr, La, Ti, Sn, Si, Y, Ta, Nb, W and Cu).

Five spectrometers were used to collect the counts; the details of the crystals and standards used are available from the senior author. The run time for one analysis was 12 minutes. The 'trace analysis programme' (assuming Al = 52.4 wt% and O = 46.6 wt%) was used at 30 kV and 60 nA (at 25 kV and 200 nA for repeat analysis of samples from CKEP and BPEP) to optimize count rates for trace elements. Altogether, 491 analyses were collected (307 analyses from Thai-Laos corundum samples and 184 analyses from world corundum samples).

Results

Although the LA-ICP-MS method requires further refinement to produce accurate results, it is still useful for screening a wide range of elements within a short time. In this study Ta, Nb, W and Cu have been found in samples from Ban Huai Sai (CKEP) and Bo Phloi (BPEP) by using LA-ICP-MS and the EPMA has been used to verify their presence and abundance. The only trace element results presented here are results obtained from the EPMA analysis.

Compositions to three decimal places are given in *Tables II* and *III* and some oxides and ratios are plotted in the diagrams of *Figures 3* and *4*. Note that the limit of detection (*Table II*, column 12) is the concentration of background at $x+3\sigma$ of its signal distribution (Potts, 1987, 16; Walsh, 1997). All analysed elements are described below (the results of the corundum samples from Ban Huai Sai are grouped with the Thai corundum samples).

Vanadium

Thai corundum samples have vanadium contents of less than 0.032 wt% V_2O_5 and in most samples, the element is below the limit of detection (0.0026 wt% of V_2O_5), bdl in *Table II*. The highest value (0.032 wt%) belongs to a violet sample from Bo Phloi.

Corundum samples from outside Thailand have higher contents of vanadium than the Thai samples, ranging between 0.001 and ca 0.200 wt% V_2O_5. Of these, the Al-rich restite pelitic xenoliths from Mull and Bushveld have corundums with relatively high vanadium contents and the highest value (0.196 wt%) is from the Bushveld sample.

Nickel and manganese

Nickel contents in corundum were beneath the limit of detection. Manganese contents are also very low but above the detection limit (0.001%) in 17 samples. However, of these, only two analyses show significant MnO concentrations: BKCEP9, 0.0070 wt% and BREP22, 0.0044 wt%.

Gallium

Gallium, like titanium and iron, is present in almost all samples. The plots of Ga_2O_3 contents for Thai corundum samples show a bimodal distribution (*Figure 3*). Most ruby samples (in purple, red and pink) contain Ga_2O_3 between 0.001 and 0.010 wt%. Most sapphire samples (in blue, green, yellow and brown) contain Ga_2O_3 between 0.010 and 0.100 wt%.

The corundum samples from outside Thailand contain Ga_2O_3 from 0.001 to 0.054 wt%. A sample from an unknown geological origin from Vietnam (VNEP) contains the highest Ga_2O_3 (0.054 wt%).

Iron

Thai corundum samples contain relatively high iron contents compared to the samples from other parts of the world. The Fe_2O_3 contents of most Thai corundum samples fall in a range between *ca.* 0.300 and 3.000 wt%, rather narrower than that found for samples from outside Thailand. The sample BKCEP9 contains the highest value (3.334 wt% of Fe_2O_3) beyond the major range. The Fe_2O_3 values of the samples with high iron contents (BKCEP and NYEP) match those of the igneous corundum sample from Natal (Δ1556).

The Fe_2O_3 contents of corundum samples from outside Thailand lie mainly in the range 0.100 to 2.000 wt%. Exceptionally, the restitic emery samples from Sithean Sluain (Δ1378) have high values of Fe_2O_3, including the highest value found (4.895 wt%). In contrast, ruby samples from marble at Mong Hsu (TYEP, MSEP) and from an unknown geological origin in North Vietnam (NVEP) have very low iron contents (less than 0.010 wt%).

Chromium

Chromium contents in the corundum samples from Thailand show a bimodal distribution in the graph, like gallium (*Figure 3*). The ruby samples have Cr_2O_3 values between 0.028 and 0.564 wt%, while the sapphire samples have lower values of Cr_2O_3 from 0.053 wt% down to below the limit of detection (0.0047 wt%).

In corundums from outside Thailand Cr_2O_3 contents are up to 1.700 wt%. The highest value belongs to a sample from Mong Hsu (MSEP4), while the Cr_2O_3 contents of the igneous corundum from Natal (Δ1556), the corundum in the meta-syenite-gneiss from Bancroft (BC21), and the corundums of unknown geological origin from Vietnam (VNEP) and Nigeria (NAEP) are below the limit of detection (0.0047 wt%).

Lanthanum

Thai corundum samples contain very low concentrations of lanthanum compared to V, Ga, Fe, Cr and Ti. In most samples, La could not be detected (limit of detection 0.0016 wt% La_2O_3). Sample BKCEP9 contains the highest La_2O_3 (0.0053 wt%).

In corundum samples from outside Thailand, the highest La_2O_3 content is 0.004 wt% in metabauxite from Naxos, 577, but in most samples La_2O_3 was below the limit of detection (0.0016 wt%).

Titanium

The limit of detection for TiO_2 is 0.0003 wt% (*Table II*) which is low compared with the limits for other elements analysed in this study. Thai ruby samples have TiO_2 contents mainly between 0.007 and 0.073 wt%, but in Thai sapphires, there is a wider range from 0.003 to 0.554 wt% with those from Ban Huai Sai (CKEP) at the upper end of this range.

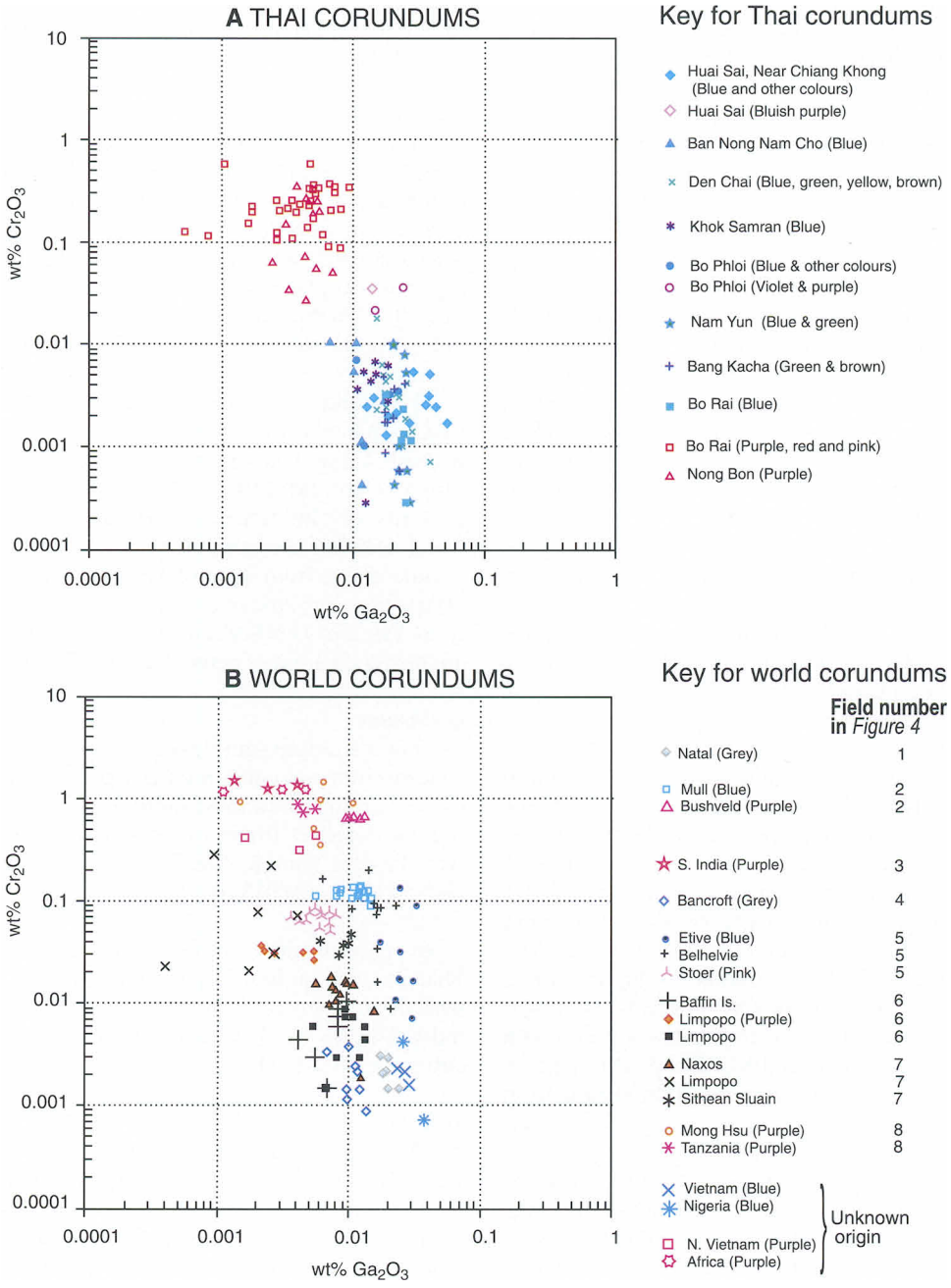

Figure 3: *Plots of wt% of Cr_2O_3 against Ga_2O_3 for Thai corundum and corundum outside Thailand. Thai corundum (A) shows two discrete populations compared to the corundum outside Thailand (B).*

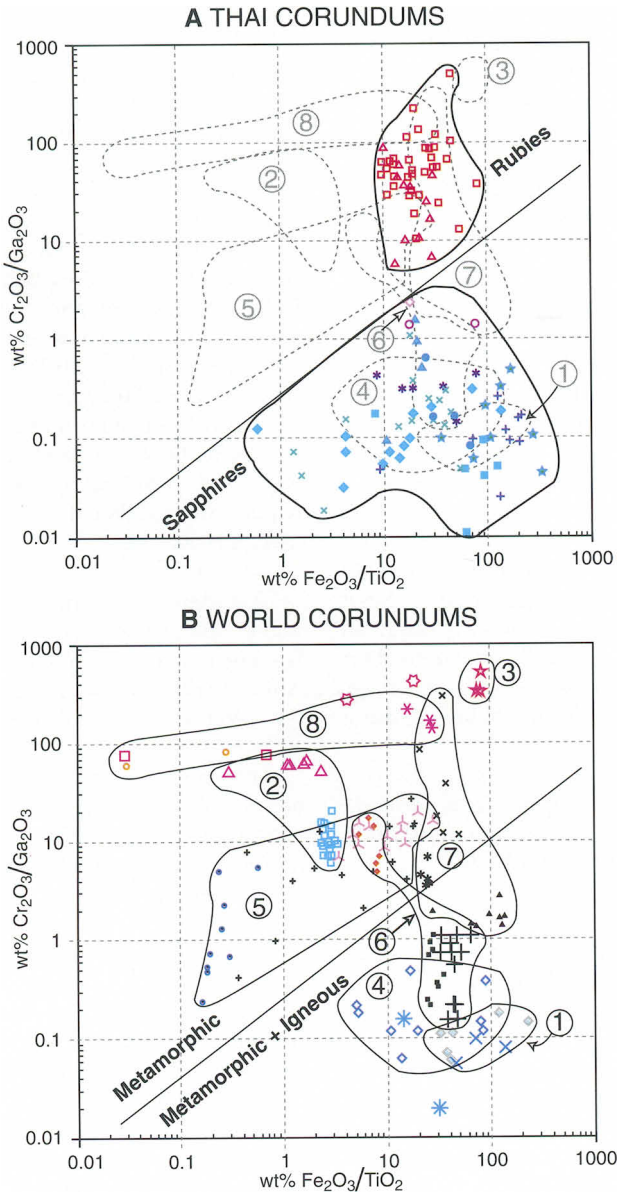

Figure 4: *(A) Plot of wt% Cr_2O_3/Ga_2O_3 against wt% Fe_2O_3/TiO_2 in Thai corundums for comparison with the well-characterized origins of the world corundums in B. Thai corundums can be considered as two groups: group I), rubies with high Cr and low Ga contents and group II), sapphires of all colours other than red with high Ga and low Cr contents. (B) Plot of similar ratios for the world corundums separated into 8 groups on geological criteria.*

Note: Key for **Figure 4** is the same as in **Figure 3**.

Titanium in the corundum samples from outside Thailand shows a wide range with the highest value of TiO_2 (0.915 wt%) in a pelitic hornfels from Etive (MM125A) and the lowest value (0.002 wt%) in a meta-syenitic corundum from Bancroft. Note that the wide range of TiO_2 in the samples is probably due to patchy rutile inclusions.

Tin

Tin is one of the granitophile metals (Sn, Nb, Ta, W, Be, Li) derived from crustal sources (Smirnov, 1968). The limit of detection of this element can be relatively high (min. 0.0025, max. 0.0317 wt% SnO_2) compared to those of the other elements. A blue sapphire sample from Ban Huai Sai contains the highest value of SnO_2 (0.075 wt%) and other samples from this locality have relatively high Sn contents. Most samples from Ban Huai Sai have high Sn contents, which are generally above the limit of detection (Min. = 0.025 wt% of SnO_2). This agrees with the results obtained using the LA-ICP-MS.

The corundum samples from outside Thailand show very low concentrations of tin and in most SnO_2 was not detected.

Silicon

Like tin, silicon has a very high detection limit and there is low precision in measurements of background.

In Thai corundum, silicon is more abundant in ruby than in sapphire. Moreover most SiO_2 values in the rubies are higher than the limit of detection and the highest is in sample BREP37 (0.049 wt%).

In most corundum samples from outside Thailand, SiO_2 is below the limit of detection (0.0059 wt%). A sample in a meta-bauxite from Naxos (577) has an anomalously high SiO_2 value of 0.256 wt%.

Yttrium

All values of Y_2O_3 for Thai corundum samples are lower than the mean of the limit of detection. The results of the samples from outside Thailand are also lower than the limit of detection except for the igneous corundum in plumasite from Natal (sample 1556) which shows the highest Y_2O_3 value (0.325 wt%).

Tantalum niobium, tungsten and copper

Four elements were measured in samples from two Thai localities: Ban Huai Sai and Bo Phloi. The tantalum and niobium contents in samples from Ban Huai Sai are highest (up to 0.271 wt% of Ta_2O_5; 0.382 wt% of Nb_2O_3), whereas in samples from Bo Phloi both are very low. The maximum values of Ta_2O_5 and Nb_2O_5 in Bo Phloi samples are only 0.006 wt% and 0.003 wt% respectively. These results are consistent with those obtained using LA-ICP-MS.

Tungsten in sapphires from Bo Phloi is higher than in the samples from Ban Huai Sai. The maximum value in Bo Phloi samples is 0.093 wt% of WO_3, compared with 0.023 wt% WO_3 in the sample from Ban Huai Sai.

The copper contents are low with most below the limit of detection. The maximum values found were 0.004 wt% and 0.006 wt% of CuO in the samples from Ban Huai Sai and Bo Phloi respectively.

Discussion

Several models for the origin of the corundum in basaltic terrains have been generated. Most models involve plutonic crystallization from melt, although regional metamorphism of Al-rich rocks subducted below the continental crust has been proposed by Levinson and Cook (1994). In the Thailand context, this model has the weakness that the subduction zone (Sunda trench, west of Myanmar and Indonesia) is too far away (>1000 km) from the basalt outcrops. Corundum-bearing basalts also occur in Cambodia, Viet Nam and China, having a similar age range (Cenozoic) to that in Thailand (e.g. Barr and Macdonald, 1981). They do not seem to be related to a subduction zone. Several models invoke

alkaline Si- and Al-rich melts, either evolved from basaltic magmas (Coenraads *et al.*, 1990; Coenraads, 1992a) or derived from melting of amphibolitised mantle (Sutherland, 1996). A more complex melt origin was proposed by Guo *et al.* (1996), who claimed that mineral inclusions in the corundums reflect the reaction between Si-rich and carbonatitic magmas under relatively low temperatures around 400°C at mid-crustal levels around a depth of 10-20 km. Although this model is consistent with the origin of sapphires, it does not clearly account for rubies. Sutherland *et al.* (1998a) proposed the means of generating basaltic-type gem corundum and favoured melting of mantle source-rocks containing amphibole at depths of 35–40 km near the crust-mantle boundary; such melting could produce a final Si- and Al-rich rock with over 5 wt% corundum. Moreover the different metamorphic or pegmatitic sources and assemblages (e.g. corundum-sapphirine-spinel assemblage) must exist under basaltic regions. Using trace-element and inclusion approaches, Sutherland *et al.* (1998b) and Sutherland (1998) classify corundum in basaltic terrains into metamorphic corundum (including ruby) and basaltic-type (including blue, green, yellow, brown, white, grey, opaque and black corundums).

The trace element variation diagram using data from this study (*Figure 3, A*) shows that Thai corundums have a bimodal distribution based on the Cr and Ga contents. The purple and pink ruby samples (simply called rubies) contain high chromium (up to 0.57 wt% Cr_2O_3 but low gallium (<0.01 wt% Ga_2O_3). The samples with blue, green, brown and violet colours (simply called sapphires) contain high gallium (up to 0.10 wt% Ga_2O_3) but low chromium (<0.05 wt% Cr_2O_3). This evidence agrees well with the results obtained by Sutherland *et al.* (1998b) who designated the ruby group as having a metamorphic origin and the sapphire group as having an igneous origin. Thus although both sapphire and ruby occur together in the same deposits in Thailand, their origins are most probably different.

Sapphire genesis

Both Ga and Cr substitute readily for Al in corundum, which can be explained by the simple rules of similar ionic charge and radius (Ga^{3+} = 0.620 Å, Cr^{3+} = 0.615 Å and Al^{3+} = 0.535 Å; 6-coordinate). Moreover Ga has chemical properties similar to Al and it is always present with Al. Ga is enriched in felsic and intermediate rocks, whereas Cr is enriched in ultramafic and mafic rocks (Krauskopf and Bird, 1995, 542-5).

Figure 4A shows the plots of Thai sapphire samples superimposed on the fields of corundums in syenitic gneiss from Bancroft (field 4), in pegmatitic plumasite from Natal (field 1), in Al, Mg-pelite from Baffin Island and Limpopo (part of field 6). A high-grade metamorphic rock consisting of corundum, sillimanite, minor zircon and a trace of hercynite and found in alluvium of a corundum mine in Bo Phloi is believed to be derived from the same source as the corundums brought to the Earth's surface by alkali basalt (Pisutha-Arnond *et al.*, 1999). Hercynite is also found as inclusions in sapphires from this locality (Saminpanya, 2000, 216-7). On this basis, the crystallization of sapphires from Thailand in magma of pegmatitic plumasite or directly from an alkali basalt magma will be ruled out. An origin related to metamorphism is more likely.

However the study of fluid inclusions in sapphires from Bo Phloi (Srithai and Rankin, 1999) suggested a magmatic source. Moreover the U-Pb dating of zircon inclusions in sapphires from New South Wales and a zircon associated with sapphire from Chanthaburi (Coenraads *et al.*, 1990; Coenraads *et al.*, 1995) suggested that sapphires have a genetic link to alkali basalt. Guo *et al.* (1996) suggested that at the high temperatures of basaltic magmas, the U-Pb in zircons can be reset within the time of the magma's eruption and cooling due to Pb diffusion so that the results could then give the same age as the basalt and not the true age of sapphire. Other circumstantial

evidence includes: failed experimental attempts to grow corundum from a corundum-bearing basaltic composition under different pressure, temperature and hydrous conditions have been reported (e.g. Green *et al.*, 1978); and surface features of sapphires (e.g. Coenraads, 1992a, 1992b; Krzemnicki *et al.*, 1996; Saminpanya, 2000, 116-22) indicate that the sapphires were not in equilibrium with the magma of basalt host rock. These factors suggest that sapphires crystallized elsewhere and that the alkali basaltic magma picked them up and carried them to the Earth's surface.

In *Figure 4*, the Thai sapphire data lie mostly in the field of the syenitic gneiss from Bancroft. The pre-existing rock of the corundum-bearing syenitic gneiss from Bancroft is a dark paragneiss of the Precambrian Grenville series (Gummer, 1946). According to Gummer (1946) and Moyd (1949), metasomatic alteration converted the dark paragneiss, into a nepheline-corundum syenitic gneiss. By analogy to the syenitic gneiss of Bancroft, Thai sapphires could have originated from Precambrian paragneiss that experienced metasomatism by emanations from felsic magma (enriched in gallium and incompatible elements) or carbonatite (enriched in Nb-Ta) at deep levels beneath Thailand. Note that the main source of Nb-Ta is granitic pegmatites, carbonatite or peralkaline granite (Möller *et al.*, 1989). In this case a carbonatite magma might have intruded the gneiss source rock to form fenite (syenitic composition). In addition to Bancroft, another corundum-bearing fenite has been reported from the Khibina alkaline complex, Russia (Barkov *et al.*, 1997; Barkov *et al.*, 2000). However, as Thai sapphires occur extensively throughout the country, any such process or processes will have to have been widespread and not necessarily limited to a single intrusive complex. The process introduced in this study is slightly different from that described by Guo *et al.* (1996) who said that the carbonatite reacted with the pegmatitic magma giving corundum-bearing lenses at mid-crustal levels.

The abundances of Ga, Ti and Fe, incompatible elements (e.g. Ta, Nb, Sn) and mineral inclusions in sapphires (zircon, alkali feldspar, nepheline and spinel) suggest that the sapphires formed in a highly evolved melt of peralkaline syenitic or granitic composition. This agrees well with the studies of some authors, e.g. Aspen *et al.*, (1990) and Upton *et al.* (1999), but it is different from those of Sutherland *et al.* (1998a) who maintain that sapphires crystallized when amphibole-bearing mantle underwent partial melting because of an advancing thermal aureole.

Nb, Ta and Sn could possibly have been carried to the country rocks by felsic or carbonatitic magma during a process in which the gneissic country rock was metamorphosed to the syenitic gneiss as in the Bancroft area. Nepheline ($Ne_{68.3}Ks_{28.6}Q_{3.0}$; n=4) is found as an inclusion in corundum from Bo Phloi (Saminpanya, 2000, 215). This is consistent with the sapphire originating in a nepheline-corundum syenitic gneiss. Nepheline coexisting with sapphire is also found in syenitic rock and nepheline-aegirine intrusive rock (urtite) in Mogok, Myanmar (Waltham, 1999).

The lower crust beneath Thailand is thought to be composed of Precambrian-metamorphic granulite-facies rocks (Bunopas, 1992). The data in *Figure 4B* show that the plots of Thai sapphires also overlap the field of corundum from Al- and Mg-rich pelites from Baffin Island, Canada and Limpopo, Zimbabwe. This suggests that the parent rocks could have been the Precambrian paragneiss of Thailand, which originated from the marine (flysch) sediments of a continental margin (of Gondwanaland) and were deeply buried and metamorphosed (Bunopas, 1992).

Ruby genesis

The ruby group, consisting of red, pink and purple corundum is confined to the areas of Bo Rai and Nong Bon. In *Figure 4*, their analyses lie in or close to field 7, corundum of bauxitic origin (e.g. BB19 from the Limpopo belt). Some analyses fall in the gap between field 8 (corundums in marble) and field 5 (corundums in normal pelitic rocks), and this suggests that Thai rubies probably crystallized in a different environment from these rocks. The inclusion suite in the rubies which includes garnet, sapphirine and fassaite pyroxene, also suggests that Thai rubies have a metamorphic origin (Sutthirat *et al.*, 2001).

In Thailand rubies are always found with sapphires. Sapphires are dominant in the localities in the western part of the country (Shan-Thai block) but rubies are dominant in the east (Indochina block). The proportional change from sapphire to ruby is apparent in the Chanthaburi and Trat areas (Vichit, 1992; Hughes, 1997, 427-43). This suggests that the source beneath Thailand which produced both rubies and sapphires was at the base of very thick continental crust or within the upper mantle. The fact that rubies are rich in chromium and poor in gallium suggests that they formed in pre-existing metamorphic rock with mafic composition. Sapphires are rich in Ga and high field strength elements and poor in Cr, and these features are consistent with their formation in syenitic metamorphic rocks by reaction with a highly evolved fractionated magma such as a carbonatitic magma. It is envisaged that such a magma might move from the mantle to deep in the crust where it reacted with the syenitic metamorphic rock. Cr is generally precipitated early in magmatic fractionation (Matzat and Shiraki, 1978) and so in highly fractionated magmas such as carbonatites and syenites is not available for reaction. In contrast, Ga is present in fractionated magmas and they and the host rocks could be the source of gallium in sapphires.

Conclusions

Thai sapphires contain high Ga, Ti and Fe and incompatible elements (e.g. Ta, Nb, Sn) whereas Thai rubies are rich in Cr but poor in those elements found in Thai sapphires. However both the rubies and the sapphires have metamorphic-related origins. Thai sapphires could have originated from Precambrian paragneiss that experienced metasomatism by emanations from felsic magma (enriched in Ga and incompatible elements) or carbonatite (enriched in Nb-Ta) at deep levels beneath Thailand. Thai rubies have a metamorphic origin and formed in a pre-existing metamorphic rock with mafic composition. It was at a later stage that alkali magmas penetrated the metamorphic rocks and carried sapphires and rubies to the surface to be erupted as basalts in many localities in Thailand.

Acknowledgements

The authors would like to thank Dave Plant and Dr Chris Hayward at the Department of Earth Sciences, University of Manchester for help with EPMA analysis of corundum samples and Paul Lythgoe for help with LA-ICP-MS analysis of corundum samples.

References

Aspen, P., Upton, B.G.J., and Dickin, A.P., 1990. Anorthoclase, sanidine and associated megacrysts in Scottish alkali basalts: high-pressure syenitic debris from upper mantle sources? *European Journal of Mineralogy*, **2**, 503-17

Barkov, A.Y., Laajoki, K.V.O., Men' Shikov, Y.P., Alapieti, T.T., and Sivonen, S.J., 1997. First terrestrial occurrence of titanium-rich pyrrhotite, marcasite and pyrite in a fenitized xenolith from the Khibina alkaline complex, Russia. *Canadian Mineralogist*, **35**(4), 875-85

Barkov, A.Y., Martin, R.F., Men' Shikov, Y.P., Savchenko, Y.E., Thibault, Y., and Laajoki, K.V.O., 2000. Edgarite, $FeNb_3S_6$, first natural niobium-rich sulfide from the Khibina alkaline complex, Russian Far North: evidence for chalcophile behaviour of Nb in a fenite. *Contributions to Mineralogy and Petrology*, **138**, 229-36

Barr, S.M., and Macdonald, A.S., 1981. Geochemistry and geochronology of late Cenozoic basalts of Southeast Asia. *Geol. Soc. Amer. Bull.*, **92** (Part 2), 1069-142

Brearley, A.J., 1986. An electron optical study of muscovite breakdown in pelitic xenoliths during pyrometamorphism. *Mineralogical Magazine*, **50**, 385-97

Bunopas, S., 1992. Regional stratigraphic correlation in Thailand. In: *Proceedings of the National Conference on 'Geologic Resources of Thailand: Potential for Future Development'*, C. Piencharoen (ed. in chief), Dept. Mineral Resources, Bangkok, Thailand, pp. 189-208

Calligaro, T., Poirot, J.-P., and Querré, G., 1999. Trace element fingerprinting of jewellery rubies by external beam PIXE. *Nuclear Instruments and Methods in Physics Research B*, **150**, 628-34

Cartwright, I., and Barnicoat, C., 1986. The generation of quartz-normative melts and corundum-bearing restites by crustal anatexis: petrogenetic modelling based on an example from the Lewisian of North-West Scotland. *Journal of Metamorphic Geology*, **3**, 79-99

Christensen, J.N., Halliday, A.N., Lee, D-C., and Hall, C.M., 1995. In situ Sr isotopic analysis by laser ablation. *Earth and Planetary Science Letters*, **136**, 79-85

Coenraads, R.R., 1992a. Sapphires and rubies associated with volcanic provinces: Inclusions and surface features shed new light on their origin. *Australian Gemmologist*, **18**(3), 70-8

Coenraads, R.R., 1992b. Surface features on natural rubies and sapphires derived from volcanic provinces. *Journal of Gemmology*, **23**(3), 151-60

Coenraads, R.R., Sutherland, F.L., and Kinny, P.D., 1990. The origin of sapphires: U-Pb dating of zircon inclusions sheds new light. *Mineralogical Magazine*, **54**, 113-22

Coenraads, R.R., Vichit, P., and Sutherland, F.L., 1995. An unusual sapphire-zircon-magnetite xenolith from the Chanthaburi Gem Province, Thailand. *Mineralogical Magazine*, **59**, 465-79

Dirlam, D.M., Misiorowski, E.B., Tozer, R., Stark, K.B., and Bassett, A.M., 1992. Gem wealth of Tanzania. *Gems & Gemology*, **28**(2), 80-102

Droop, G.T.R., and Charnley, N.R., 1985. Comparative geobarometry of pelitic hornfelses associated with the Newer Gabbros: a preliminary study. *Journal of Geological Society of London*, **142**, 53-62

Droop, G.T.R., and Treloar, P.J., 1981. Pressures of metamorphism in the thermal aureole of the Etive Granite Complex. *Scottish Journal of Geology*, **17**(2), 85-102

Droop, G.T.R., 1989. Reaction history of garnet-sapphirine granulites and conditions of Archaean high-pressure granulite-facies metamorphism in the Central Limpopo Mobile Belt, Zimbabwe. *Journal of Metamorphic Geology*, **7**, 383-403

Du Toit, A.L., 1918. Plumasite (corundum-aplite) and titaniferous magnetite rocks from Natal. *Transactions of Geological Society of South Africa*, **21**(53), 53-75

Feenstra, A., 1985. *Metamorphism of bauxites on Naxos, Greece*. Geologica Ultraiectina, Mededelingen van het Instituut voor Aardwetenschappen der Rijksuniversiteit te Utrecht, No. **39**, 206 pp

Frye, K., 1974. *Modern mineralogy*. Prentice-Hall, Inc., New Jersey, 325 pp

Game, P.M., 1954. Zoisite-amphibolite with corundum from Tanganyika. *Mineralogical Magazine*, **30**(226), 458-66

Green, T.H., Wass, S.Y., and Ferguson, J., 1978. Experimental study of corundum stability in basalts (abstract). *Abstr. Programme 3rd Aust. Geol. Conv., Townsville*, p. **34**

Gummer, W.K., and Burr, S.V., 1946. Nephelinized paragneisses in the Bancroft area, Ontario. *The Journal of Geology*, **54**(3), 137-68

Guo, J., O'Reilly, S.Y., and Griffin, W.L., 1996. Corundum from basaltic terrains: a mineral inclusion approach to the enigma. *Contributions to Mineralogy and Petrology*, **122**, 368-86

Horrocks, P.C., 1983. A corundum and sapphirine paragenesis from the Limpopo Mobile Belt, southern Africa. *Journal of Metamorphic Geology*, **1**, 13-23

Hughes, R.W., 1997. *Ruby and sapphire*. RWH Publishing, Boulder, 511 pp

Jackson, S.E., Longerich, H.P., Dunning, C.R., and Fryer, B.J., 1992. The application of laser ablation microprobe-inductively coupled plasma-mass spectrometry (LA-ICP-MS) to in-situ trace element determinations in minerals. *Canadian Mineralogist*, **30**, 1049-64

Jarvis, K.E., Gray, A.L., and Houk, R.F., 1992. *Handbook of inductively coupled plasma mass spectroscopy*. Blackie, Glasgow, 375 pp

Jeffries, T.E., Perkins, W.T., and Pearce, N.J.G., 1995. Measurements of trace elements in basalts and their phenocrysts by laser probe microanalysis inductively coupled plasma mass spectroscopy (LA-ICP-MS). *Chemical Geology*, **121**, 131-44

Joseph, D., Lal, M., Shinde, P.S., and Padalia, B.D., 2000. Characterization of gem stones (rubies and sapphires) by energy-dispersive X-ray fluorescence spectrometry. *X-Ray Spectrometry*, **29**, 147-50

Krauskopf, K., and Bird, D., 1995. *Introduction to geochemistry*. 3rd edn. McGraw-Hill, Inc. , New York, 647 pp

Krzemnicki, M.S., Hänni, H.A., Guggenheim, R., and Mathys, D., 1996. Investigations on sapphires from an alkali basalt, South West Rwanda. *Journal of Gemmology*, **25**(2), 90-106

Levinson, A.A., and Cook, F.A., 1994. Gem corundum in alkali basalt: Origin and occurrence. *Gems & Gemology*, **30**(4), 253-62

Matzat, E., and Shiraki, K., 1978. *Chromium. In*: Wedepohl, K.H. (ed.). Handbook of geochemistry vol II/3, Element Cr (24) to Br (35). Springer-Verlag, Berlin

Moazzen, M., 1999. *Contact metamorphic process in Etive aureole, Scotland*. PhD Thesis, Department of Earth Sciences, The University of Manchester. 392 pp

Möller, P., Cernỳ, P., and Saupé F. (ed.), 1989. *Lanthanides, tantalum, and niobium mineralogy, geochemistry, characteristics of primary ore deposits, prospecting, processing, and applications, Workshop Papers*. Springer-Verlag, Berlin, New York, 380 pp

Moyd, L., 1949. Petrology of nepheline and corundum rocks of Southeastern Ontario. *American Mineralogist*, **34**, 736-51

Muhlmeister, S., Fritsch, E., Shigley, J.E., Devouard, B., and Laurs, B.M., 1998. Separating natural and synthetic rubies on the basis of trace-element chemistry. *Gems & Gemology*, **34**(2), 80-101

Nassau, K., 1983. *The physics and chemistry of color: the fifteen causes of color*. John Wiley and Son, New York, 454 pp

Osipowicz, T., Tay, T.S, Orlic, I., Tang, S.M., and Watt, F., 1995. Nuclear microscopy of rubies: Trace elements and inclusions. *Nuclear Instruments and Methods in Physics Research B*, No. 104: 590-4

Pearce N.J.G., Perkins, W.T., Abell, I., Duller, G.A.T., and Fuge, R., 1992. Mineral microanalysis by laser ablation inductively coupled plasma mass spectrometry. *Journal of Analytical Atomic Spectrometry*, **7**, 53-7

Peretti, A., Mullis, J., and Mouawad, F., 1996. The role of fluorine in the formation of colour zoning in rubies from Mong Hsu, Myanmar (Burma). *Journal of Gemmology*, **25**(1), 3-19

Peretti, A., Schmetzer, K, Bernhardt, H-J., and Mouawad, F., 1995. Rubies from Mong Hsu. *Gems & Gemology*, **31**(1), 2-26

Pisutha-Arnond, V., Wathanakul, P., and Intasopa, S., 1999. New Evidences on the origin of Kanchanaburi Sapphire. *Symposium on Mineral, Energy, and Water Resources of Thailand: Towards the year 2000*. Bangkok, Thailand (abstract)

Potts, P.J., 1987. *A handbook of silicate rock analysis*. Blackie, London, 621 pp

Reed, S.J.B., 1996. *Electron microprobe analysis and scanning electron microscopy in geology*. Cambridge University Press, Cambridge, 201 pp

Reed, S.J.B., 1997. *Electron microprobe analysis*, 2nd ed. Cambridge University Press, Cambridge, 326 pp

Saminpanya, S., 2000. *Mineralogy and origin of gem corundum associated with basalt in Thailand*. PhD Thesis, Department of Earth Sciences, The University of Manchester, 395 pp

Sanchez, J.L., Osipowicz, T., Tang, S.M., Tay, T.S., and Winn, T.T., 1997. Micro-PIXE analysis of trace element concentration of natural rubies from different locations in Myanmar. *Nuclear Instruments and Methods in Physics Research B*, No. 130, 682-6

Schairer, J.F., and Yagi, K., 1952. The system FeO-Al_2O_3-SiO_2. *American Journal of Science*, Bowen Vol., 471-512

Schmetzer, K., and Bank, H., 1980. Explanations of the absorption spectra of natural and synthetic Fe- and Ti-containing corundums. *Neues Jahrbuch für Mineralogie, Abhandlungen*, **139**, 216-25

Smirnov, V.I., 1968. The sources of ore-forming fluids. *Economic Geology*, **63**, 380-9

Smith, D.G.W., 1969. Pyrometamorphism of phyllites by a dolerite plug. *Journal of Petrology*, **10**(1), 20-55

Srithai, B., and Rankin, A.H., 1999. Fluid inclusion characteristics of sapphires from Thailand. In: *Mineral deposits: Processes to Processsing*, Stanley, C.J., *et al.* (Eds), Balkema Press, Rotterdam, 107-10

Stern, W.B., and Hänni, H.A., 1982. Energy dispersive X-ray spectrometry: A non-destructive tool in gemmology. *Journal of Gemmology*, **18**(4), 285-96

Sutherland, F.L., 1996. Alkaline rocks and gemstones, Australia: a review and synthesis. *Australian Journal of Earth Sciences*, **43**, 323-43

Sutherland, F.L., 1998. Gem corundum origins from eruptive sources. In: *Abstract and Programme of 17th General Meeting*, International Mineralogical Association, August 9-14, Toronto, Canada. p. A13

Sutherland, F.L., and Coenraads, R.R., 1996. An unusual ruby-sapphire-sapphirine-spinel assemblage from the Tertiary Barrington volcanic province, New South Wales, Australia. *Mineralogical Magazine*, **60**, 623-38

Sutherland, F.L., Hoskin, P.W.O., Fanning C.M., and Coenraads, R.R., 1998a. Models of corundum origin from alkali basaltic terrains: a reappraisal. *Contributions to Mineralogy and Petrology*, **133**, 356-72

Sutherland, F.L., and Schwarz, D., 1997. Gem corundum from Australia and Southeast Asia. In: Johnson, M.L., and Koivula, J.I., Gem News. *Gems & Gemology*, **33**(4), 302

Sutherland, F.L., Schwarz, D., Jobbins, E.A., Coenraads, R.R., and Webb, G., 1998b. Distinctive gem corundum suites from discrete basalt fields: a comparative study of Barrington, Australia, and West Pailin, Cambodia, gemfields. *Journal of Gemmology*, **26**(2), 65-85

Sutthirat, C., Saminpanya, S., Droop, G.T.R., Henderson, C.M.B., and Manning, D.A.C., 2001. Clinopyroxene-corundum assemblages from alkali basalt and alluvium, eastern Thailand: constraints on the origin of Thai rubies. *Mineralogical Magazine*, **65**(2): 277-95

Sylvester, P.J., and Ghaderi, M., 1997. Trace element analysis of scheelite by excimer laser ablation - inductively coupled plasma spectrometry (ELA-ICP-MS) using a synthetic silicate glass standard. *Chemical Geology*, **141**, 49-65

Tang, S.M., Tang, S.H., Mok, K.F., Retty, A.T., and Tay, T.S., 1989. A study of natural and synthetic rubies by PIXE. *Applied Spectroscopy*, **43**(2), 219-23

Tang, S.M., Tang, S.H., Tay, T.S., and Retty, A.T., 1988. Analysis of Burmese and Thai rubies by PIXE. *Applied Spectroscopy*, **42**(1), 44-8

Thomas, H.H., 1922. On certain xenolithic Tertiary minor intrusions in the Island of Mull (Argyllshire). *The Quarterly Journal of the Geological Society of London*, **78**(311), 229-61

Upton, B.G.J., Hinton, R.W., Aspen, P., Finch, A., and Valley, J.W., 1999. Megacrysts and associated xenoliths: evidence for migration of geochemically enriched melts in the upper mantle beneath Scotland. *Journal of Petrology*, **40**(6), 935-56

Vichit, P., 1992. *Gemstones in Thailand*. National conference on 'Geologic resources of Thailand: Potential for future development', 17-24 November. Department of Mineral Resources, Bangkok, Thailand. 124-50

Walsh, J.N., 1997. Inductively coupled plasma-atomic emission spectrometry (ICP-AES). In: Gill, R. (ed.). *Modern analytical geochemistry*. Longman, Singapore, pp. 41-66

Waltham, T., 1999. The ruby mines of Mogok. *Geology Today*, **15**(4), 143-49

Willemse, J., and Viljoen, E.A., 1970. The fate of argillaceous material in the gabbroic magma of the Bushveld complex. *The Geological Society of South Africa*, Special Publication 1, Symposium on the Bushveld Igneous Complex and other Layered Intrusions, 336-66

International Jewellery LONDON 2003

31 August to 3 September
Earls Court 2, London

Seminar Programme

A full and varied programme of seminars at IJL 2003

Sunday 31 August

11:30 *Michael Hoare*, NAG. History and hysteria – drivers behind jewellery retail
13:00 *Matthew Hall*, GIA. Research update on diamond treatments
14:30 *Doug Garrod*, Gem-A. Everything included – internal features of gemstones
15:30 *Violet Bailey*. Recruiting staff for profit

Monday 1 September

11:30 *Vivienne Becker*. Directions and trends in jewellery design in 2004
13:00 *Matthew Hall*, GIA. Research update on coloured stone treatments
14:30 *Dr Christopher Corti*, World Gold Council. What is a white gold? – the consumer may be confused
15:30 *Violet Bailey*. Recruiting staff for profit

Tuesday 2 September

11:30 *Vicky Morrison*, Platinum Public Relations in association with NAG – Get yourself talked about
13:00 *Matthew Hall*, GIA. Research update on coloured stone treatments
15:00 *Richard Bailey and Nigel Lubbock,* legal advisors to the BJA. Money laundering Regulations 2003/Proceeds of Crime Act 2002 – *Risks for jewellery retailers*
16:00 Doug Garrod, Gem-A. Everything included – internal features of gemstones

Wednesday 3 September

10:30 *Carrie Soucy*, JCK Magazine. What women want – why fashion matters to jewellers
11:30 *Nine months on the Kimberley Process is embedded in the psyche*. But is it?
14:30 *Doug Garrod*, Gem-A. Everything included – internal features of gemstones
15:30 *Jennifer Bloy*, Jewellery Designer. The Goldsmiths Craft and Design Council Competition – How it has influenced my career

Visit the IJL website at www.jewellerylondon.com for further information on the fair.

Gem-A will again be exhibiting at the IJL. Visit us at Stand G28 adjacent to the Seminar Theatre

Caesium-rich morganite from Afghanistan and Madagascar

Prof. Dr H.A. Hänni FGA and Dr M.S. Krzemnicki FGA

SSEF Swiss Gemmological Institute, Basel, Switzerland

email: gemlab@ssef.ch

ABSTRACT: Quite saturated pink beryl of Madagascar and Afghanistan are described. They display densities between 2.91 and 3.10 g/cm^3 and RI values up to 1.608 (n_e) and 1.615 (n_o) which exceed the values reported so far in the literature. Chemical analyses reveal very high caesium concentrations (up to 15.18 wt.% Cs_2O). The incorporation of Cs in the structural channels of beryl is mainly coupled with a substitution on the tetradhedrally-coordinated beryllium site. Such stones belong to the so-called tetrahedral beryls. UV-Vis-NIR spectra show manganese and water absorption features typical for morganite. XRD data and Raman spectra reveal a distinct increase in cell parameters (mainly c_0) compared to pure beryl, thus underlining the unusual character of the studied material. While the sample from Afghanistan is semi-transparent, transparent stones are found among the samples from Madagascar. Inclusions consist mainly of fine tubes parallel to the *c*-axis, flat fluid-filled inclusions parallel to the basal pinacoid, and tension fractures. Based on chemical composition, spectral data and colour saturation we suggest that the simple term morganite be retained to describe the stones, unless a new term is approved by the IMA to recognize the extraordinary composition and structure of the material.

Introduction

In mid-2002 a small quantity of pink to raspberry-red beryls were mined in Madagascar (*Figure 1*). Some time before that, a minor amount of similar specimens had already been found in Afghanistan. Pink to red varieties of beryl have been reported with various names in the gemmological literature. In this paper we intend to describe the new stones and compare them with earlier material of similar colours, i.e. morganite and red beryl. Initial measurements have indicated high values for refractive indices and density, and therefore we felt it necessary to determine not only the customary gemmological properties, but also to carry out a sound mineralogical investigation including chemical analyses, structural data and spectral characteristics in UV-Vis and NIR.

When the composition of beryl is close to the ideal formula $Be_3Al_2Si_6O_{18}$, it is considered as n-beryl (normal beryl). The crystal structure of beryl is characterized by Be-O tetrahedra and distorted Al-O octahedra, linked with six Si-O tetrahedra forming a hexagonal ring structure. The stacking of the Si_6O_{18} rings forms large

 ISSN: 1355–4565

Figure 1: *Morganite crystals from Madagascar and Afghanistan from left: M2, M1, M3 and A1; faceted stones from Madagascar, from left: M5, M4, M6. The largest faceted stone is 3.025 ct.*

structural channels parallel to the crystallographic *c*-axis of the beryl and the structure offers a large number of possible substitutions both on the different lattice sites and in the channels (Deer *et al.*, 1992).

When the main substitution takes place on the octahedral lattice site, commonly occupied by aluminium, we speak of o-beryl (octahedral beryl). Partial substitutions of Al^{3+} by ions such as Fe^{3+}, Cr^{3+}, V^{3+}, or Mn^{3+} are common in this kind of material. Bivalent ions such as Mg^{2+}, Fe^{2+}, Mn^{2+} require a charge compensation that may be satisfied by monovalent alkalis (e.g. Na^{+}), which are incorporated in the channels of the structure. Most emeralds and aquamarines are o-beryls. When Be^{2+} on the tetrahedral lattice site is partially replaced, we speak of t-beryl (tetrahedral beryl). Based on our investigations it soon became obvious that the new pink beryls belong to this group. Substitution of Be^{2+} by monovalent ions (mainly lithium) requires a charge compensation, which may be realized by introducing a further monovalent ion in the channel structure (Bakakin *et al.*, 1970). The structural channel can accommodate large alkali ions and other large molecules such as H_2O or CO_2.

Both substitutions, octahedral and tetrahedral, as well as the absorption of ions and molecules in the channels, have the effect of increasing the density and refractive indices of beryl (Cerny and Hawthorne, 1976; Hänni, 1980; Sinkankas, 1981). We can thus assume that beryls with high constants contain more substitute elements and are relatively impure. Data from the literature demonstrate that high constants are usually related to high alkali contents, particularly of the heavy alkalis Cs and Rb (Evans *et al.*, 1966).

Sample description and origin

The present report is based on a small number of samples, which were obtained in March 2002 and January 2003. The first sample (A1) of a surprisingly strong pink colour was presented to one of the authors by Haleem Khan, of Hindukush Mala Gems & Minerals, Pakistan. It consists of a tabular crystal with flat hexagonal hillocks on the basal plane, similar to those described as a consequence of rapid growth by Flamini *et al.* (1983) on red beryl from Utah (*Figure 2*). The translucent material is more saturated than would be expected in morganite in the gem trade, but it is less saturated than the red beryl from Utah, USA. The sample was reported to have come from

the Deva mine, Paroon Valley (Konar, Nuristan) in Afghanistan (Haleem Khan, pers. comm. 2002). The other samples are from Madagascar and are similar in colour to sample A1. Sample M2 is a flat hexagonal tabular crystal of an orangey-pink colour. Alexander Leuenberger (Switzerland) provided that stone in December 2002. A short time later, five more samples were obtained from Denis Gravier (Le Mineral Brut, St. Jean-le-Vieux, France) during the Tucson Mineral and Gem Show 2003. Two of the samples (M1, M3) consist of rough translucent stones with broken surfaces. Three more samples (M4, M5, M6) are faceted transparent and semi-transparent stones. They are reported to come from Mandrosonoro, approximately 150 km SW of Antsirabe (Central Madagascar). Some dealers give Ambatovita as the local name for the origin of Madagascar samples. The source is described as a pegmatite which also contains danburite, tourmaline and kunzite. The pink beryls are intergrown with lepidolite and amazonite feldspar (F. Danet, pers. comm., 2003). On one of our rough samples dark green tourmaline is also present, and this supports a pegmatitic origin.

As reference samples, red beryl (R1, R2) from the Wah Wah Mountains and Thomas Range, Utah (courtesy Ted and Rex Harris, Delta, 1983), and light pink morganite (R3) from Madagascar (courtesy Werner Spaltenstein, Chanthaburi) were used. Red beryl is well described in the literature (Nassau and Wood, 1968; Hänni, 1980; Flamini *et al.*, 1983; Shigley and Foord, 1984). A remarkable property of the rhyolitic red beryls is their sectorized colour zoning which resembles an hourglass pattern. The prismatic growth sectors are intensely coloured as they attracted more Mn and Fe, while the basal growth sector is pale.

The colours of the faceted samples were compared with the Biesalski Pflanzenfarben-Atlas DIN 6164 colour chart. Since the stones possess a distinct pleochroism (orangey-red and purplish-pink), the perceived colour depends on the orientation selected for the cutting. When viewed in the *c*-axis direction the colour was orangey-pink and described as

Figure 2: *From left to right: Morganite from Madagascar (M2), red beryl from Utah (R1), and morganite from Afghanistan (A1).*

7.5:3:1 following DIN 6164 (observed in samples M4 and M5). Perpendicular to the *c*-axis the colour is more purplish-pink and described as 10.5:2:1.5 (sample M6).

Specific gravities and refractive indices

Specific gravity (SG), refractive index (RI) and birefringence were determined by usual gemmological testing methods. Both SG and RI of the new material from Afghanistan and Madagascar distinctly exceed the values so far reported in the literature (*Table I*). The birefringence, however, is not affected by these increases. The values for the reference samples (light pink morganite and red beryl) are consistent with those reported in the literature. The increases in SG and RI correlate with the amount of substitution by the heavy alkali ions, Cs and Rb (*Table I*).

UV-Vis spectra

Spectra of morganite and red beryl have been published by Wood and Nassau, 1968; Nassau and Wood, 1968; and Shigley and Foord, 1984. Both pink and red colours in beryl have been attributed to the incorporation of manganese on the aluminium site in the beryl structure, but the situation is complicated by the possibility of two manganese related colour types of beryl,

Table I: Specific gravities, refractive indices and caesium contents of morganites and red beryl.

Sample		SG	RI n_e	RI n_o	Birefringence	Cs_2O wt.%
pink morganite (Madagascar)	M4	3.103	1.608	1.615	-0.007	14.27
	M5	3.101	1.608	1.615	-0.007	14.63
	M6	3.089	1.604	1.611	-0.007	14.31
pink morganite (Afghanistan)	A1	2.906	1.598	1.606	-0.008	9.70
morganite (Madagascar)	R3	2.760	1.592	1.600	-0.008	1.09
red beryl (Wah Wah, Utah)	R1	2.670	1.564	1.570	-0.006	0.13
red beryl (Thomas Range, Utah)	R2	2.670	1.568	1.575	-0.007	

which are dependent on the valence state of manganese (Mn^{2+} or Mn^{3+}) (after Deer *et al.*, 1992 and Wood and Nassau, 1968).

In morganite (light pink), bivalent manganese is incorporated probably by substitution for Al according to the formula [Mn^{2+} + alkali$^+$ = Al^{3+}] where the alkali (e.g. Na^+, K^+, Rb^+, Cs^+) is in the structural channels of beryl. Other substitutions involving Mn^{2+} may also be possible in morganite. As the concentration of Mn^{2+} generally is much lower than the alkalis in such morganites, the proposed substitution remains essentially based on charge balance and bond length considerations.

In red beryl from Utah trivalent manganese acts as a chromophore element by a simple substitution of Mn^{3+} for Al^{3+} in o-beryl. Platonov *et al.* (1989) have described the spectral characteristics of the two Mn-related colours and underlined a clear difference in pleochroism: morganite exhibits distinct dichroism despite having a weaker colour saturation.

UV-Vis-NIR spectra were recorded on the samples from Afghanistan (A1), Madagascar (M5) and Utah (R1) with a Varian Cary Scan 500 spectrometer, using polarization filters to obtain ω- and ε-absorption spectra (*Figure 3*). The spectra of samples Al and M5 showed a strong correlation with spectra reported by Platonov *et al.* (1989) for morganite. In the spectrum of the o-vibration a strong maximum at 570 nm and a general absorption below 370 nm are present. The ε-vibration curve is characterized by a main absorption at 489 nm, with a side peak at 476 nm, and a second maximum at 550 nm, with an absorption edge at 370 nm.

Red beryl from the Wah Wah Mountains, Utah (R1) produced an ω-ray spectrum with an absorption maximum at 562 nm, and a peak at 428 nm, with general absorption below 350 nm. The ε-ray spectrum has its maximum at 535 nm, and a very weak peak at 428 nm. The 370 nm peak is absent, and the absorption edge is again at about 350 nm (compare also Shigley and Foord, 1984).

Near infrared (NIR) spectra

The NIR spectra of our samples were studied with a Varian Cary Scan 500 spectrometer between 800 and 2500 nm. A polarization unit could only be used from 250–900 nm. For morganite samples A1 and M2, three main absorption features near 1412 nm (7082 cm^{-1}), 1907 nm (5244 cm^{-1}) and 2267

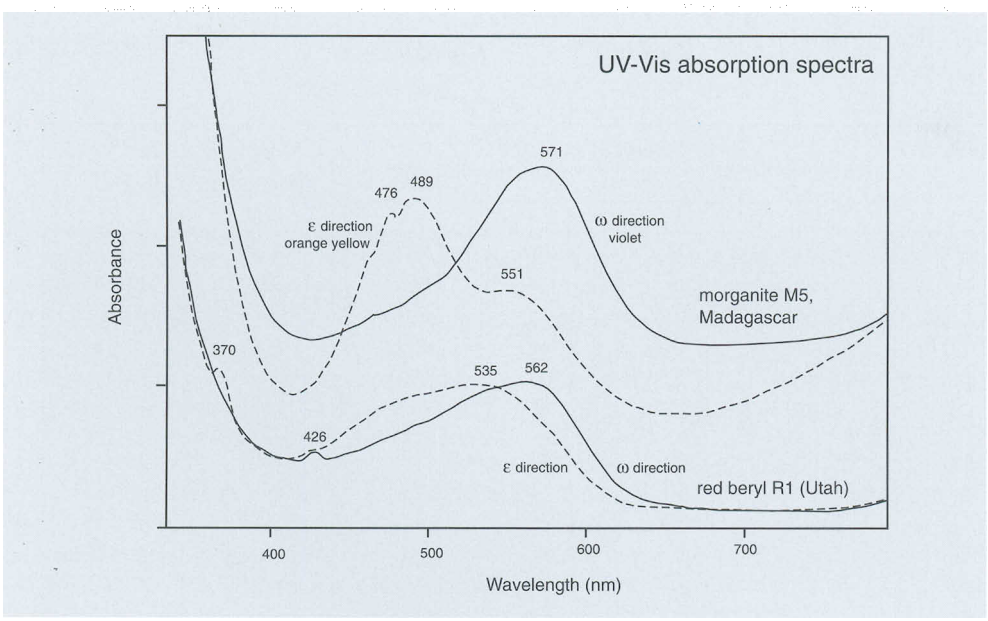

Figure 3: *UV-VIS spectra of morganite M5 from Madagascar and red beryl R1 from Utah (USA). The spectra reveal a distinct difference between these two beryl varieties with manganese Mn^{2+} as chromophore in morganite and Mn^{3+} in red beryl.*

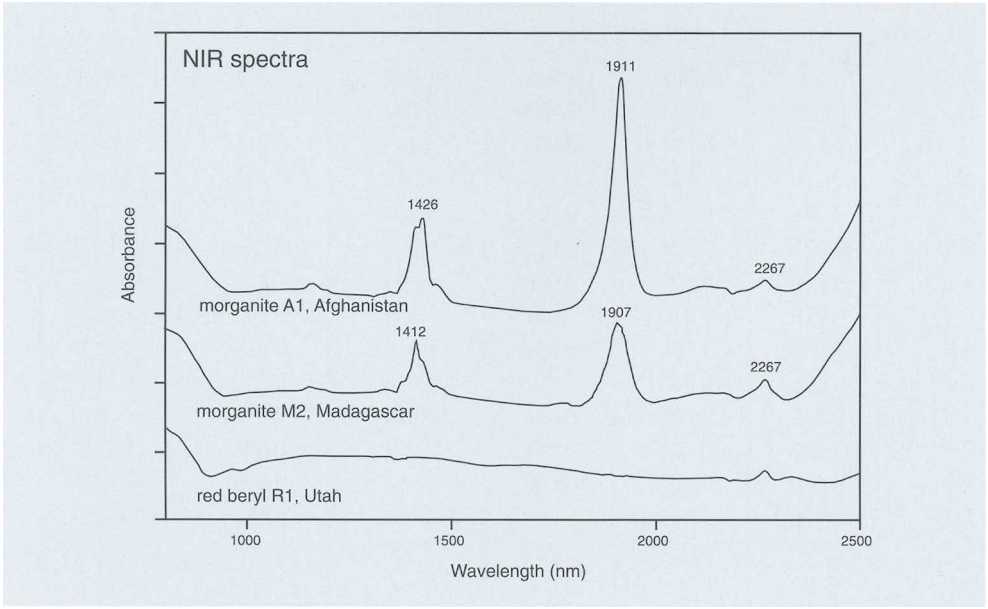

Figure 4: *Unpolarized NIR spectra of morganites A1 (Afghanistan), M2 (Madagascar), and red beryl R1 (Utah). Absorption peaks due to water occur near 1420 and 1910 nm in the morganite spectra but are absent in the red beryl spectrum.*

Table II: *Electron microprobe analyses of morganites from Madagascar and Afghanistan, and red beryl from USA.*

Wt.%	*Pink morganite*				*Morganite*	*Red beryl*	
	Madagascar			*Afghanistan*	*Madagascar*	*Utah, USA*	
	M4	*M5*	*M6*	*A1*	*R3*	*R1*	
BeO*	6.36	6.21	6.28	8.13	11.20	13.78	Be-site
Li_2O*	1.84	1.86	1.83	1.35	0.68	0.09	
Cs_2O	14.27	14.63	14.31	9.70	1.09	0.13	channel
Na_2O	0.56	0.50	0.52	1.15	1.35	0.07	
K_2O	0.14	0.16	0.15	0.03	0.07	0.20	
Rb_2O	0.38	0.39	0.39	0.14	0.09	0.14	
MgO	b.d.	b.d.	b.d.	b.d.	b.d.	0.11	
CaO	0.17	0.17	0.19	0.98	0.01	b.d.	
Al_2O_3	15.84	15.70	15.62	15.72	17.52	16.59	Al-site
Cr_2O_3	b.d.	b.d.	b.d.	b.d.	b.d.	b.d.	
V_2O_3	0.05	0.09	0.09	0.06	b.d.	0.04	
Fe_2O_3	0.03	0.03	0.02	0.02	0.02	2.10	
TiO_2	b.d.	b.d.	b.d.	b.d.	b.d.	0.27	
MnO	b.d.	b.d.	b.d.	0.02	b.d.	0.29	
Sc_2O_3	b.d.	b.d.	b.d.	b.d.	b.d.	b.d.	
SiO_2	59.01	58.60	58.42	61.32	64.82	66.91	Si-site
Total	98.65	98.33	97.82	98.60	96.85	100.69	
Normalization to a total of 11 cations							
Be^{2+}	1.552	1.528	1.549	1.910	2.490	2.968	
Li^{+}	0.753	0.765	0.755	0.532	0.298	0.032	
Cs^{+}	0.619	0.639	0.626	0.405	0.043	0.005	
Na^{+}	0.110	0.099	0.103	0.218	0.242	0.012	
K^{+}	0.018	0.020	0.020	0.004	0.009	0.023	
Rb^{+}	0.025	0.026	0.026	0.009	0.005	0.008	
Mg^{2+}	0.000	0.000	0.000	0.000	0.000	0.015	
Ca^{2+}	0.019	0.018	0.021	0.103	0.001	0.000	
Al^{3+}	1.899	1.895	1.890	1.813	1.911	1.753	
Cr^{3+}	0.000	0.000	0.000	0.000	0.000	0.000	
V^{3+}	0.004	0.007	0.008	0.004	0.000	0.003	
Fe^{3+}	0.002	0.002	0.001	0.001	0.001	0.142	
Ti^{4+}	0.000	0.000	0.000	0.000	0.000	0.018	
Mn^{2+}	0.000	0.000	0.000	0.001	0.000	0.022	
Sc^{3+}	0.000	0.000	0.000	0.000	0.000	0.000	
Si^{4+}	6.000	6.000	6.000	6.000	6.000	6.000	
Total	11.000	11.000	11.000	11.000	11.000	11.000	
H_2O*	0.460	0.570	0.749	0.456	0.973	0.000	

N.B. *BeO, Li_2O and H_2O have been calculated. b.d. = below detection limit

nm (4411 cm^{-1}), are present (*Figure 4*). Without polarisation measurements detailed attributions could not be made and the above absorptions could only be attributed to H_2O vibrations in general. H_2O molecules may be present in two perpendicular positions (type I or II) in the beryl channels (Wood and Nassau, 1968; Charoy, 1998). Infrared analysis of beryl sample powder mixed with KBr would allow an identification of water type and this work is planned for the future. According to the literature, however, most of the water molecules in morganites possess a molecular axis parallel to the structural channels in beryl and are type II. The red beryl reference sample did not show molecular response in the NIR spectral range except for a small peak at 2267 nm, which is in agreement with the H_2O-free nature of this material (Nassau and Wood, 1968; Hänni, 1980).

Chemical composition

Preliminary compositions of the new material were obtained from ED-XRF analyses, which indicated major Si, Al and also the presence of minor Fe, Mn, Cs and Rb in all samples (red beryl and morganite).

Quantitative chemical analyses of pink samples A1, M4, M5 and M6, light pink morganite R3 (Madagascar) and a red beryl R1 (Utah, USA) (see *Table II*) were carried out. On each sample six measurements were taken along a traverse of about 3 mm, to gain some information about their homogeneity.

The analyses were carried out with a JEOL-JXA 8600 electron microprobe (Geochemical Laboratory, University of Basel, Switzerland), operated in wavelength-dispersive mode (WDS) at an accelerating potential of 20 kV and a beam current of 20 nA. Fourteen elements were measured on their $K\alpha_1$ or $L\alpha_1$ lines, respectively, using well-characterized silicates (pollucite for caesium) and oxides as standards. The raw data were fully corrected for matrix effects by a ZAF-type online procedure. Vanadium was further corrected for peak overlap by caesium $L\beta_5$.

The measurements revealed (*Table II*) that the pink samples are relatively homogeneous and that the red beryl has zones of different composition. Samples M4, M5 and M6 contain caesium (Cs_2O) up to 15.18 wt.%, which is distinctly higher than reported so far in the literature (11.3 wt.% Cs_2O reported by Evans and Moore, 1966). Specimen A1 is less rich in caesium (Cs_2O up to 10.05 wt.%), whereas morganite with Cs_2O up to 1.25 wt.% and red beryl with Cs_2O up to 0.19 wt.% are in the range commonly determined in such beryls (Deer *et al.*, 1992; Nassau and Wood, 1968). Further R^+ and R^{2+} in pink beryl M4, M5 and M6 are sodium, rubidium, potassium and calcium, whereas magnesium is below detection limit. Compared to this, specimen A1 has higher contents of sodium, but shows lower values for rubidium. Potassium and magnesium are at or below detection limit. Based on these data, the new pink samples from Afghanistan and Madagascar belong to the alkali beryls, further classified as lithian caesian beryls after Deer *et al.* (1992).

The aluminium concentration is slightly below that required for ideal stoichiometry. This may perhaps be explained by single-site substitutions on the Al-site, but is more likely to be due to the presence of coupled substitution involving caesium. Transition elements, such as iron, chromium, vanadium, titanium and manganese, commonly involved in such substitutions on the Al-site, were only found at the detection limit or below using either the microprobe or the ED XRF. As vanadium had to be corrected for Cs $L\beta_5$ interference, these values near the detection limit are only indications. We suspect that the pink beryls do not contain any vanadium. Although there is a general consensus that manganese is the chromophore for the pink and red colours in natural beryl (Nassau and Wood, 1968; Deer *et al.*, 1992), only in the red beryl could the manganese be measured quantitatively (*Table II*, column 6). However, UV-Vis spectra of the samples where the manganese was below the detection limit of the electron microprobe contain absorption peaks typical for manganese.

All data were further normalized, on a basis of six silicon atoms per formula unit (pfu), assuming full site occupancy on the tetrahedrally-coordinated Si sites (see *Table II*). Furthermore, beryllium and lithium were calculated for a stoichiometric total of 11 cations, although some Cs-rich beryls with total cations up to 11.25 have been described (Deer *et al.*, 1992).

Since beryllium and lithium contents can not be obtained by means of the electron microprobe, these contents were calculated taking into account any possible substitution mechanisms. Although several single-site and coupled substitutions involving alkalis have been described, most of them are based on unsupported stoichiometry (Wood and Nassau, 1968). Based on the data for the pink beryls, and on charge balance and bond length considerations, the most important substitution mechanism in samples A1, M4, M5 and M6 may be formulated as:

$$(i)\ Be^{2+} = Li^{+} + Cs^{+}$$

where for charge balance reasons, lithium on the beryllium site (Hawthorne and Cerny, 1977) is coupled with caesium in the channels of the beryl structure. Due to their large ionic size compared to tetrahedrally coordinated beryllium, all alkalis except lithium can only occupy positions in the channels of the beryl structure. This suggests that the other alkalis present (Na^{+}, K^{+}, Rb^{+}) may be charge balanced mostly by a similar mechanism with the possibility of involvement also with a coupled mechanism involving the Al site,

$$(ii)\ Al^{3+} = R^{2+} + R^{+}$$

where R^{2+} stands for bivalent ions (Mg^{2+}, Ca^{2+}, Fe^{2+}, Mn^{2+}) and R^{+} stands for monovalent alkalis except lithium (Na, K, Rb).

Usually substitution mechanisms can be confirmed by plotting the quantities of the involved cations against each other in a diagram. A distinct correlation with a negative slope between Be and Cs would support the most important suggested substitution mechanism in our pink samples. However, as beryllium and lithium have been calculated in relation to the total amount of cations (in our pink samples basically dependent on the caesium concentration), any diagram representing beryllium content plotted against caesium (or lithium) would necessarily produce a very good negative correlation, due to the so-called constant sum effect (Rollinson, 1993). Therefore no correlation diagram is given in this study.

The indicated amounts of beryllium and lithium in *Table II* are necessarily given as approximate concentrations. Light elements can now be measured in gemstones by laser ablation inductively coupled mass spectrometry LA ICP MS, if a small amount of damage on the surface is acceptable (Hänni and Pettke, 2002).

Laser ablation inductively coupled mass spectrometry (LA ICPMS) results, produced after delivery of the manuscript of this paper confirm the presence and quantities of calculated values for BeO and Li_2O. The Afghan sample A1 gave BeO 7.93 wt%, LiO_2 2.30 wt% and Cs_2O 9.21 wt%. The Madagascar sample M3 gave BeO 8.09 wt%, LiO_2 2.04 wt% and Cs_2O 13.85 wt%.

NIR-spectrometry revealed the presence of water in the structural channels of pink beryl from Madagascar and Afghanistan, whereas the sample from Utah showed no water peaks. This was also confirmed by the chemical analyses. Based on total sum considerations, the pink samples A1, M4, M5, and M6 contain 1/2 H_2O molecule per formula unit. This is in good agreement with published analyses, which mention H_2O concentrations commonly from 0.3 to 0.8 molecules (Charoy, 1998). The light pink morganite specimen contains 1.0 molecules of H_2O per formula unit, whereas the calculated water concentration in the red beryl from Utah is zero, which

again is in good agreement with published figures (Nassau and Wood, 1968; Hänni, 1980).

Crystal structure

Bakakin *et al.* (1970) described a correlation between chemical composition and unit cell parameters of beryl. This was further confirmed by Hänni (1980), who showed that an increase of a_0 in o-beryls was correlated to the extent of substitution on the octahedral Al-site, whereas the c_0 value remained virtually unaffected. The c/a ratio commonly is slightly below 1.0 in such beryls. For alkali (caesium) rich beryl, Sosedko (1957) demonstrated an increase in c_0 related to the content of caesium, with a_0 remaining reasonably constant. They show c/a values slightly above 1.000, consistent with the results of Sosedko (1957) and Charoy (1998) for caesium rich t-beryls (see *Table III*).

Preliminary crystal structure investigations by powder XRD (X-ray diffraction) seem to confirm this correlation. However, ongoing studies by the authors will clarify if and how the high caesium content affects (enlarges) the crystal structure of these samples. First powder XRD analyses revealed that two of the most important diffraction reflections of beryl are not present in samples M2 and A1.

Raman spectra

The Raman-shift spectra of samples M4, M5, M6 and A1 have been obtained using a Renishaw Raman microprobe. These are compared with spectra from o-beryls (red beryl from Utah, synthetic red beryl and aquamarine) and in *Figure 5* a partial peak shift of the pink caesium-rich specimens compared to the above-mentioned o-beryls can be seen. The pink caesium-rich samples show a distinct peak at 1097 cm^{-1}, which compares with 1069 cm^{-1} of the reference samples. A second but less distinct shift can be observed at 402 cm^{-1} (M4, M5, M6, A1), compared to 394 cm^{-1} fo reference samples. All other peaks are con or show only minor peak shifts. This ma explained by the fact, that substitution

Table III: *Cell parameters and contents of Cs and Al.*

Beryl variety	*Beryl sample*	a_0	c_0	*c/a*	*Substitution type*	*Wt.%* Cs_2O	Al_2O_3	*Source*
morganite	Madagascar M2				tetrahedral	14.4		this study
	Afghanistan A1					9.7		
	Russia 3*	9.200	9.227	1.003	tetrahedral	4.13		Sosedko 1957
	Russia 2*	9.202	9.209	1.001		0.67		
	Russia 1*	9.202	9.183	0.998		0.27		
red beryl	Utah R1 light centre	9.214	9.206	0.999	octahedral		17.42	this study
	Utah R1 red rim	9.227	9.205	0.998			15.74	
colourless beryl	Switzerland, Hänni 4	9.211	9.196	0.998	octahedral		18.1	Hänni 1980
aquamarine	Switzerland, Hänni 1	9.233	9.208	0.997	octahedral		15.5	
	Switzerland, Hänni 3	9.257	9.197	0.994			14.6	
	Switzerland, Hänni 3	9.288	9.189	0.989			10.6	

* after Deer *et al.*, 1962

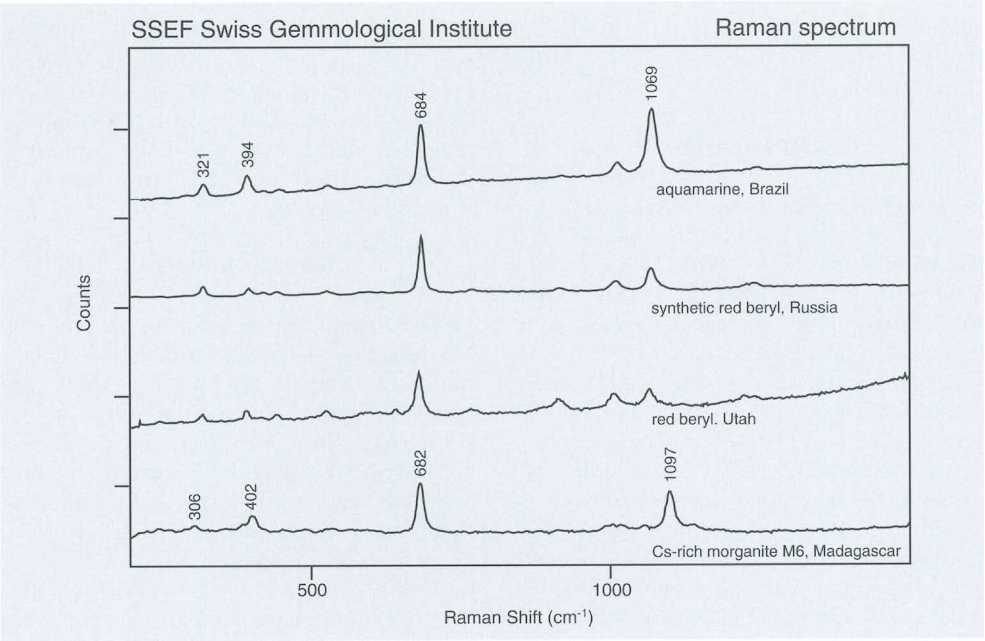

Figure 5: *Raman spectra of morganite M6 red beryl R1, synthetic red beryl (Russia), and aquamarine (Brazil). Cs-rich morganite from Madagascar shows a distinct peak shift at 1097 cm^{-1} compared with the other beryls.*

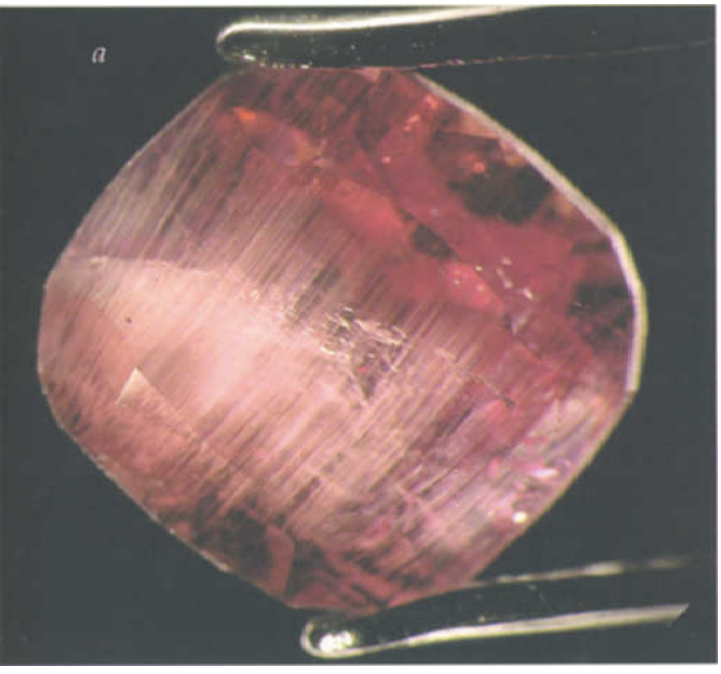

Figure 6: *(a) Morganite from Madagascar (M5) with hollow tubes parallel to the c-axis.*

(b) Detail of M5 showing hollow tubes parallel to the c-axis, flat fluid inclusions parallel to the basal pinacoid, and tension fractures (magnification 20×).

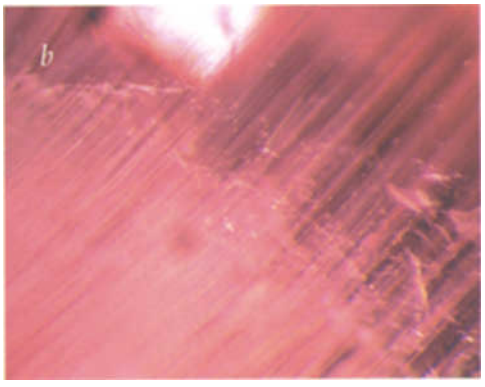

Figure 7: Cat's-eye Cs-rich morganite from Madagascar, provided by D. Gravier (magnification 10×).

place mostly on the Be-site (coupled with incorporation of large alkalis in the structural channels) enlarging locally the structure, whereas the aluminium- and silicon-sites remain virtually unchanged. Further studies will be done to attribute molecular vibrations to their relative Raman peaks.

Inclusions

The specimen from Afghanistan shows strong basal growth zoning and a few tension fractures of conchoidal shape. The samples from Madagascar contain fine tubes parallel to the *c*-axis, and fluid inclusions flattened along the basal plane. The tubes may be so dense in parts that cat's-eye stones may be expected from this source. (*Figure 6a, 6b and 7*). With only a small number of samples, only a few inclusions have been encountered and a wider range may emerge when more stones are seen.

Comparison with synthetic pink, red or purple beryl

For some years hydrothermally grown red and purple beryl has been available. The crystals appear in different colours and owe their colours to different chromophore elements. Some of the stones have been described for example by Henn and Milisenda (1999) and Shigley and Foord (1984). None of the synthetic crystals contain Rb or Cs, but are characterized by distinct concentrations of Ti, Mn or Ni (unpublished SSEF analyses).

The oldest commercially available synthetic material seems to be the pink synthetic beryl from Biron (Australia), which contains Ti as a chromophore element (Brown, 1993). Later, crystals with darker

Figure 8: Hydrothermally grown synthetic beryls from Biron (right) and Novosibirsk, Russia (left).

colours appeared; these were produced in Russia (*Figure 8*) and showed distinct contents of Mn, Fe and Ni. Henn and Milisenda (1999) reported on synthetic red beryl from Russia and found that Co^{2+} was the chromophore. For all these hydrothermal synthetic beryls, the reported densities and refractive indices are clearly lower than for natural morganite as described in this study. It should thus not be difficult to distinguish them from natural morganites. Furthermore, in most of the red to purple and pink hydrothermal synthetic material, characteristic chevron-like growth inhomogeneities could be expected (Johnson and Koivula, 1997).

Terminology considerations

A number of terms are related and used for rose coloured, pink or red beryls. Not all of them are, however, applied in current gemmological publications. Vorobyevite is a caesium beryl of colourless or pink colour, first described in 1908 from Lipovka, Ural Mountains (Sinkankas, 1981). Rosterite is another name for caesium beryl of colourless or pink colour from Elba, Italy. However, these variety names are nowadays only rarely found in the literature.

Much better known is the term morganite (Sinkankas, 1981), given to pink beryl by G.F. Kunz in 1910 to honour J.P. Morgan. Most authors relate the pink colour to the incorporation of some manganese and, at the same time, mention the presence of Cs, which is however not contributing to the colour. Red beryl from Utah owes its name to the intensity of its redness which is far more saturated than the colour associated with morganite. The weak pleochroism of red beryl compared with morganite is a further hint that colour is not the only difference between these minerals.

The new samples studied from Afghanistan and Madagascar strongly resemble in all aspects the properties attributed to morganite. In the trade the investigated samples were sold as 'raspberry beryl' or 'pink beryl', rather than morganite. It seems that for the trade the term morganite is related to a weak colour, and this might negatively influence the new material. However, reconsidering the literature, the term morganite has for a long time precisely described the available light to intensely saturated rose to pink beryl varieties with variable amounts of Mn, Cs and Rb, and no fancy name is required to describe these stones. In the CIBJO rules (CIBJO 2002), application of morganite is related to a mineralogical variety, while morganite, pink beryl and red beryl are also mentioned as commercial names.

Discussion

Caesium and lithium are typical lithophile elements involved in formation of minerals in rhyolites (Christiansen *et al.*, 1983) and pegmatites. While these elements are found only in trace levels in the red beryl from Utah, in the samples from Afghanistan and Madagascar they are present in minor to major quantities. The Madagascar samples are particularly rich in caesium and exceed the Cs_2O contents of other beryls reported in the literature. A consequence of the higher Cs contents is the higher RI and SG values, which exceed the values quoted in many gemmological identification tables for morganite.

Several substitution mechanisms are proposed for the incorporation of alkalis and manganese in these samples. It has been confirmed that Mn^{2+} colours these pink beryls in the same way that it does in morganite (Shigley and Foord, 1984; Platonov *et al.*, 1989) whereas red beryl shows a different manganese absorption pattern, which is attributed to Mn^{3+} (Wood and Nassau, 1968; Lehmann, 1978). Preliminary structural data and the Raman-shift spectra support the idea that incorporation of Cs and perhaps other alkalis has caused an increase of cell dimensions mainly along the *c*-axis.

Summarizing, studied morganites from Afghanistan and Madagascar represent an extreme position in respect to all measured data (density, RI, Cs-concentration, cell parameters) compared to any beryls described so far in the literature. The new material might require a new mineral name due to chemical and structural differences to the classical morganite.

Acknowledgements

The authors are grateful to Haleem Khan (Hindu Kush Minerals, Peshawar, Pakistan), Alexander Leuenberger (Switzerland) and Denis Gravier (Le Mineral Brut, St. Jean-le-Vieux, France), for providing research samples. Fabrice Danet gave valuable information about the occurrence of the morganite samples from Madagascar. Light pink morganite reference material was donated by Werner Spaltenstein (Chantaburi, Thailand). Ted and Rex Harris, Delta, U.S.A., kindly provided the red beryl reference material in 1983. We acknowledge contributions by Dr K. Schmetzer (Petershausen) and Prof. S. Graeser (Mineralogical Institute, University of Basel, Switzerland) for offering the X-ray diffraction facility, Dr T. Pettke, Isotope Geochemistry and Mineral Resources, Swiss Federal Institute of Technology (Zürich) for LA ICP MS data of the Madagascar caesium beryl material, and Peter Giese (SSEF, Basel) for measuring the UV-Vis and NIR spectra. The manuscript was reviewed by our colleagues Dr Lore Kiefert and J.-P. Chalain at SSEF, Basel.

References

Bakakin, V., Rylov, G.M., and Belov, N.V., 1970. Correlation between chemical composition and unit cell parameters of beryl. *Doklady Akademiya Nauk SSSR. Earth Science section* (New York), **173**, 129-32

Biesalski Pflanzenfarben Atlas, 1957. DIN 6164, Musterschmidt-Verlag, Gottingen

Brown, G., 1993. Australian titaniferous synthetic beryl. J. *Gemmol. Assoc. Hong Kong*, **16**, 5-6

Cerny, P., and Hawthorne, F.C., 1976. Refractive indices versus alkali contents in beryl: general limitations and applications to some pegmatitic types. *Canadian Mineralogist*, **14**, 491-7

Charoy, B., 1998. Cristallochimie du béril: l'état des connaissances. In: Didier Giard (Ed.), *L'émeraude*, Association Françáise de Gemmologie, 47-54

Christiansen, E.H., Burt, D.M., Sheridan, M.F., and Wilson, R.T., 1983. The petrogenesis of topaz rhyolites from Western United States. *Contrib. Mineral. Petrol.*, **83**, 16-30

CIBJO, 2002. *Gemstones – terminology and classification: Annex B1: Stones, gemstones and ornamental stones.* Coloured Stone Commission, 2001-2, NYC

Danet, F., 2003. Personal communication

Deer, W.A., Howie, R.A., and Zussman, J., 1962. *The rock forming minerals*. Vol. I. Longman Group Ltd., England

Deer, W.A., Howie, R.A., and Zussman, J., 1992. *The rock forming minerals*. Vol. IB (2nd edn). Longman Group Ltd., England

Evans, H.T., and Moore, M.E., 1966. Crystal chemical studies of cesium beryl. *Abstracts: Geological Society of America Meeting*, 1966, 63

Flamini, A., Gastaldi, L., Grubessi, O., and Viticoli, S., 1983. Sulle caratteristiche particolari del berillo rosso dell' Utah. *La gemmologia*, **IX**, (1/2), 12-20

Hänni, H.A., 1980. *Mineralogische und mineralchemische Untersuchungen an Beryll aus alpinen Zerrklüften*. Dissertation. Universität Basel

Hänni, H.A., and Pettke, T., 2002. Eine neue Diffusionsbehandlung liefert orangefarbene und gelbe Saphire. *Gemmologie. Z. Dt. Gemmol. Ges,*. **51**(4), 137-52

Hawthorne, F.C., and Cerny, P., 1977. The alkali-metal positions in Cs-Li beryl. *Canadian Mineralogist*, **15**, 414-2

Henn, U., and Milisenda, C., 1999. Synthetische rote Berylle aus Russland. *Gemmologie. Z. Dt. Gemmol. Ges.*, **48**(2), 97-104

Johnson, M.L., and Koivula, J.I., 1997. Red and purple hydrothermal synthetic beryl. Gem news. *Gems & Gemology*, **33**(1), 68-9

Khan, H., 2000. Personal communication

Lehmann, G., 1978. Farben von Mineralien und ihre Ursachen. *Fortschr. Mineral.*, **56**(2), 172-252

Nassau, K., and Wood, D.L., 1968. An examination of red beryl from Utah. *Am. Min.*, **53**, 801-6

Platonov, A.N., Taran, M.N., and Klyakin, V.A., 1989. On the two colour types of Mn^{3+} bearing beryls. *Z. Dt. Gemmol. Ges.*, **38**(4), 147-54

Rollinson, H., 1993. *Using Geochemical Data: Evaluation, presentation, interpretation*. Longman Group Ltd., Essex, UK

Shigley, J.E., and Foord, E.E., 1984. Gem quality red beryl from the Wah-Wah mountains, Utah. *Gems & Gemology*, **20**(4), 208-21

Sinkankas, J., 1981. *Emerald and other beryls*. Chilton Book Company, Radnor, Pennsylvania, USA

Sosedko, T. A., 1957. The change of structure and properties of beryls with increasing amounts of alkalies. *Mem. All. Union Min. Soc.*, **86**, 495

Wood, D.L., and Nassau, K., 1968. The characterization of beryl by visible and infrared absorption spectroscopy. *Am. Mineral.* **53**, 777-800

Abstracts

Diamonds

Gems and Minerals

Instruments and Techniques

Synthetics and Simulants

Diamonds

Study of diamonds from chromitites in the Luobusa ophiolite, Tibet. (Chinese with English abstract.)

W. Bai, J. Yang, P. Robinson, Q. Fang, Z. Zhang, B. Yan and X. Hu. *Acta Geologica Sinica*, **75**(3), 2001, 404-9.

A newly discovered occurrence of diamonds in chromitites of the Luobusa ophiolite, Tibet, is described, together with details of the diamonds and of their numerous metallic inclusions. Examination of 25 grains of diamond recovered from the chromite ores revealed about 70 varieties of native elements (Cr, Cu, Ni, Fe, C, Si, Au, Pb, W, Ir, Os, Ru), alloys (Fe-Ni, Fe-Co, Fe-Mn, Fe-Si, Fe-Ni-Cr, Fe-Ni-Co, Si-C, Cr-C, Ir-Os, Os-Ir, Or-Ir-Ru, Fe-Pt), silicates and sulphides. Photomicrographs of the diamonds are accompanied by IR and Raman spectra and a plot of their B-defects *vs* H (x 10^{-6}). R.A.H.

Two age populations of zircons from the Timber Creek kimberlites, Northern Territory, as determined by laser-ablation ICP-MS analysis.

E.A. Belousova, W.L. Griffin, S.R. Shee, S.E. Jackson and S.Y. O'Reilly. Australian Journal of Earth Sciences, 48(5), 2001, 757-65.

Two populations of kimberlite zircons are present in the Timber Creek kimberlites, Northern Territory, Australia. Laser-ablation ICP-MS U-Pb dating yields age ranges of 1483 ± 15 and 179 ± 2 m.y. this distinction being supported by Hf isotope data. The trace element patterns of both populations are typical of mantle-derived zircons, but there are differences that indicate the two populations were derived from different magma sources. The dating results indicate that the emplacement age of the Timber Creek kimberlites cannot be older than the age of the younger zircon population. These data clarify an inconsistency between previously reported SHRIMP age of Timber Creek zircons (1462 ± 53 m.y.) and the much younger age (1200 m.y.) of the sediments into which the kimberlites have intruded. The Timber Creek kimberlites are therefore a newly recognized extension of widespread Jurassic kimberlite activity in Western Australia and South Australia. W.D.B.

The mystery about coloured diamonds.

C. Carrington. *Australian Gemmologist*, **21**(8), 2002, 295-8.

Australia's Argyle mine has become famous for its coloured diamonds, which include brown (champagne and cognac) and pink to red stones. The chemistry and physics of coloured diamonds is discussed, valuing and marketing of the Argyle brown and pink/red diamonds is described. P.G.R.

Morphology of diamond crystals from the Bingara range, northern New South Wales, Australia.

J.D. Hollis. *Australian Gemmologist*, **21**(9), 2003, 350-9, 4 plates, 3 tables.

Due to their unusual occurrence and certain rare features, diamonds from the Bingara range are of special interest and are representative of diamonds from the other scattered locations along the length of eastern Australia. This paper is based on a study of over 300 diamond euhedra selected from over 8700 crystals sampled from bulk at the Monte Christo Prospect, Bingara by Cluff Resources Pacific NL during 1999-2000. The crystal forms observed in the study are illustrated as sketches 1-54 in four plates. These are referred to in the text by their sketch number, and a description of their morphology is listed in one of the tables. Diamond morphology of these crystals is largely the result of oscillations between etching and resorption stages prior to eruption. Subsequent events imprinted crystals with final eruption and post-eruption experiences. The crazing, impacting and pitting stages are most unusual and distinguish the Bingara range diamonds from classical suites. P.G.R.

Mineral inclusions in diamonds: associations and chemical distinctions around the 670 km discontinuity.

M.T. Hutchison, M.B. Hursthouse and M.E. Light. *Contributions to Mineralogy and Petrology*, **142**(1), 2001, 119-26.

New mineral associations within diamonds from the Juina district of Brazil include a previously unrecorded Na-Al-(Mg, Fe)SiO_3 phase, associated with ferropericlase and the tetragonal almandine-pyrope phase, an association of corundum with aluminous pyroxene, and an olivine

Abstractors

W.D. Birch	W.D.B.	R.A. Howie	R.A.H.	P.G. Read	P.G.R.
A.M.Clark	A.M.C.	R.K. Harrison	R.K.H.	E. Stern	E.S.
J. Flinders	J.F.	P.B. Leavens	P.B.L.	P.M. Whelan	P.M.W.
		M. O'Donoghue	M.O'D.		

For further information on many of the topics referred to, consult *Mineralogical Abstracts*

 ISSN: 1355–4565

phase associated with ferropericlase. The minerals in each association occur within the same diamonds, and also within individual diamonds in different combinations. High-*P* experimental data show these associations formed at different depths within ~ 60 km either side of the upper–lower mantle boundary. Mineral compositions show the sampled regions of the deep transition zone and lower mantle are distinct and heterogeneous. Also, contrary to some recent experimental studies, Al is not solely accommodated within perovskite-structured (Mg, Fe)SiO_3 in the uppermost lower mantle. J.F.

Rb-Sr of kimberlites and lamproites from eastern Dharwar craton, south India.

A. KUMAR, K. GOPALAN, K.R.P. RAO AND S.S. NAYAK. *Journal of the Geological Society of India*, **58**(2), 2001, 135-41.

Rb-Sr phlogopite isochron ages for Kotakonda and Mudaebid kimberlites, in the Narayanpet kimberlite field NW of the Cuddapah basin, of 1085 ± 14 and 1099 ± 12 m.y. respectively, are younger than recently reported K-Ar (1363 ± 48 m.y.) and ^{40}Ar-^{39}Ar (1402 ± 5 m.y.) ages for the Kotekonda kimberlite. This supports previous conclusions from these authors that S Indian kimberlites erupted episodically at ~ 1090 m.y. Rb-Sr ages of lamproites from Ramannapeta (1224 ± 14 m.y., NE basin margin), and Chelima and Zangamarajupalle (1354 ± 17 and 1070 ± 22 m.y. respectively), within the Cuddapah basin are distinctly different. While this Rb-Sr age of the Ramannapeta lamproite is younger than an earlier K-Ar age (1381 ± 18 m.y.), it is similar to many spatially close alkaline complexes (Elchuru, Kunavaram). The Chelima and Zangamarajupalle ages are considered imprecise, since these rocks contain a large secondary carbonate component whose Sr isotope composition is genetically unrelated to that of their phlogopites. J.F.

Gem Trade Lab Notes.

T.M. MOSES, I. REINITZ, S.F. MCCLURE AND M.L. JOHNSON (EDS). *Gems & Gemology*, **39**(1), 2003, 38-46.

Notes are given on two intensely coloured type IIa diamonds, one was 1.15 ct pear-shaped brilliant which had been subjected to HPHT treatment and was graded fancy intense green-yellow and the other was a 4.15 ct natural diamond graded fancy vivid pinkish-orange; both stones contained substantial nitrogen-related defects. Also noted are quartz coloured greyish-blue by inclusions of indicolite and a metamict zircon from Sri Lanka showing bright play-of-colour. R.A.H.

Diamond, former coesite and supersilicic garnet in meta-sedimentary rocks from the Greek Rhodope: a new ultra high-pressure metamorphic province established.

E.D. MPOSKOS AND D.K. KOSTOPOULOS. *Earth and Planetary Science Letters*, **192**(4), 2001, 497-506.

The discovery of UHP indicator minerals and textures from the Rhodope metamorphic province (RMP), N. Greece, is reported. Exsolution of quartz, rutile and apatite in sodic garnet from metapelites (garnet-biotite-kyanite gneisses) identifies a Si-Ti-Na-P-rich precursor garnet phase. These textures in garnet have only once before been reported, from eclogites in Su Lu UHP metamorphic province, China. Microdiamonds and multicrystalline quartz pseudomorphs after coesite occur in garnet from both both eclogites and metapelites. It is argued that these rocks were transported into the upper mantle, to depths >220 km, establishing the RMP as a UHP metamorphic belt. J.F.

Archean subduction recorded by Re-Os isotopes in eclogitic sulfide inclusions in Kimberley diamonds.

S.H. RICHARDSON, S.B. SHIREY, J.W. HARRIS AND R.W. CARLSON. *Earth & Planetary Science Letters*, **191**(3-4), 2001, 257-66.

Eclogitic sulphide minerals within diamonds from the deepest part of the continental mantle keel beneath the Kaapvaal craton, and brought to the surface in kimberley kimberlites, have low Ni and Os contents and high Re/Os, typical of a basaltic protolith. Sulphide inclusions with the lowest Os give late Archaean single-grain absolute ages, whereas those with higher Os give a well-constrained 2900 m.y. isochron age and radiogenic i_{Os} (γ_{Os} = +45). This implies a significant time between basaltic precursor generation and eclogitic diamond crystallization, consistent with lengthy residence in a near-surface environment before subduction, resulting from accretion of the Kimberley block to the craton, and subsequent diamond formation. These data suggest subduction-related crustal recycling was viable during continent formation in the mid-Archaean, and may have been involved in eclogitic diamond formation ever since. J.F.

Découvertes diamantifères au Québec-Novembre 2002.

G. RIONDET. *Revue de Gemmologie*, **147**, 2003, 7-10.

Update of diamond finds in Quebec, Canada, from the first discovery of two diamondiferous kimberlites in December 2001 to the present. A short history and maps are given. M.O'D.

Abundance and composition of mineral inclusions in large diamonds from Yakutia.

N.V. SOBOLEV, E.S. EFIMOVA, A.M. LOGVINOVA, O.V. SUKHODOL'SKAYA AND YU. P. SOLODOVA. *Doklady, Russian Academy of Sciences Section*, **376**(1), 2001, 34-8. (English translation.)

The abundance of inclusions in 2334 diamonds from the Mir, Udachnaya and Aikhal kimberlite pipes is presented. Chromite, garnet and olivine inclusions were abundant and EPMA results for garnet and chromite are given. The results indicate that the inclusion assemblages are similar in diamonds of varying size from the same pipe. Sulphide inclusions are predominant only in large diamonds from the Mir pipe. A.M.C.

Tectonic controls on kimberlite location, southern Africa.

S. VEARNCOMBE AND J.R. VEARNCOMBE. *Journal of Structural Geology*, **24**(10), 2002, 1619-25.

A geometric method of spatial analysis (SpaDiS™), which requires neither statistics nor algebraic models, has been used to show that crustal architecture is critical in the location of kimberlites. Distinct corridors of kimberlites are parallel to, but not within prominent shear zones and crustal faults. Instead the kimberlites occur in relatively homogeneous, strong crust capable of maintaining the very high CO_2 *P* necessary for rapid emplacement. Archaean directional trends in kimberlite distribution are recognised on the craton, whereas Proterozoic and Carboniferous-Permian (Karoo) age trends are recognized both on and off the Archaean craton. R.A.H.

Gems and Minerals

Anwendung der Laser-Raman-Spektroskopie zur Identifizierung von synthetischen Opalen aus Russland.

A. Banerjee. *Gemmologie. Z. Dt. Gemmol. Ges.* **51**, 2002, 191-3. 1 diagram, bibl.

Short description of the use of Raman spectroscopy in distinguishing synthetic opal from Russia, when other methods do not yield satisfactory results. E.S.

Update of Australia's gemstone and pearl resources.

G. Brown. *Australian Gemmologist*, **21**(8), 2002, 273-7, 1 map.

This status report covers Australia's diamond, opal, South Sea cultured pearl, sapphire and ruby, chrysoprase and nephrite industries, and suggests reasons for economic changes that have occurred over recent years. P.G.R.

Der Stein ist wirklich echt!

W. Bürgi. *Schweizer Strahler*, 2003/1, 37-8.

Note on an exceptional specimen of rough transparent quartz containing pyrite crystals of considerable size. The specimen was due to be shown at a special exhibition at the Lucerne Bourse during April 2003. M.O'D.

On the problem of the occurrence of dispersed bunsenite (NiO) in chrysoprases.

K. Dyrek, Z. Sojka, W. Zabinski and F. Bozon-Verdura. *Mineralogica Polonica*, **32**(2), 2001, 308.

The nickel oxide bunsenite is identified as the source of nickel from which chrysoprase obtains its green colour. UV-VIS-NIR spectroscopic tests showed that the Ni^{2+} ions were attached to the SiO_2 crypto-crystalline matrix in positions of distorted octahedral symmetry outside the framework. Specimens from Lower Silesia, Poland, Marlborough Creek, Australia and an unspecified African location were examined. M.O'D.

Edelsteinbergbau im Festgestein: zwei Beispiele aus Pakistan.

H.C. Einfalt. *Gemmologie. Z. Dt. Gemmol.* **51**, 2002, 153-170. 10 photographs, 1 table, 3 flow-charts, bibl.

The article is a revised version of the lecture given to the German Gemmological Association in spring 2001. It deals with the geological and mineralogical background of two mines in Northern Pakistan, the Katlang topaz mine (and the newly opened Shomzo mine nearby) and the Gujar Kili emerald mine. In both cases geology and actual mining are described and the future prospects discussed. E.S.

Eine grosse Topasdruse am Waldstein im Fichtelgebirge.

J. Frankenberger. *Lapis*, **27**(6), 2002, 46-8.

Light blue crystals of topaz are described from Waldstein in the Fichtelgebirge of Bavaria, Germany, where they occur with orthoclase and light green crystals of apatite. M.O'D.

Le nouveau traitement produisant des couleurs orange à jaune dans les saphirs.

E. Fritsch, J.-P. Chalain, H. Hänni, B. Devouard, G. Chazot, D. Giuliani, D. Schwarz, C. Rollion-Bard, V. Garnier, S. Barda, D. Ohnenstetter, F. Notari and P. Maitrallet. *Revue de gemmologie*, 147, 2003, 11-23.

Detailed description of recent treatments of sapphire giving orange to yellow colours. Sapphires from Songea, Tanzania, Ilakaka, Madagascar, and some from Burma and Thailand have been heated at high temperatures in an oxidizing atmosphere and with the diffusion of beryllium into the stone from outside. Notes on appearance, properties and testing are given. M.O'D.

Le jade, valeur et terminologie en Occident et en Chine.

E. Gonthier. *Revue de gemmologie*, **147**, 2003, 31-35.

Notes on jade classification, valuation and varietal nomenclature in China and in the West. The Chinese characters for 'jade' and 'precious stone' are explained. M.O'D.

Geochemistry of agates; a trace element and stable isotope study.

J. Götze, M. Tichomirowa, H. Fuchs, J. Pilot and Z.D. Sharp. *Chemical Geology*, **175**(3-4), 2001, 523-41.

Trace-element and stable isotope data on Precambrian-Tertiary agate within felsic-mafic volcanic rocks from 18 locations worldwide, help elucidate agate formation and the origin of mineral-forming fluids. Samples are generally LREE-enriched, while some have a positive Eu anomaly. Similar REE patterns for the agates and their parent volcanic rocks suggests mobilization of elements by circulating fluids during syn- and post-volcanic wallrock alteration. Deuterium (δD-44 to -130‰) and O(δ^{18}O+16.4 to +33.4‰) data on agates and associated quartz incrustations show variable compositions for samples

from different localities, but also within single agates (<10‰ for $\delta^{18}O$); attributed to either kinetic effects during isotope fractionation or mixing of meteoric and magmatic fluids. High $\delta^{18}O$ of parent volcanic rocks (<+19.5‰) suggest circulation of ^{18}O-enriched hydrothermal fluids that originated from heated meteoric water and/or residual magmatic fluids. Agate formation occurred at 50-250°C. J.F.

Tiefblaue Afghanit-Kristalle von Sar-e-Sang, Badakshan, Afghanistan.

A. GUASTONI AND F. DEMARTIN. *Lapis*, **27**(6), 2002, 22-3.

Dark blue crystals of afghanite, some translucent and perhaps of ornamental quality, are described from Sar-e-Sang, Badakshan, Afghanistan. Prismatic crystals show pyramidal terminations. M.O'D.

Eine neue Diffusionsbehandlung liefert orangefarbene und gelbe Saphire.

H.A. HÄNNI AND T. PETTKE. *Gemmologie. Z. Dt. Gemmol. Ges.*, **51**, 2002, 137-52. 10 photographs, 1 table, 3 graphs, bibl.

New orange sapphires appeared on the market in 2001. They had been treated in Thailand and showed an orange to yellow thick layer parallel to the cut surface. It became obvious that the corundum originated in Tanzania and Madagascar and were heat treated together with foreign substances, but it was shown that beryllium plays an important role in the coloration. The terminology of the new material is debated as it presents an identification problem as the diffusion of beryllium may penetrate the complete stone. E.S.

The occurrence of gagate in southern Soltykow (The Holy Cross Mts).

V. HEFLIK, B. KWIECINNSKA AND A. ZMUDZKA. *Mineralogia Polonica*, **32**(2), 2001, 47-55, 3 colour photographs.

Gagate [jet] is found with brown coals of the Zagaje series in Lower Jurassic sediments at a nature reserve, Gagates of Soltykow, near Kielce, Poland. The material was found to be a fossil coal with a banded structure and jet-black colour. Despite its fine colour the material is not easily fashioned into ornaments due to the high pyrite content. Details of chemical analyses are given, showing that the jet can be placed within the mixed terrestrial-marine type of organic matter. M.O'D.

Mikrokristalline SiO_2 – mineralisationen in rhyolithischen Rotliegendvulkaniten des Thüringer Waldes und ihre Genese.

G. HOLZHEY. *Aufschluss*, **54**, 2003, 95-110.

Lower Rotliegend-age volcanic rocks of the Thüringer Wald, Germany, host agate-bearing rhyolite spherulites. While the paper discusses the genesis of the spherulites there are also implications for the types of patterns observed in many specimens. The paper was first published in *Chemie der Erde*, **59**, 1999, 183-205. M.O'D.

Australian sedimentary opal - why is Australia unique?

D. HORTON. *Australian Gemmologist*, **21**(8), 2002, 287-94, illus. in colour, 1 table.

Sedimentary opal deposits are widely scattered throughout central Australia and constitute about 95 per cent of the world's precious opal. These opal deposits occur along generally flat-lying horizontal layers within 30 metres of the surface. The unique combination of geological events (deposition, weathering, remobilisation, preservation) that gave rise to these deposits over a 100 million year period may account for the conditions which resulted in Australia's many sedimentary opal fields. P.G.R.

Agate Creek agates.

P. HOWARD. *Australian Gemmologist*, **21**(8), 2002, 299-300, illus. in colour.

Agates are one of the most attractive varieties of crypto-crystalline quartz. In Australia, an important source of quality agates is located in north Queensland in the vicinity of three creeks (Agate Creek, Spring Creek and Black Soil Creek) some 100km south of George Town. At this abundant source, agates occur as nodules in the valley at the head of the three creeks. When polished the agates display a great variety of colour and pattern as is demonstrated in the accompanying illustrations. P.G.R.

Bergkristalle als funkelnde Meisterwerke der Kunst.

G. KANDUTSCH. *Lapis*, **28**(3), 2003, 31-8.

Notes on an exhibition of worked rock crystal shown at the Kunsthistorisches Museum in Vienna during 2003. M.O'D.

Edelsteine aus dem Gebiet nördlich von Araçuai (Minas Gerais, Brasilien): Vorkommen, Eigenschaften und Behandlungsmethoden.

J. KARFUNKEL, J. QUÉMÉNEUR, K. KRAMBROCK, M. PINHEIRO, G.O. DIAS AND R. WEGNER. *Gemmologie. Z. Dt. Gemmol. Ges.*, **51**, 2002, 171-84, 5 photographs, 4 graphs, 1 diagram, 1 map, glossary, bibl.

Gemstones have been mined in this area for over 100 years, the main ones being: tourmaline (green, red, blue and multi-coloured), beryl (colourless, blue, pink and yellow), spodumene (colourless, yellow and green), quartz (smoky quartz, rock crystal and citrine), amblygonite, petalite and andalusite. The geology of the district is discussed as are the various possibilities of treatment, mainly in order to purify the desired colour. E.S.

Genesis and gemmology of sapphires from the Nezametnoye deposit, Primorye region, Russia

A. KHANCHUK, B. ZALISHCHAK, V. PAKHOMOVA, E. ODARICHENKO AND V. SAPI. *Australian Gemmologist*, **21**(9), 2003, 369-75, 8 illus., 1 map, 4 tables.

Corundums and sapphires from the Nezametnoye placer deposit in far eastern Russia are found both as

crystals of about 20mm size and sometimes larger, and as derived fragments. Both the crystals and fragments are rounded to varying degrees. The problem of determining an origin for corundum – one of the fundamental questions in geology – until now has remained debatable. Based on the established association of this sapphire's mineral inclusions (columbite, albite, zircon, zinc-bearing hercynite, rutile), the composition of the sapphire's glassy inclusions, and the presence of accessory corundum in the granite- and granosyenite porphyries that underlie the Nezametnoye deposit of alluvial sapphires, the conclusion was made that the sources of the corundums in this deposit were rare-metal pegmatites, greisens, and metasomatites associated with Mesozoic granitoid bodies that are widespread in the area. P.G.R.

Achat vom Donnersberg, Pfalz.

K. KOHOUT. *Lapis*, 27(6), 2002, 51.

Specimens of agate are described from Donnersberg in the German Pfalz. Some examples contain amethyst. M.O'D.

Gem news international

B.M. LAURS (ED.). *Gems & Gemology*, **39**(1), 2003, 48-64.

Items mentioned include the occurrence and faceting of a purplish-pink Cs-'beryl' from Madagascar; this had ε 1.608, ω 1.616-1.617, SG ~ 3.10. EPMA for one with a purplish-pink core and pale pinkish-orange rim gave Cs_2O 13.57 and 15.33 wt.%, respectively. Also mentioned are a new find of demantoid at a historic Russian site in the Urals and 'LifeGem' synthetic diamonds grown using purified carbon derived from human remains during cremation as a personal individualized memorial. R.A.H.

Achate aus dem Vorland des Riesengebirges, Tschechien.

M. LÜTTICH. *Lapis*, **8**(4), 2003, 21-6.

Agate with attractive patterning is described from several sites in the Riesengebirge, Czech Republic. M.O'D.

Nouvelles expositions à Lausanne.

R. MARCHANT. *Schweizer Strahler*, 2003/1, 5-9 and 23-7.

French- and German-language descriptions of the re-arranged exhibits at the Musée cantonale de géologie, Lausanne, Switzerland [the canton is Vaud], include notes on gem materials displayed. Text and illustrations in both French and German versions need to be consulted as they do not correspond. M.O'D.

The processing and heat treatment of Subera (Queensland) sapphire rough.

M. MAXWELL. *Australian Gemmologist*, **21**(8), 2002, 279-86.

The author of this paper is the Technical Services Manager of Great Northern, a subsidiary of GTN Resources. The Subera corundum deposit, located some 5km east of Rubyvale, is mined by Great Northern. This deposit has large reserves of low quality sapphire and several attempts have been made to develop a viable bulk heat treatment programme aimed at enhancing the colour of the sapphire rough. Despite modifications none of these treatments was successful, and the latest process introduced experimentally by Crystal Chemistry resulted in as many stones being reduced in value as those gaining value. From this it was concluded that the economic bulk heat treatment of Subera sapphire rough was not feasible and the process has been discontinued. P.G.R.

Prächtiger Spessartin-Granat aus den Pegmatiten von Fujian, China.

B. OTTENS. *Lapis*, **28**(4), 2003, 13-20

Fine quality well-crystallized spessartine is reported from a pegmatite in the area of Tongbei-Yunling, Fujian Province, China. The spessartine is associated with well-formed rock crystal: other minerals from the area are described. M.O'D.

Luminescent geochemical anomalies in the lithosphere and haloes of ore bodies.

A. PORTNOV, B. GOROBETS, A. ROGOZHIN, A. BUSHEV AND T. KVITKO. *Periodico di Mineralogia*, **71**(1), 2002, 85-100.

Haloes of luminescent minerals occur around kimberlite pipes, emerald-bearing bodies in metasomatic rocks, gold-bearing bodies, mica pegmatites and quartz veins. These are special cases of luminescent geochemical anomalies which occur in those parts of the Earth's crust where considerable interaction has taken place between rocks and abyssal fluids. These fluids leached trace elements, including the luminogenous transition metals of *3d*, *4f* and some other groups from the country rocks, accumulating and then depositing them. Accumulations of Mn, *REE*, U and other luminogenous elements form glow centres in secondary minerals. Outcrops of photoluminescent calcite, apatite, zircon, fluorite, cerussite, chlorargyrite and uranyl minerals in altered rocks may serve as indicators of mineral deposits. Photoluminescent grains of apatite with a violet-blue glow (Ce^{3+}, Eu^{2+}) detected by sand analysis allow mapping of secondary mechanical haloes (scattering), of help in prospecting for kimberlite pipes. R.A.H.

From mastodon ivory to gemstone: the origin of turquoise colour in odontolite.

I. REICHE, C. VIGNAUD, B. CHAMPAGNON, G. PANCZER, C. BROUDER, G. MORIN, V.A. SOLÉ, L. CHARLET AND M. MENU. *American Mineralogist*, **86**(11-12), 2001, 1519-24.

Heat-induced colour changes of fossilized Miocene mastodon ivory (13-16 m.y.) have been known at least since the Middle Ages. Cistercian monks are believed to have created odontolite, a turquoise-blue 'gemstone' by heating mastodon ivory found in Miocene geological layers next to the Pyrrenean chain, France, to use it for the decoration of medieval art objects. This material has been the object of investigations of European naturalists and gemmologists, among them Rèaumur (1683-1757). Although vivianite [$Fe_3(PO_4)_2.8H_2O$] is the commonly accepted colouring phase supposed to appear when heating fossilized mastodon ivory, previous spectroscopic studies using PIXE/PGE and TEM-EDX

indicate that the chemical composition of collection odontolite and heated mastodon ivory corresponds with well-crystallized fluorapatite [$Ca_5(PO_4)_3F$] containing trace amounts of Fe (230-890 ppm), Mn (220-650 ppm), Ba (160-620 ppm), Pb (40-140 ppm), and U (80-210 ppm). No vivianite has been detected. New insights into the physico-chemical mechanism of the colour transformation of fossilized ivory come from a combination of UV/visible/near-IR reflectance spectroscopy, time-resolved laser-induced luminescence spectroscopy (TRLIF), and X-ray absorption near-edge structure (XANES). Contrary to what had formerly been described as the colour origin in odontolite, the present study conclusively identifies traces of Mn^{5+} by UV/visible/near-IR reflective spectroscopy, TRLIF, and XANES inside the fluorapatite. Thus odontolite owes its turquoise-blue colour to Mn^{5+} ions in a distorted tetrahedral environment of four O^{2-}ions. XANES also documents oxidation of disordered octahedral Mn^{2+} ions to tetrahedral Mn^{5+} species in apatite during the heating process. P.M.W.

Seltenheiten aus Mogok, Myanmar.

R. Schlüssel, C.C. Milisenda and F. Bärlocher. *Gemmologie. Z. Dt. Gemmol. Ges.*, **51**, 2002, 185-90. 6 photographs, 1 map. bibl.

Three recently found gems are described. A violet poudretteite weighing 3 ct was found in snow-white marble. An orange-yellow periclase rough was cut as a 27.81 ct cabochon - it showed adularescence due mainly to numerous minute liquid inclusions. The third specimen was a 14 ct thorite cabochon. E.S.

The first transparent faceted grandidierite, from Sri Lanka.

K. Schmetzer, M. Burford, L. Kiefert and H.-J. Bernhardt. *Gems & Gemology*, **39**(1), 2003, 32-7.

A 0.29 ct faceted greenish-blue grandidierite is described from Sri Lanka. It has α (greenish-blue) 1.583, β (very pale yellow) 1.620, γ (blue-green) 1.622, $2V_a 25°$; SG 2.96. EPMA results show FeO 1.71 wt.% distinguishing it from lazulite; the FTIR and Raman spectra are presented. R.A.H.

Poudrettite: a rare gem species from the Mogok Valley.

C.P. Smith, G. Bosshart, S. Graeser, H. Hänni, D. Günther, K. Hametner and E.J. Gübelin. *Gems & Gemology*, **39**(1), 2003, 24-31.

A 3 ct faceted poudrettite was bought in Mogok, Myanmar [Burma], in 2000 and is the first recorded gem-quality specimen of this rare borosilicate hitherto only known in small crystals from the Mont Saint-Hilaire complex, Quebec. Its identity was confirmed (using minute scrapings) by XRD, IR, Raman spectroscopy and LA-ICP-MS; it has ω (purple-pink) 1.511, ε (very pale brown) 1.532, and also shows colour zoning; SG 2.527; trace amounts of Li and Mn were higher in the purple zone, and Ca, Rb and Cs were lower. R.A.H.

Prächtige Morionkristalle vom Blausee, Binntal, Schweiz.

I. Stalling and Y. Pellmont. *Lapis*, **28**(20), 2003, 31-4.

Well formed crystals of ornamental-quality smoky quartz (morion) are described from Blausee in the Swiss Binntal. An occurrence of blue tourmaline is also described. M.O'D.

Colour in quartz; from atomic substitutions to nanoinclusions.

P. Vasconcelos, B. Cohen and N. Calos. *Australian Gemmologist*, **21**(8), 2002, 278.

Colour in amethyst and citrine may be caused by the presence of multiple atoms and colour centres; in rose quartz, chrysoprase and precious opal the colour may be due to band gap and interference phenomena. The application of high-resolution analytical techniques (such as ICP-MS, HRTEM, XRD, XAFS and TEM) permits unambiguous identification of dispersed elements or mineral inclusions, thus clarifying our understanding of colour in this mineral. P.G.R.

The *Mineralogical record* library: fifty early collection catalogs.

W.E. Wilson. *Journal of the Geo-Literary Society*, **18**(1), 2003, 4-28.

The library of the *Mineralogical Record* has concentrated on assembling mineral collection catalogues which are notoriously hard to find on the second-hand market. The catalogues listed in chronological order range from the 16th to the early 20th century: some collections contain ornamental materials and many collections have been broken up and are now hard to trace. Some illustrations are reproduced in black-and-white. M.O'D.

Origin of a dolomite-related jade deposit at Chuncheon, Korea.

T.-F. Yui and S.-T. Kwon. *Economic Geology*, **97**(3), 2002, 593-601.

The Chuncheon nephrite deposit is among the world's largest; it is hosted in Precambrian dolomitic marble and amphibole schist that were intruded by the late Triassic Chuncheon granite. Carbonates in the marble have O and C isotope composition in the range of -0.1 to +18.2 and -4.3 to + 0.9‰, and -0.4 to + 3.5 and -9.9 to 4.7‰, respectively. These data are in agreement with the decarbonation process driven by fluid infiltration forming the nephrite deposit from dolomitic marble in the T range 330-430°C. Stable isotope compositions of silicates from the nephrite are homogeneous and extremely depleted in ^{18}O and D. It is suggested that formation of the deposit post-dated metamorphism of the country rocks. Model calculations show that the fluid/rock ratios were high, and that both O and H isotope compositions of nephrite were mainly buffered by the fluid phase, and that XCO_2 of the fluid phase was very low during nephrite formation. R.A.H.

Instruments and Techniques

A compilation of infrared absorption spectra of some specific gemstones as an aid to their identification.

S. FERNANDES, M. KHAN AND G. CHOUDHARY. *Australian Gemmologist*, **21**(9), 2003, 361-7, 1 illus., 6 tables.

Although the individual gemstones selected for this study can usually be identified by their unique optical and other physical properties, these gemstones were also chosen because they shared a common colour (e.g. blue stones such as iolite, kyanite, sapphire and blue glass). In this study comparative observations were made of the IR spectra recorded from twenty-five samples of each selected species, each group consisting of faceted stones, rough specimens and, when these were the only samples available, fine chips. Spectra were recorded using a Nicolet Avatar 360 FTIR spectrometer that was equipped with a diffuse reflectance attachment. The study has resulted in the production of several sets of 'fingerprint' IR patterns for consideration as a possible means of identification for five colour ranges of gemstones and similarly coloured man-made materials. In some cases clearly defined regions of their IR spectra have to be investigated before a positive identification can be made for some of the gemstones of similar colour. P.G.R.

Photomicrography for gemologists.

J.I. KOIVULA. *Gems & Gemology*, **39**(1), 2003, 4-23.

The basic requirements for gemmological photomicrography are reviewed and new techniques, advances and discoveries in this field are introduced. Just because you don't see it, doesn't mean it isn't there. Proper illumination is the most critical factor in obtaining the best results with gem material, coupled with the cleanliness of the photomicroscope and its surroundings. Also critical is the understanding of the features seen and the role they might play in the identification process. R.A.H.

Spectrométrie de fluorescence du chrome (Cr^{3+}) dans les spinelles. Identification des spinelles synthétiques produits par dissolution anhydre et des autres matériaux dits "spinelles synthètiques" produits par fusion Verneuil.

F. NOTARI AND C. GROBON. *Revue de gemmologie*, **147**, 2003, 24-30.

Fluorescence spectroscopy is useful in the detection of synthetic red spinels. Details of the procedures and results are given. M.O'D.

Synthetics and Simulants

Diamond nucleation and growth by reduction of carbonate melts under high-pressure and high-temperature conditions.

A. ARIMA, Y. KOZAI AND M. AKAISHI. *Geology*, **30**(8), 2002, 691-4.

Experiments were carried out in the $CaMg(CO_3)_2$-Si and $CaMg(CO_3)_2$-SiC systems at 7.7 GPa and T of 1500-1800°C. No graphite was added to the run powder as a carbon source; the carbonate-bearing melts supply the carbon for diamond formation. Diamond grows spontaneously from the carbonatitic melt by reducing reactions: $CaMg(CO_3)_2 + 2Si = CaMgSi_2O_6 + 2C$ in the $CaMg(CO_3)_2$-Si system, and $CaMg(CO_3)_2 + 2SiC = CaMgSi_2O_6 + 4C$ in the $CaMg(CO_3)_2$ -SiC system. The results provide strong experimental support for the view that some natural diamonds crystallized from carbonatitic melts by metasomatic reducing reactions with mantle solid phases. P.B.L.

Imaging the atomic arrangements on the high-temperature reconstructed α-Al_2O_3 (0001) surface.

C. BARTH AND M. REICHLING. *Nature*, **414**(6859), 2001, 54-7.

Dynamic scanning force microscopy is used to image directly the atomic structure of the (0001) surface of α-Al_2O_3 heated to >1300°C in ultrahigh vacuum. The results show surface domains with hexagonal atomic symmetry at the centre, and disorder of the periphery. The dominant feature of the surface shortly after preparation is figured and is a rhombic grid representing the unit cell. On exposing the surface to H_2O and H_2, the surface structure forms hydroxide clusters forming rings attributed to self-organization involving cluster-surface and cluster-cluster interactions. R.K.H.

[Influence of silicates upon the growth of synthetic diamond crystals.]

A.A. CHEPUROV, V.M. SONIN AND A.I. CHEPUROV. *Proceedings of the Russian Mineralogical Society*, **131**(1), 2002, 107-10. (Russian with English abstract.)

The synthesis and growth of diamond crystals at 5.5 GPa and 1500°C in the system Fe-Ni-C was performed with the aid of silicate components (natural olivine and balsalt) up to 20 wt.%. The introduction of >5% of silicates leads to changes in the morphology of the diamond crystals, manifested in the loss of morphological stability by the {111} faces, with triangular vicinal hillocks with step-like lateral surfaces becoming transformed into sub-individuals. In so doing, the initial single crystal is eventually transformed into a parallel aggregate. In the growth process, the diamond crystals accept the inclusion of silicate phases, with local concentrations screening off diamond growth and stopping it entirely at 20% silicate content. R.A.H.

Evolution of crystal morphology of natural diamond in dissolution processes: experimental data.

A.F. Khokhryakov, Yu. N. Pal'yanov and N.V. Sobolev. *Doklady, Russian Academy of Sciences, Earth Sciences Section*, **381**(8), 2001, 884-8. (English translation.)

This was an experimental study of the morphological evolution of the main types of natural diamond crystals during their dissolution in modelled systems at mantle *P-T* conditions; 112 crystals (55 pseudo-octahedra, 27 pseudorhombic dodecahedra and 30 cubic crystals) were investigated. The experimental data are tabulated and the results show that the dissolution of diamond with the formation of ditrigonal layers occurs at 2.5-5.7 GPa and 1100-1450°C. The rate of diamond dissolution in water-containing silicate systems is an order of magnitude higher than in carbonate systems due to the carbonization reaction. The semi-rounded and rounded crystals of the natural diamonds serve as an indication of a fluid regime. A.M.C.

Crystallization of metamorphic diamond: an experimental modelling.

Yu N. Pal'yanov, V.S. Shatsky, A.G. Sokol, A.A. Tomilenko and N.V. Sobolev. *Doklady, Russian Academy of Sciences, Earth Sciences Section*, **381**(8), 2001, 935-8 (English translation).

This study was aimed at determining whether diamond crystallized in the metamorphic host-rock medium or was formed elsewhere and later captured as inclusions. The experimental results confirm the critical role of water-bearing carbonate melt in the genesis of metamorphic diamonds. Garnet-pyroxene rock from the Kumdykol deposit in the Kokchetav Massif does not melt and remains inert relative to diamond and graphite. Therefore, it may be regarded as a restite. The experiments succeeded in obtaining the joint experimental crystallization of diamond and garnet. A.M.C.

Diamond formation through carbonate-silicate interaction.

Y.N. Pal'yanov, A.G. Sokol, Y.M.B.F. Khokhryakov and N.V. Sobolev. *American Mineralogist*, **87**(7), 2002, 1009-13.

Crystallization of diamond and graphite from the carbon component of magnesite occurs upon the latter's decarbonation in reactions with coesite and enstatite at *P* of 6-7 GPa and *T* of 1350-1800°C. In a series of experiments, diamond was obtained in association with enstatite, coesite and magnesite, as well as with forsterite, enstatite and magnesite. Octahedral diamond crystals were studied by FTIR spectroscopy and were found to contain nitrogen and hydrogen, which are known as the most abundant impurities in natural type 1a diamonds. Growth of diamond on the cubic faces of seed crystals proceeds with formation of a cellular surface structure, which is similar to natural fibrous diamonds. The isotopic composition of synthesized diamonds ($\delta^{13}C$ = -1.27‰) was close to that of the initial magnesite ($\delta^{13}C$= -0.2‰). P.M.W.

Crystallization of diamond and syngenetic minerals in melts of diamondiferous carbonatites of the Chagatai Massif, Uzbekistan: experiment at 7.0 Gpa.

Yu. A. Litvin, A.P. Jones, A.D. Beard, F.K. Divaev and V.A. Zharikov. *Doklady, Russian Academy of Sciences, Earth Sciences Section*, **381A**(9), 2001, 1066-1069. (English translation.)

The aim of this work was an experimental study of the possibility of high-*P* diamond crystallization in the melts of the diamondiferous carbonatites in the melts of the diamondiferous carbonatites of the Chagatai Massif, as well as high-*P* transformations of natural carbonate-silicate rocks under *P-T* conditions of diamond stability. Major element analyses are given for 12 mineral phases crystallizing simultaneously with diamond in these experiments with deep-seated carbonatites. It was established that carbon-oversaturated melts of natural diamondiferous mantle carbonatites serve as a highly intense diamond-forming medium within the diamond stability field. A.M.C.

Mechanisms of layered spiral growth of synthetic diamond crystals based on SEM data.

N.D. Samotoin. *Doklady, Russian Academy of Sciences, Earth Sciences Section*, **381**(8), 2001, 925-8. (English translation.)

High-voltage (100 kV) SEM was applied to the study of fine growth surface morphology of diamond crystals. Various factors governing the layered spiral growth of diamond were found and investigated. Their contributions, abundances and factors controlling the minimum height of growth steps were estimated. The data obtained show that the diamond crystal growth from a hydrocarbon gas phase is provided by various mechanisms even under the same physiochemical conditions. The layered spiral mechanism generated by various sources dominates in the collective formation of diamond crystals. A.M.C.

Opal identification and value.

P.B. DOWNING, 2003. Majestic Press, Inc., Estes Park, CO, U.S.A. pp xii, 212, illus. in colour. Hardcover: ISBN 0 9625311 8 9. £32.00.

A revised, expanded and updated edition of a book first published in 1992, this is a beautifully illustrated coverage of all gem varieties of opal, their man-made counterparts and the qualities that make some colour varieties more desirable than others in the world's opal markets. Pricing is also discussed and there are also useful notes on opal in jewellery.

Opal from different world locations is described, the sites including not only Australia and Mexico but also Ethiopia, Brazil, Canada and Indonesia. Each chapter concludes with a brief summary. The book is attractively produced with excellent photographs and can be highly recommended. M.O'D.

Colored gemstones. The Antoinette Matlins buying guide.

A. MATLINS, 2003. Gemstone Press, Woodstock, Vermont (Sunset Farm Offices, Route 4, PO Box 237, Woodstock VT, U.S.A.). pp xv, 180, illus. in colour. Softcover. ISBN 0 943763 33 9. US $16.95 (higher outside the US).

Simple and easy-to-read guide to the major gemstones, their qualities and how they are priced. While the text is adequate there is insufficient colour differentiation in the photographs so that the red stones in particular appear the same colour. The best parts of the book are those dealing with buying and its possible pitfalls. Some small inaccuracies have crept in but they are nothing to worry about. M.O'D.

Diamonds. The Antoinette Matlins buying guide.

A. MATLINS, 2003. Gemstone Press, Woodstock, Vermont (Sunset Farm Offices, Route 4, PO Box 237, Woodstock VT, U.S.A.). pp xv, 184, illus. in colour. Softcover. ISBN 0 943763 32 0. US $16.95 (higher outside the US).

Useful guide to the commerce of gem diamond with notes on diamond qualities and grading systems, buying at auction, on the internet and on gemstone investment telemarketing scams (there are lots of them). Most of the facts given would be found in a gemmology text but this book is aimed at a different audience and should suit it quite well. M.O'D.

Jewelry and gems at auction. The definitive guide to buying and selling at the auction house and on internet auction sites.

A. MATLINS, 2003. Gemstone Press, Woodstock, Vermont (Sunset Farm Offices, Route 4, PO Box 237, Woodstock VT, U.S.A.). pp xiv, 309, illus. in colour. Softcover. ISBN 0 943763 29 0. US $19.95 (higher outside the US).

This is not only the best guide devoted to buying jewellery and gemstones by auction and through the internet: it appears to be the only one so far. The experience of the author virtually guarantees reliability and the whole text is easy to read for recreation as well as for common-sense information.

A particularly welcome feature which recurs throughout the book is the publicizing of various scams (including the dealers' ring). Anyone who, having read the book, thinks, "I would never have fallen for that" may be deceiving themselves just a little – the tricks are legion and the coming of internet selling has opened up fresh minefields to the feet and purses of the careless buyer.

The text is arranged by species and needs no particular comment, apart from the welcome introduction of appraisals. This is another area of anxiety: read the book to find out why. M.O'D.

Jadeite jade: a stone and a culture.

C. M. OU YANG, 2003. Yang Mulia Gems Ltd, Hong Kong [26/F Tung Hip Comm. Bldg, Des Voeux Rd, Central, Hong Kong]. pp. xiv 184, illus. in colour. Hardcover ISBN 962 86987 1 0. Price on application.

The first impression given by this attractively produced and illustrated book is that it covers the commerce of jade particularly well although other details that the reader might expect are present. Should any reader contemplate starting in the jade business this would be an excellent book to begin with (a knowledge of Chinese and family connections would have their uses too). The world of jade is just as individual as that of diamond.

The text begins with a mineralogical description of both nephrite and jadeite, and a note on the probable origin of the term *Fei-Tsui*, used today to denote Burmese jadeite of especially fine colour. Gemmological characteristics are given before the text embarks upon a study of the occurrence and deposits of jadeite. Even now, the author tells us, there appears to be no known deposit of jadeite in mainland China. She makes the interesting point that the name *Yunnan jade* referred originally to the jadeite from the Myitkyina are of Burma which borders Yunnan. Boundaries were not clearly marked and confusion would have been easy.

The jadeite deposits of Burma are described in considerable detail as the reader might expect. Deposits currently known in the area as *Old mine* and *New mine* might, the author believes, be better classified as primary [New mine] and secondary deposits [Old mine] since this would take into account the geological times of formation.

The next chapters describe the colours and varieties of jadeite with notes on their relative popularity (in China): Chinese names are appended. Chapter 5 deals with the classification of rough jadeite, including the different types of skin to be found on the boulders. Chapter 6 describes

processing techniques and the classification of finished jade products, including carving. The jade processing centres of China are introduced.

Jade-like minerals and simulants are described in the next chapter: the gemmologist will be familiar with them and will probably turn quickly to the descriptions of treatments in chapter 8. Here we have examples of B type, B+C type and C types of jadeite and how to detect treatments and composites. The accompanying photographs are very helpful and the best available I have seen in any gemmological text so far published. It has always been difficult to find really well-illustrated accounts of these processes and tests since so many of the most authoritative ones are in Chinese.

Chapter 9 tells the reader how to appraise and value jadeite, and chapter 10 describes the operation of jade markets and the government-run auctions in Burma. The main text concludes at this point with a set of photographs of fine examples of worked jadeite. There is a useful bibliography which includes mostly papers, citations of which may be hard to root out elsewhere. Only an index is lacking. One or two typos do nothing to distract the eye and this is a most welcome book. M.O'D.

Beryllium-treated rubies and sapphires.

T. THEMELIS, 2003. The Author, Bangkok, Thailand (distributed in the UK by *Aspara*, PO Box 230, Tadworth, Surrey KT20 5ZA). pp 48, illus. in colour. Softcover. ISBN 0 940965 40 2. Price on application.

The author summarizes and illustrates some of the techniques used in the heat treatment of rubies and sapphires involving the addition of beryllium. Using a series of colour photographs Themelis (a pioneer and well-known author in this field) describes the apparatus necessary for this treatment, noting on the way the health hazards of beryllium and the stages of the process from the cleaning of the material to the finished stone. Particular attention is given to surface abnormalities.

Examples of beryllium treatment are given for rubies and sapphires from Madagascar, Songea, Morogoro and Umba (Tanzania), Montana, Australia, Sri Lanka, Mong-Hsu and Vietnam. Notes follow on the gemmological features of the treated stones and their characteristic inclusions. Notes on stability, disclosure and future prospects for this kind of treatment complete the main text which is followed by a short but very useful bibliography in which the author's presentations and useful references are given.

The standard of production is high and the pictures a welcome sight – few illustrations of these processes seem to get published and the same can be said of the notes on techniques. This is a welcome addition to the literature of treatments. M.O'D.

Proceedings of the Gemmological Association and Gem Testing Laboratory of Great Britain and Notices

Photographic Competition

The 2003 Photographic Competition on the theme All Shapes and Sizes drew a record number of entries of a particularly high quality, illustrating interesting crystal shapes, fascinating inclusions, and unusual cuts and carvings.

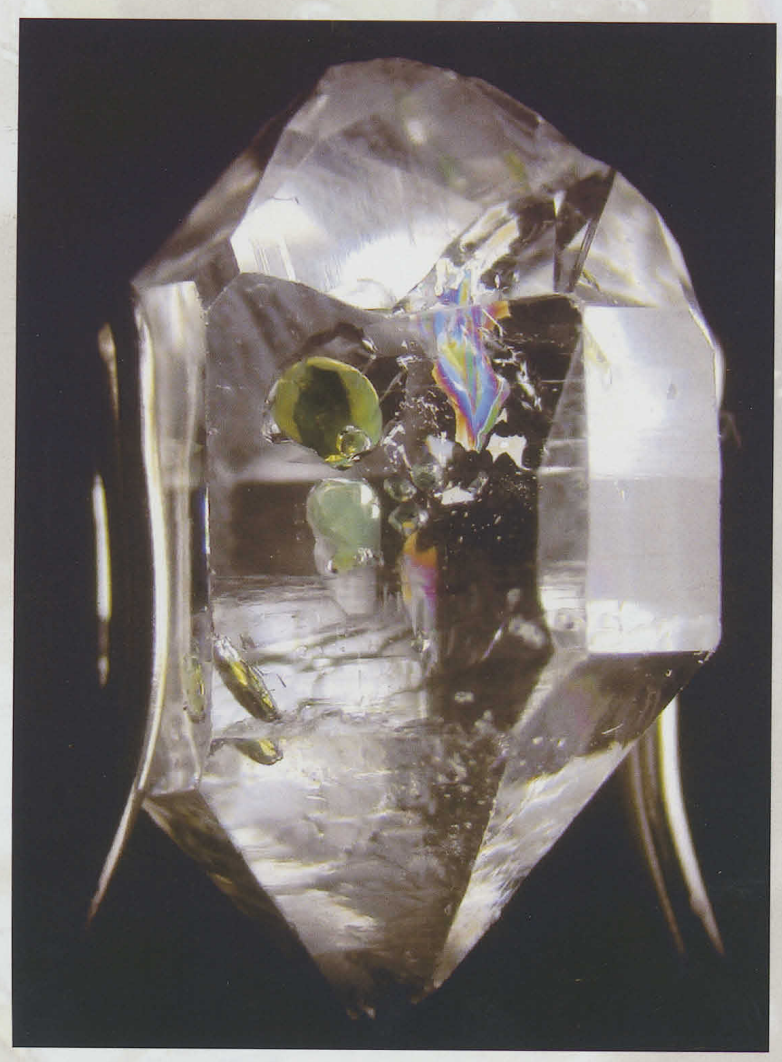

First Prize

Zeng Chunguang FGA, Singapore

Quartz with green and iridescent inclusions

(also illustrated on front cover).

ISSN: 1355–4565

Second Prize

Anthony de Goutière GG, Victoria, BC, Canada

Topaz cleavage

Third Prize

Luc Genot FGA, Brussels, Belgium

Mabe pearl

We are pleased to announce that the prizes were sponsored by Harley UK, and the Association is most grateful to them for their generosity. The winning entries will be exhibited at the Annual General Meeting to be held on 9 September and at the Gem-A Annual Conference on 2 November 2003.

ASSOCIATE MEMBERSHIP

A number of members have expressed the view that the 'Ordinary member' is not a particularly desirable title. Therefore, at a meeting of the Council of Management held on 30 April 2003 it was agreed that Ordinary membership of the Association should be retitled Associate membership.

Anyone with an interest in gemstones may apply for Associate membership – no qualifications are necessary.

Membership subscriptions and donations are vitally important for the Association to continue its work in studying and testing gemstones, and in the publication and promotion of reliable gemmological knowledge. The Council of Management is therefore most grateful to all members for their continued interest in and support of the Association.

MEMBERS' MEETINGS

London

On 15 May at the Gem Tutorial Centre, Gem-A, 27 Greville Street, London EC1N 8TN, a talk entitled 'The gem market of Chanthaburi and the heat treatment of gems in Thailand' was presented by Professor Theerapongs Thanasuthipitak of Chiang Mai University, northern Thailand, and his two colleagues from Chanthaburi, Anuphap Chinudompong and Prajak Angkahiran. A summary of their research results and views on terminology will be published in the September issue of *Gem & Jewellery News*.

Midlands Branch

On 25 April 2003 at the Earth Sciences Building, University of Birmingham, Edgbaston, John Wright gave a talk entitled 'The interface of gem and jewel'. He briefly explored the design, materials used and manufacturing processes where gems come into contact with precious metals. The meeting also included the Branch AGM when David Larcher, Gwyn Green, Elizabeth Gosling and Stephen Alabaster were re-elected President, Chairman, Secretary and Treasurer respectively.

On 18 May at Barnt Green a one-day conference was held. The event openedwith a talk by Doug Morgan entitled 'Gemmological Diversions'.

DONATIONS

The Council of Management are most grateful to the following for responding to the appeal for donations to enable the Association to extend our membership and education services. Donation levels were Diamond (£1000 and above), Ruby (£500 to £999), Emerald (£250 to £499), Sapphire £100 to £249) and Pearl (£25 to £99). All donors will be recognized at a Gala Dinner to be held in London early next year.

A list of those who have responded to the appeal follows:

Emerald Donations

Gem-A Midlands Branch
Rita Mittal, Lusaka, Zambia

Sapphire Donations

James G. Gosling, Pattingham, Staffordshire
Kiyomi Hiraga, Nakakoma-gun, Yamanashi Pref., Japan
W. Richard Peplow and Sarah A. Riley, Worcester, Hereford and Worcester

Pearl Donations

Sylvia V.J. Baker, Bullcreek, Western Australia, Australia
Robert B.R. Gau, Taipei, Taiwan, RO China
Hui Chak Lun, Kowloon, Hong Kong
Sandra Lear, Kingston upon Thames, London
Patricia Merriman, Wallasey, Merseyside
Michael Ngan Hin Wah, Hong Kong
Malcolm J. O'Hara, Sydney, New South Wales, Australia
Andrew T. Phillips, Penang, West Malaysia
Elaine Wai Ling Ng Tang, Chesham, Buckinghamshire

Following lunch, a presentation was given on the gem market and heat treatment of corundum in Chanthaburi, Thailand. The Thai team comprised Professor Theerapongs Thanasuthipitak of Chiang Mai University, northern Thailand, and his two colleagues, Anuphap Chinudompong and Prajak Angkahiran, both of whom have long experience of treating sapphires at Chanthaburi. Dr Bill Gaskarth from Birmingham University explained how the connection between Birmingham and Thailand had started and introduced the members of the team. A summary of the presentation will be published in the September issue of *Gem & Jewellery News*. An identification competition of rough and cut gemstones was held during the day.

On 21 June at Barnt Green the annual Midsummer Supper was held.

North West Branch

On 21 May at Church House, Hanover Street, Liverpool 1, Ian Mercer, Director of Education at Gem-A, gave a talk entitled 'A jade tour'.

On 18 June at Church House, Wendy Simkiss gave a talk on 'Crystal care'.

Scottish Branch

The Annual Scottish Branch Conference was held in Perth from 2 to 5 May, keynote speaker Professor Henry Hänni. A report was published in the June issue of *Gem & Jewellery News*, **12**(3), pp. 47-9.

On 18 June at the British Geological Survey, Murchison House, West Mains Road, Edinburgh, Vanessa Paterson gave a talk entitled 'Amber – yellow, orange, green, blue, red: the ins and outs'.

South East Branch

On 8 June at Christie's South Kensington, Peter Buckie gave a talk on valuation today.

North East Branch

We are pleased to announce that a new Branch of Gem-A is to be established in the North East of England. The inaugural meeting is to be held on Wednesday 10 September 2003 in Leeds.

Full details will be circulated to all Gem-A members in the area.

OBITUARY

Nikolas Lambrinides FGA, Athens, Greece, died on 30th June 2003. A full obituary will be published in the October issue of *The Journal.*

Rodolfo Moller Duran FGA DGA (D.1978), Barcelona, Spain, died on 31 March 2003.

Reginald A. Smith FGA (D.1961), Shaftesbury, Dorset, died recently.

MEMBERSHIP

Between 1 April and 1 June 2003 the Council of Management approved the election to membership of the following:

Fellowship and Diamond Membership (FGA DGA)

Ruckel, Daphne, London. 2003/2001

Fellowship (FGA)

Brook, Judith Margaret, Leicester, 1985
Epelboym, Marina, New York, U.S.A. 2003
Fisher, Fiona Jane, Dublin, Ireland. 2003
Hing, Michael E., London. 2003
Lee Hin Chi, Cheung Chau, Hong Kong. 2003
Maeland, Egil, Sandnes, Norway. 2003
Rickard, Patricia, Dollack Pines, California, U.S.A. 1986
Ng, Wai Ling, Kowloon, Hong Kong. 2003
Pi, Zhengfan, Shenzhen, P.R. China. 2002
Tong Yung, Tony, Kowloon, Hong Kong. 2002
van Rooij-Roeloffzen, M., Almere Buiten, The Netherlands. 2003

Associate Membership

Adams, Stephen Alexander, Dorking, Surrey
Ajodah, Nawjeet, London
Blackwood, Francesca, Richmond, London
Cabaniss, Jelks H. Jr, Alexandria, U.S.A.
Cardellini, Cristina, London
Donnelly, Kerry, Palmers Green, London
Eferemo, Henry, London
Fischgrund, Edward, London
Jimanez, Mary Rosa, Paris, France
John, Wendy, London
Kane, Robert, Helena, Montana, U.S.A.
Lampson, Ming, London
McQuire, Maureen, Glasgow, Scotland

GIFTS TO THE ASSOCIATION

The Association is most grateful to the following for their gifts for research and teaching purposes:

Victor Ely, London, for a Rayner spectroscope and a Rayner SG measurement set.

Pauline Gregory FGA, Westgate-in-Weardale, Durham, for cut fluorite samples.

Maria Sanchez Sierra, Tooting, London, for emerald crystals from the Coscuez Mine in Colombia.

Mirza, Sojail, Angered, Sweden
Paganoni, Federica, Italy
Thys, Valérie Clara Louise Raymond, Belgium

Laboratory Membership

Cookson Precious Metals, Birmingham, West Midlands

Transfers

Fellowship (FGA) to Fellowship and Diamond Membership (FGA DGA)

Cheung Suk Yin, Kowloon, Hong Kong
Chun Ming Lee, Hong Kong
Marlow, Carol, Sutton Coldfield, West Midlands
Pace, Michael, Elk Grove, California, U.S.A.
Tominaga, Masami, West Finchley, London

Diamond Membership (DGA) to Fellowship and Diamond Membership (FGA DGA)

Selvamani, Parvathi, Ilford, Essex
Tse Yiu Yu, Stephen, Kowloon, Hong Kong

Associate Membership to Fellowship (FGA)

Ayer, Elizabeth C., Cambridge
Giancola, Maria Luisa, Milan, Italy
Gregory, Pauline A., Bishop Auckland, County Durham
Jones, Lorraine D., Farnworth, Greater Manchester
Okazaki, Maki, London
Pennington, Susan, Bickerstaffe, Lancashire
Tun U Myint, Lannavaara, Sweden
Whalley, Joanna, Walthamstow, London

Before you choose your insurance make sure you read the small print

At T.H March, every insurance package we supply is backed by an experience no one else can match. For over a hundred years we have provided the expertise, reliability and quality of service which has made us the premier insurance broker to the jewellery trade

T.H.MARCH
INSURANCE BROKER

London 10/12 Ely Place, London EC1N 6RY
Tel 020 7405 0009 Fax 020 7404 4629
web www.thmarch.co.uk email insurance@thmarch.co.uk

Additional offices in:
Birmingham 10A Vyse Street, Hockley, B18 6LT
Tel 0121 236 9433 Fax 0121 233 4901
Glasgow Empire House, 131 West Nile Street, G1 2RX
Tel 0141 332 2848 Fax 0141 332 5370
Manchester 1st Floor, Paragon House, Seymour Grove, M16 0LN
Tel 0161 877 5271 Fax 0161 877 5288
Plymouth Hare Park House, Yelverton Business Park, Yelverton PL20 7LS
Tel 01822 855555 Fax 01822 855566
Sevenoaks Sackville House, 55 Buckhurst Avenue, Kent TN13 1LZ
Tel 01732 462886 Fax 01732 462911

MEMBER
General Insurance
STANDARDS COUNCIL

FORTHCOMING EVENTS

27 July	**South East Branch.** *Fifty years plus in gemmology.* E. ALAN JOBBINS
7 September	**South East Branch.** *Workshop on spectroscopic techniques.* COLIN WINTER
9 September	**London.** AGM followed by *Jewellery of the Art Nouveau period.* DAVID CALLAGHAN
10 September	**North East Branch.** Inaugural meeting.
11 September	**Scottish Branch.** *Organics in ornamentation.* E. ALAN JOBBINS
17 September	**North West Branch.** *Scottish minerals.* BRIAN JACKSON
26 September	**Midlands Branch.** *Nineteenth-century jet and other black jewellery.* PEGGY HAYDEN
15 October	**North West Branch.** *Notes from the laboratory – detection, disclosure and false description.* STEPHEN KENNEDY
15 October	**Scottish Branch.** *The Cheapside Hoard.* JAMES GOSLING
19 October	**South East Branch.** *'Jem Jumble' bring-and-buy*
31 October	**Midlands Branch:** *The Naughty Nineties (1890s).* BRIAN DUNN

Gem-A Conference 2003

To be held on
Sunday 2 November
at Kempton Park Racecourse, Sunbury on Thames, Middx.

In conjunction with the Rock 'n' Gem Show

Speakers:

William E. Boyajian, Paula Crevoshay, Professor Henry Hänni
Dr Jack Ogden and Clive Wright

Further details are given on p. 391

3 November	**Presentation of Awards.** Goldsmiths' Hall, London
17 November	**Scottish Branch.** *Tales of a gemstone dealer: thoughts from a broad.* TRACY DUKES
28 November	**Midlands Branch.** *British gemstones with a Scottish flavour.* BRIAN JACKSON
6 December	**Midlands Branch.** *51st Anniversary Dinner*

Contact details

(when using e-mail, please give Gem-A as the subject):

London:	Mary Burland on 020 7404 3334; e-mail mary@gem-a.info
Midlands Branch:	Gwyn Green on 0121 445 5359; e-mail gwyn.green@usa.net
North East Branch:	Neil R. Rose on 0113 2070702 ; e-mail neil.rose@gem-ro.com
North West Branch:	Deanna Brady 0151 648 4266
Scottish Branch:	Catriona McInnes on 0131 667 2199; e-mail scotgem@blueyonder.co.uk
South West Branch:	Richard Slater on 01635 553572; mobile 07801 666172; e-mail rslater@dreweatt-neate.co.uk

Gem-A Website

For up-to-the-minute information on Gem-A events visit our website on www.gem-a.info

Guide to the preparation of typescripts for publication in *The Journal of Gemmology*

The Editor is glad to consider original articles shedding new light on subjects of gemmological interest for publication in *The Journal*. Articles are not normally accepted which have already been published elsewhere in English, and an article is accepted only on the understanding that (1) full information as to any previous publication (whether in English or another language) has been given, (2) it is not under consideration for publication elsewhere and (3) it will not be published elsewhere without the consent of the Editor.

Typescripts Two copies of all papers should be submitted on A4 paper (or USA equivalent) to the Editor. Typescripts should be double spaced with margins of at least 25 mm. They should be set out in the manner of recent issues of *The Journal* and in conformity with the information set out below. Papers may be of any length, but long papers of more than 10 000 words (unless capable of division into parts or of exceptional importance) are unlikely to be acceptable, whereas a short paper of 400–500 words may achieve early publication.

The abstract, references, notes, captions and tables should be typed double spaced on separate sheets.

Title page The title should be as brief as is consistent with clear indication of the content of the paper. It should be followed by the names (with initials) of the authors and by their addresses.

Abstract A short abstract of 50-100 words is required.

Key Words Up to six key words indicating the subject matter of the article should be supplied.

Headings In all headings only the first letter and proper names are capitalized.

A **This is a first level heading**

First level headings are in bold and are centred on a separate line.

B *This is a second level heading*

Second level headings are in italics and are flush left on a separate line.

Illustrations Either transparencies or photographs of good quality can be submitted for both coloured and black-and-white illustrations. It is recommended that authors retain copies of all illustrations because of the risk of loss or damage either during the printing process or in transit.

Diagrams must be of a professional quality and prepared in dense black ink on a good quality surface. Original illustrations will not be returned unless specifically requested.

All illustrations (maps, diagrams and pictures) are numbered consecutively with Arabic numerals and labelled Figure 1, Figure 2, etc. All illustrations are referred to as 'Figures'.

Tables Must be typed double spaced, using few horizontal rules and no vertical rules. They are numbered consecutively with Roman numerals (Table IV, etc.). Titles should be concise, but as independently informative as possible. The approximate position of the Table in the text should be marked in the margin of the typescript.

Notes and References Authors may choose one of two systems:

(1) The Harvard system in which authors' names (no initials) and dates (and specific pages, only in the case of quotations) are given in the main body of the text, (e.g. Collins, 2001, 341). References are listed alphabetically at the end of the paper under the heading References.

(2) The system in which superscript numbers are inserted in the text (e.g. ... to which Collins refers.[3]) and referred to in numerical order at the end of the paper under the heading Notes. Informational notes must be restricted to the minimum; usually the material can be incorporated in the text. If absolutely necessary both systems may be used.

References in both systems should be set out as follows, with *double spacing* for all lines.

Papers Collins, A.T., 2001. The colour of diamond and how it may be changed. *J.Gemm.*, **27**(6), 341-59

Books Balfour, I., 2000. *Famous diamonds*. 4th edn. Christie's, London. p. 200

Abbreviations for titles of periodicals are those sanctioned by the *World List of scientific periodicals* 4th edn. The place of publication should always be given when books are referred to.

Volume 28 No. 7 July 2003

Contents

The Journal of Gemmology

Cover Picture

Quartz with green and iridescent inclusions

Photograph by Zeng Chunguang FGA, Singapore

First Prize in the Photographic Competition (see p. 440)

ISSN: 1355–4565

Designed & Produced by Harley UK